Appendix A Severity Level Distribution of all Manned Aircraft Parts & sUAS for unmitigated and mitigated MACs

A.1 Commercial Transport

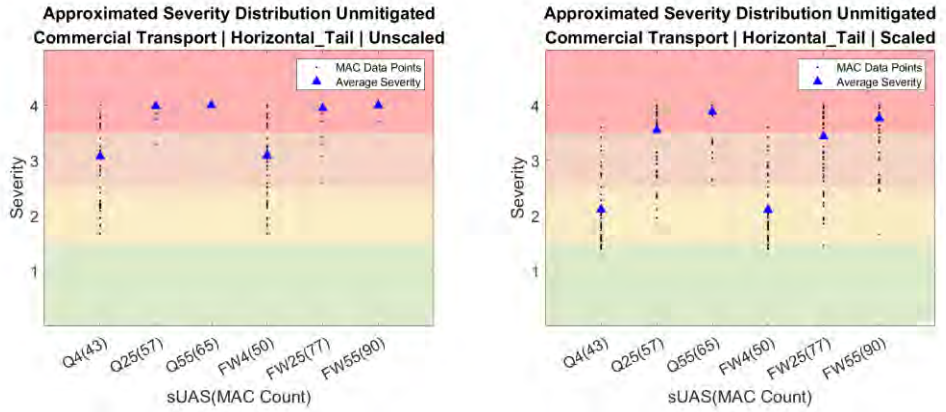

Figure 143. Approximated severity level distribution – Unmitigated commercial transport & horizontal tail.

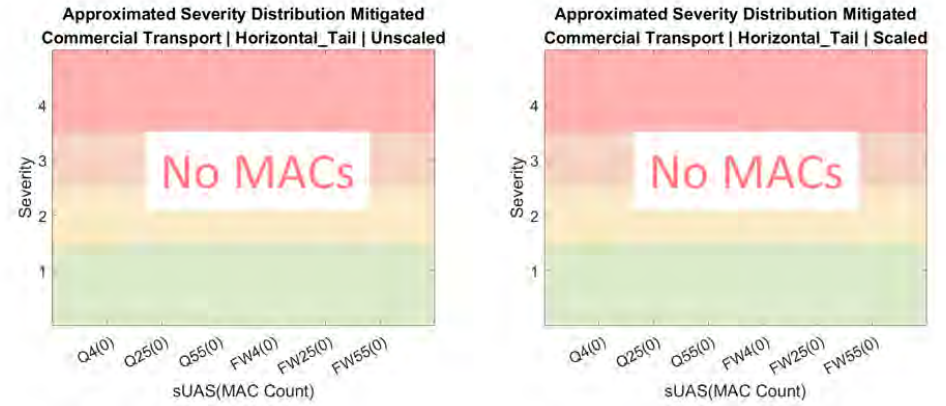

Figure 144. Approximated severity level distribution – Mitigated commercial transport & horizontal tail.

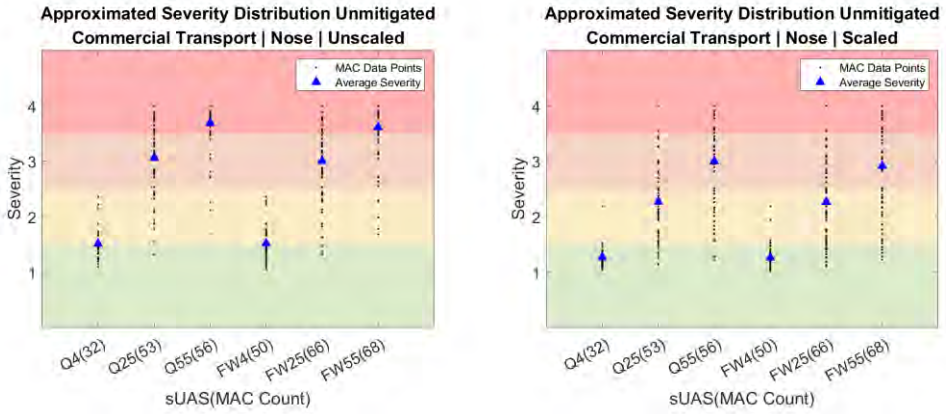

Figure 145. Approximated severity level distribution – Unmitigated commercial transport & nose cone.

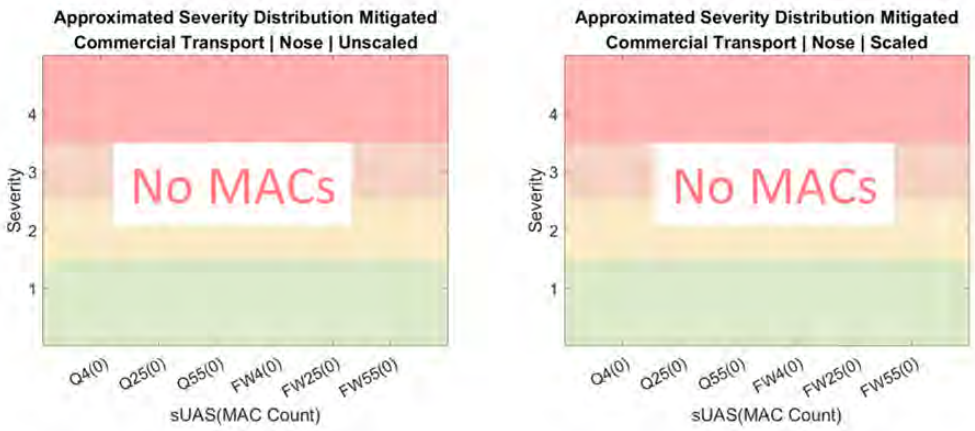

Figure 146. Approximated severity level distribution – Mitigated commercial transport & nose cone.

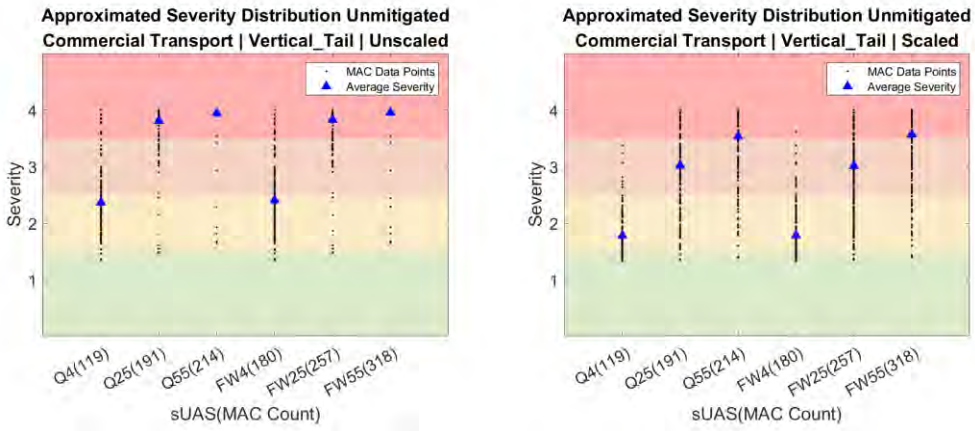

Figure 147. Approximated severity level distribution – Unmitigated commercial transport & vertical tail.

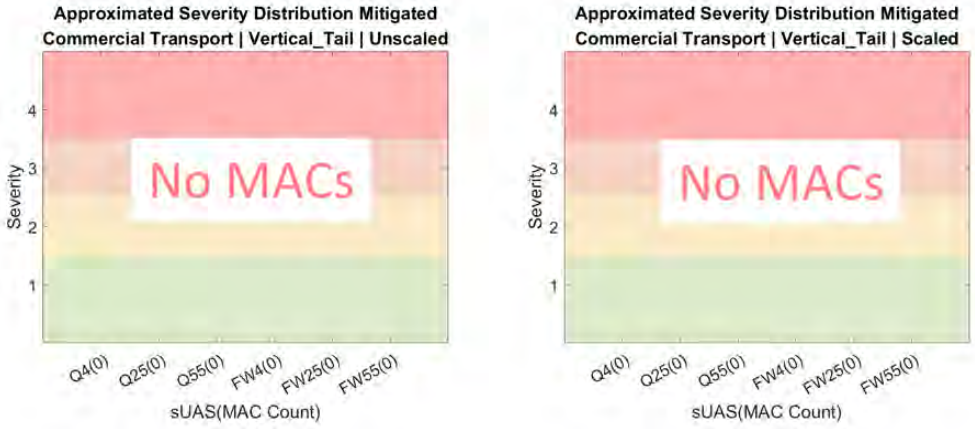

Figure 148. Approximated severity level distribution – Mitigated commercial transport & vertical tail.

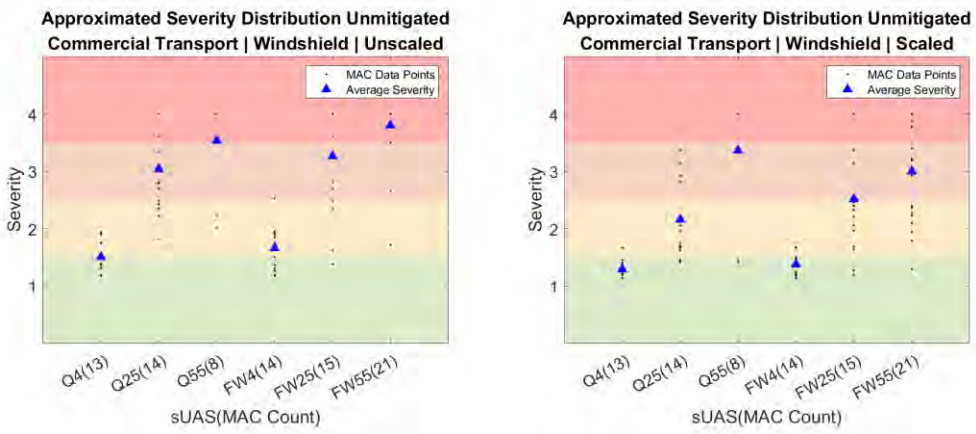

Figure 149. Approximated severity level distribution – Unmitigated commercial transport & windshield.

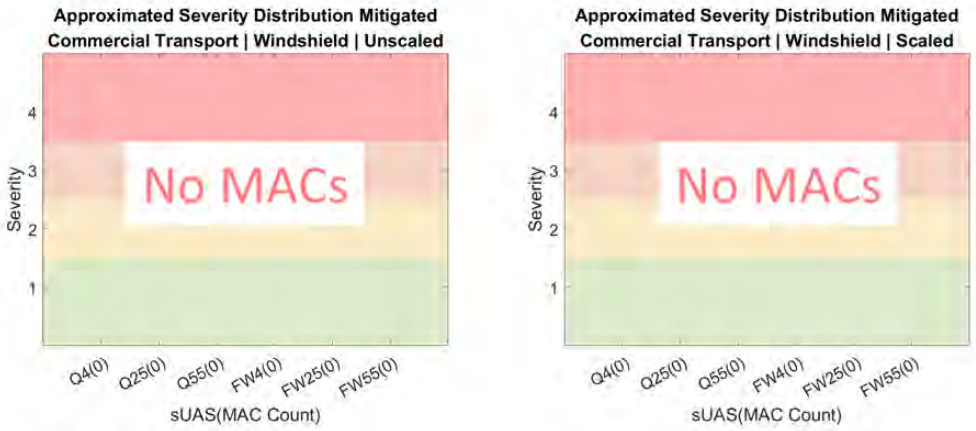

Figure 150. Approximated severity level distribution – Mitigated commercial transport & windshield.

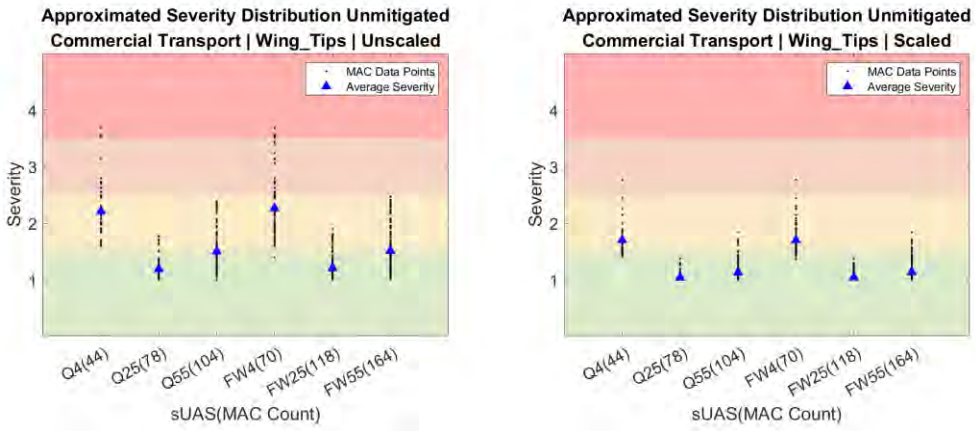

Figure 151. Approximated severity level distribution – Unmitigated commercial transport & wing tip.

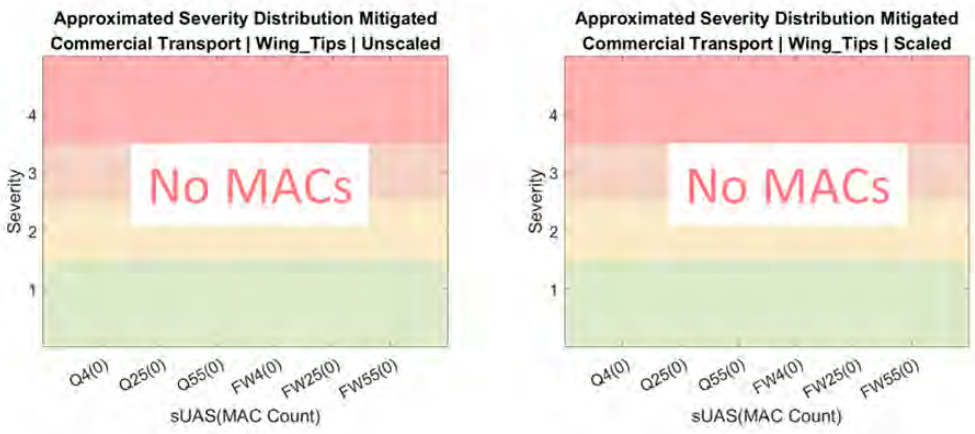

Figure 152. Approximated severity level distribution – Mitigated commercial transport & wing tip.

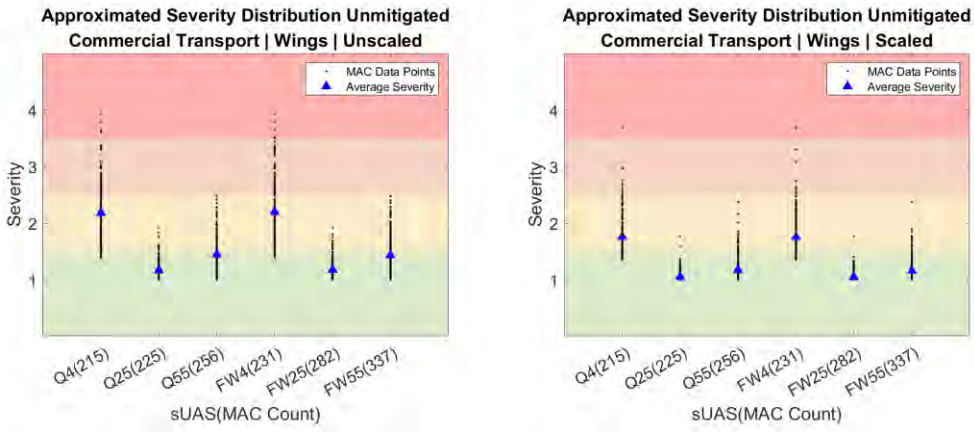

Figure 153. Approximated severity level distribution – Unmitigated commercial transport & wing.

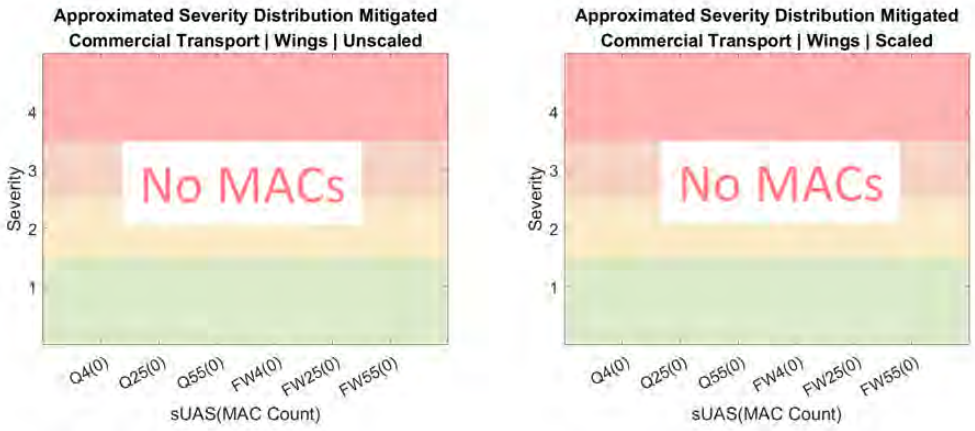

Figure 154. Approximated severity level distribution – Mitigated commercial transport & wing.

A.2 Business Jet

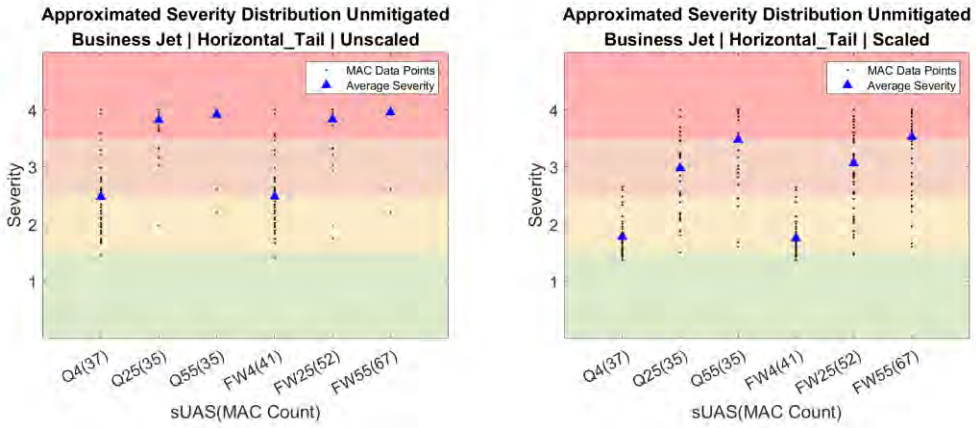

Figure 155. Approximated severity level distribution – Unmitigated business jet & horizontal tail.

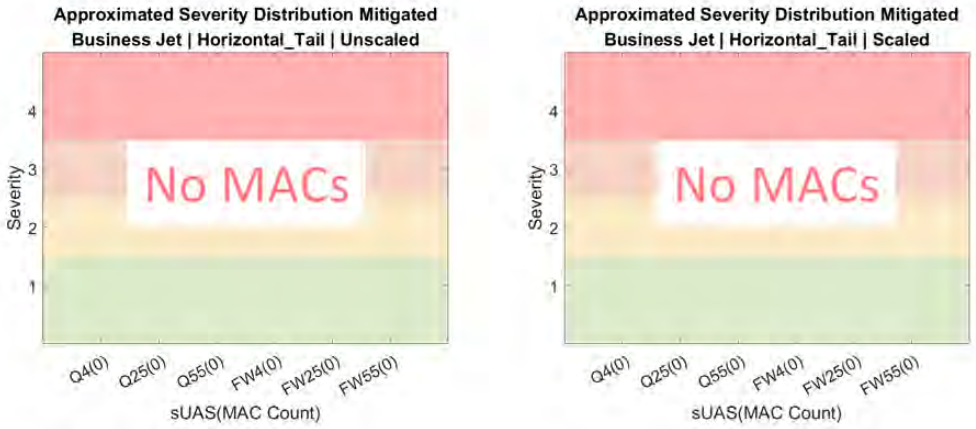

Figure 156. Approximated severity level distribution – Mitigated business jet & horizontal tail.

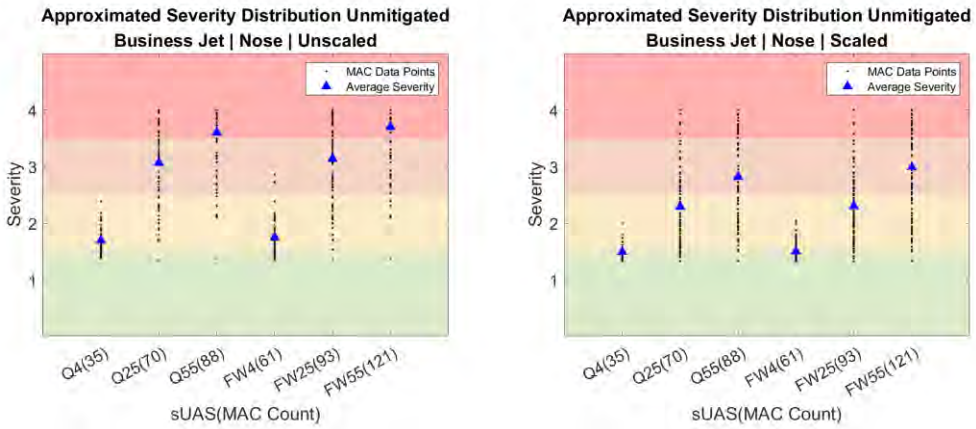

Figure 157. Approximated severity level distribution – Unmitigated business jet & nose cone.

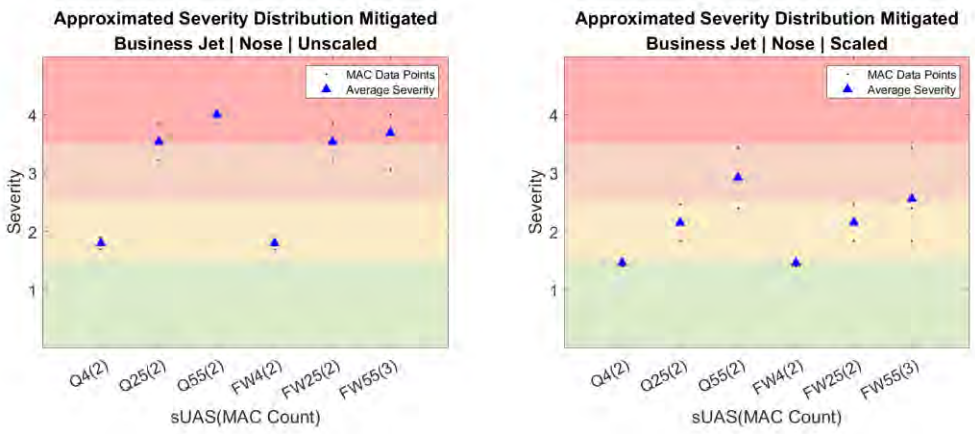

Figure 158. Approximated severity level distribution – Mitigated business jet & nose cone.

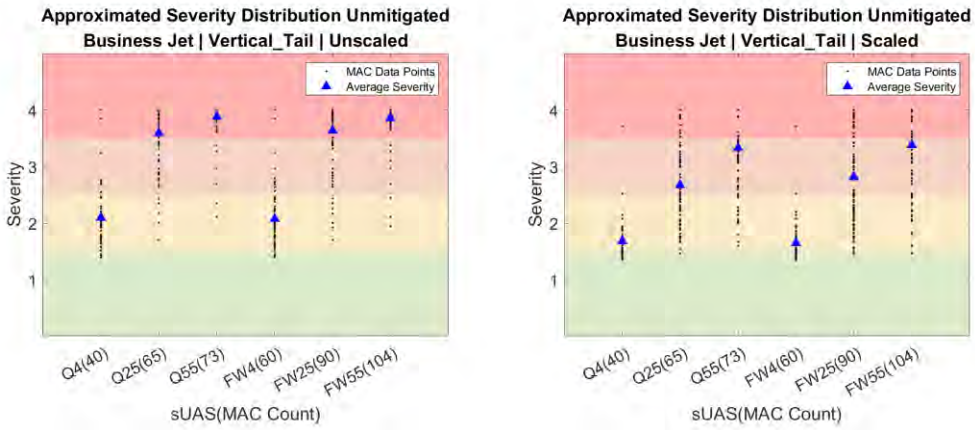

Figure 159. Approximated severity level distribution – Unmitigated business jet & vertical tail.

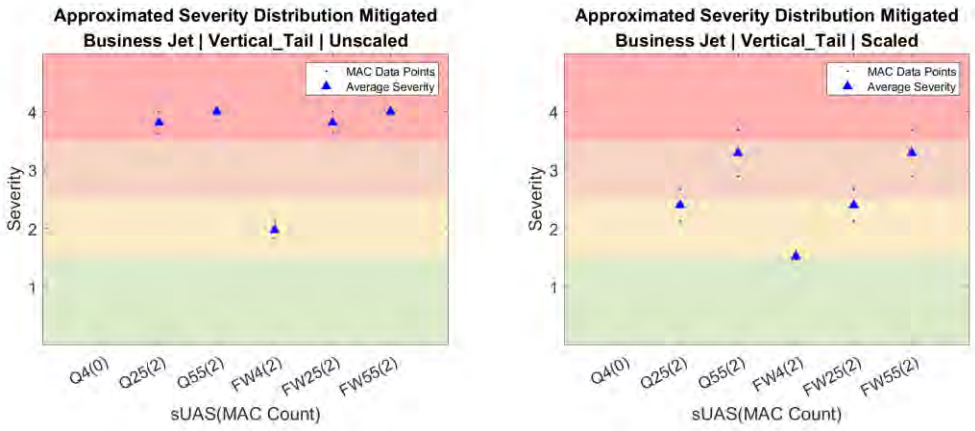

Figure 160. Approximated severity level distribution – Mitigated business jet & vertical tail.

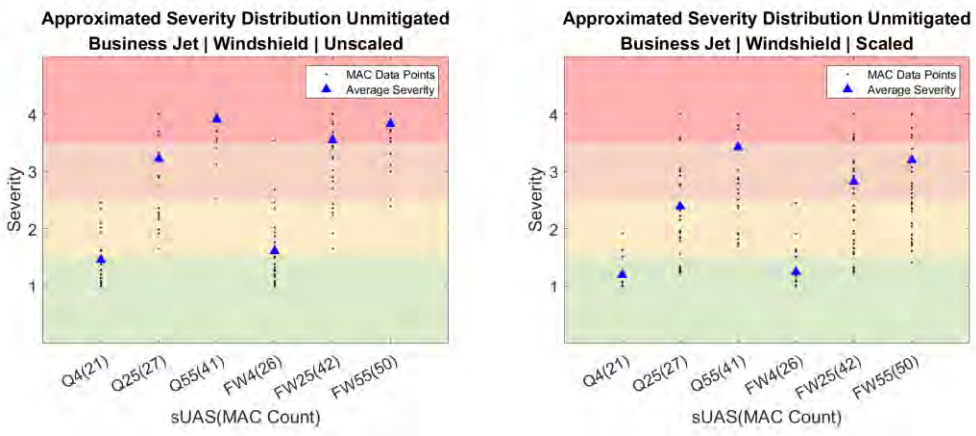

Figure 161. Approximated severity level distribution – Unmitigated business jet & windshield.

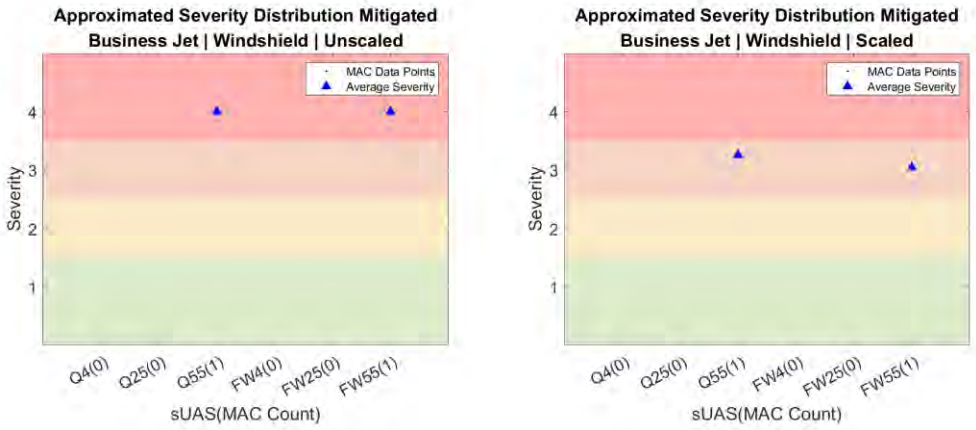

Figure 162. Approximated severity level distribution – Mitigated business jet & windshield.

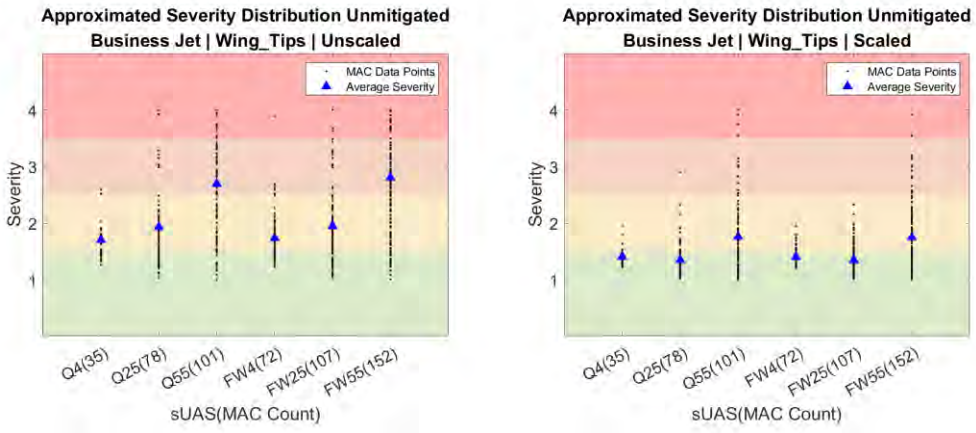

Figure 163. Approximated severity level distribution – Unmitigated business jet & wing tip.

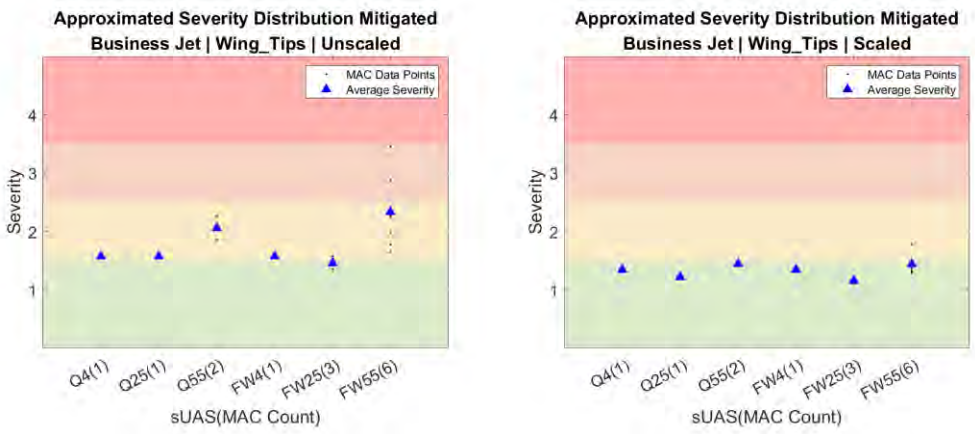

Figure 164. Approximated severity level distribution – Mitigated business jet & wing tip.

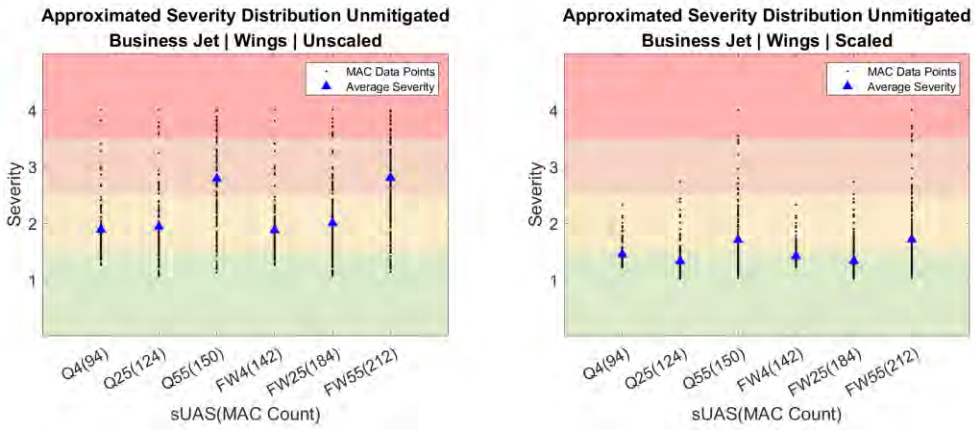

Figure 165. Approximated severity level distribution – Unmitigated business jet & wing.

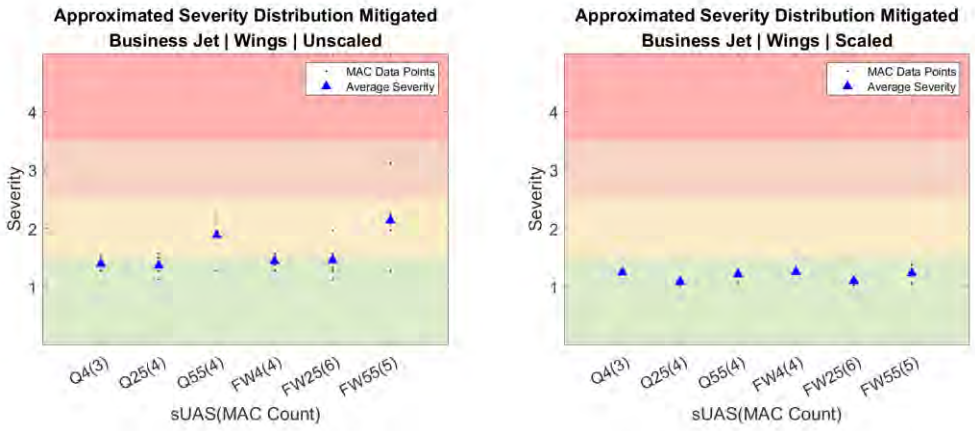

Figure 166. Approximated severity level distribution – Mitigated business jet & wing.

A.3 General Aviation (Single Engine)

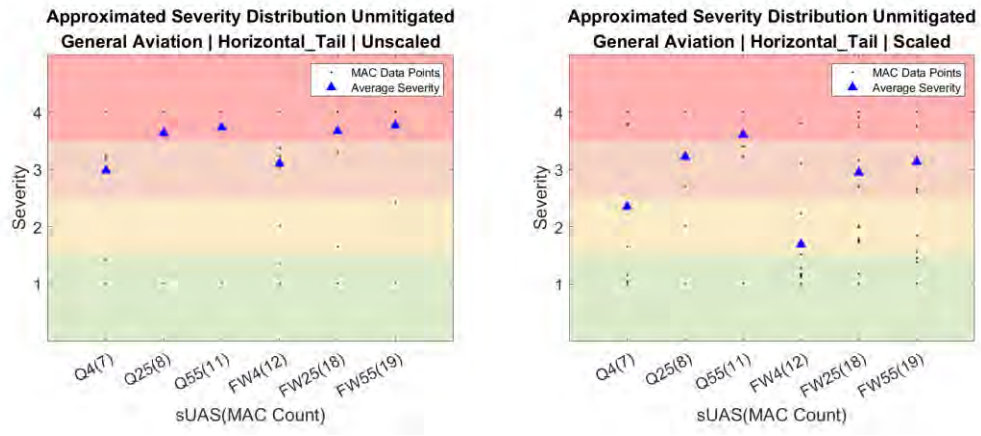

Figure 167. Approximated severity level distribution – Unmitigated general aviation & horizontal tail.

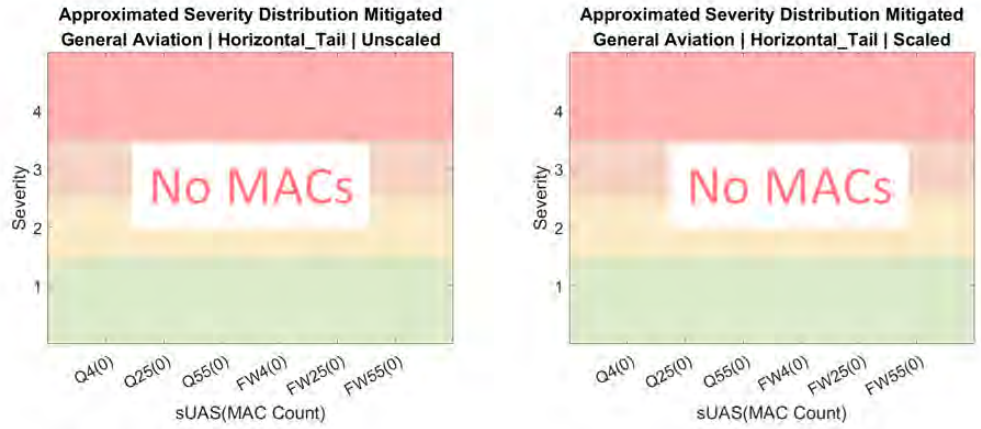

Figure 168. Approximated severity level distribution – Mitigated general aviation & horizontal tail.

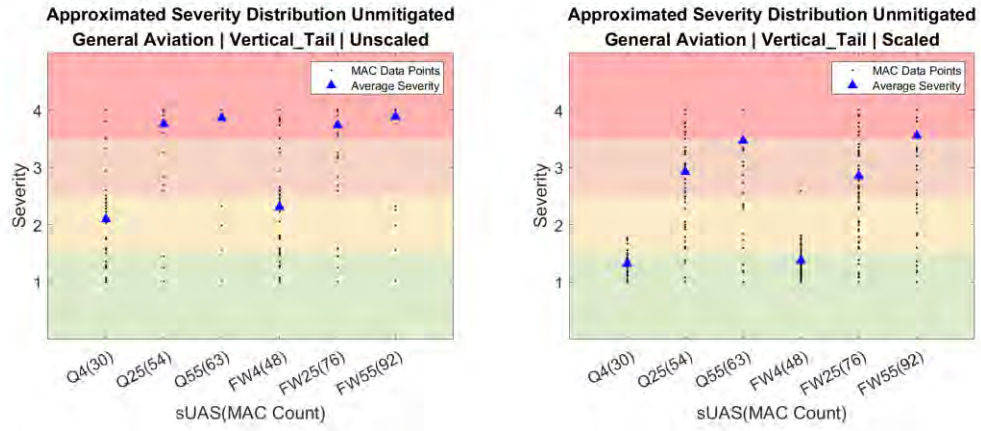

Figure 169. Approximated severity level distribution – Unmitigated general aviation & vertical tail.

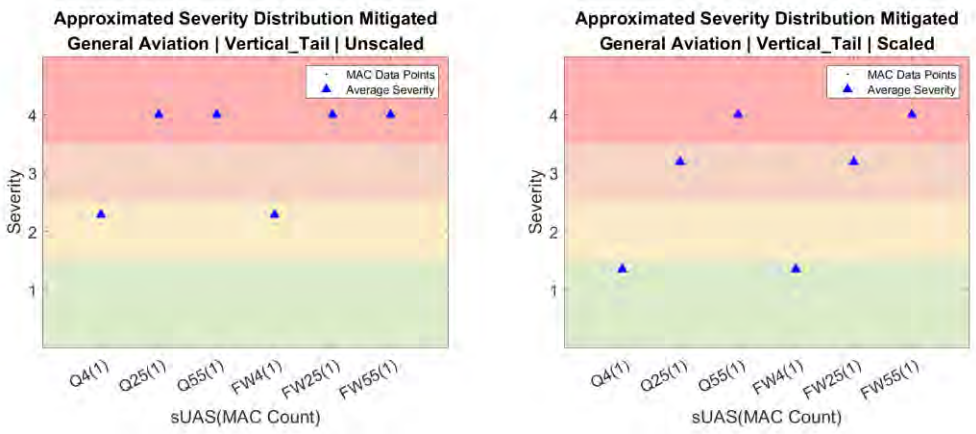

Figure 170. Approximated severity level distribution – Mitigated general aviation & vertical tail.

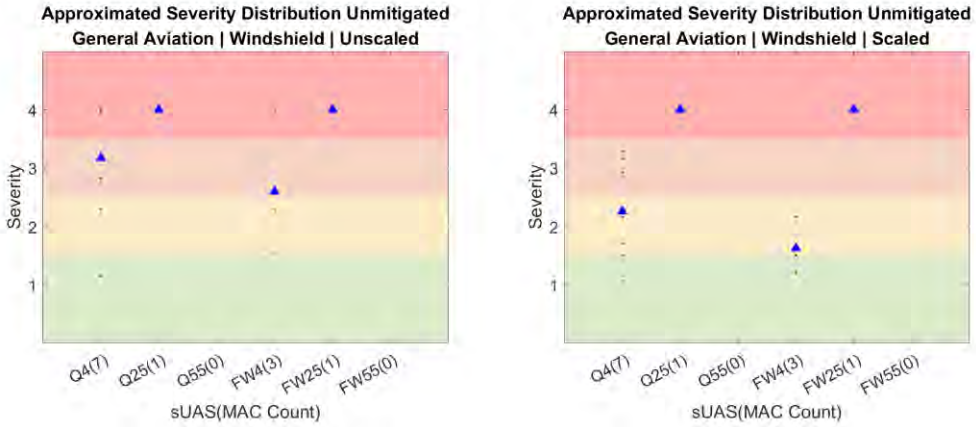

Figure 171. Approximated severity level distribution – Unmitigated general aviation & windshield.

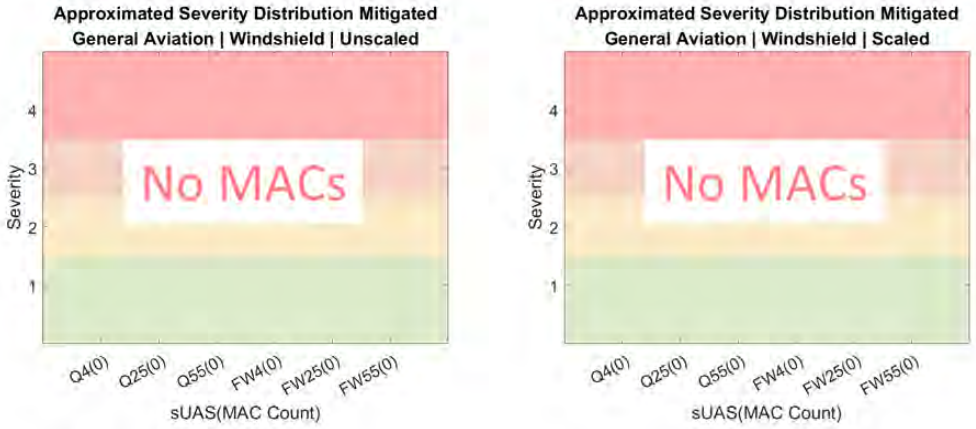

Figure 172. Approximated severity level distribution – Mitigated general aviation & windshield.

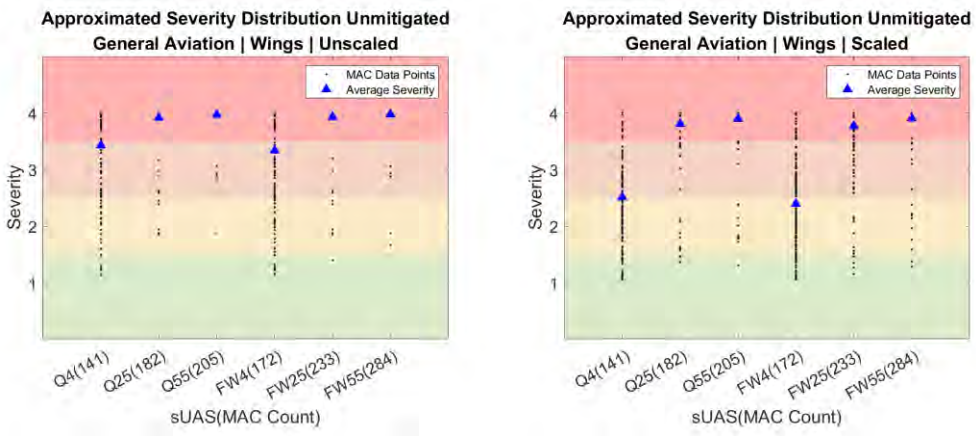

Figure 173. Approximated severity level distribution – Unmitigated general aviation & wing.

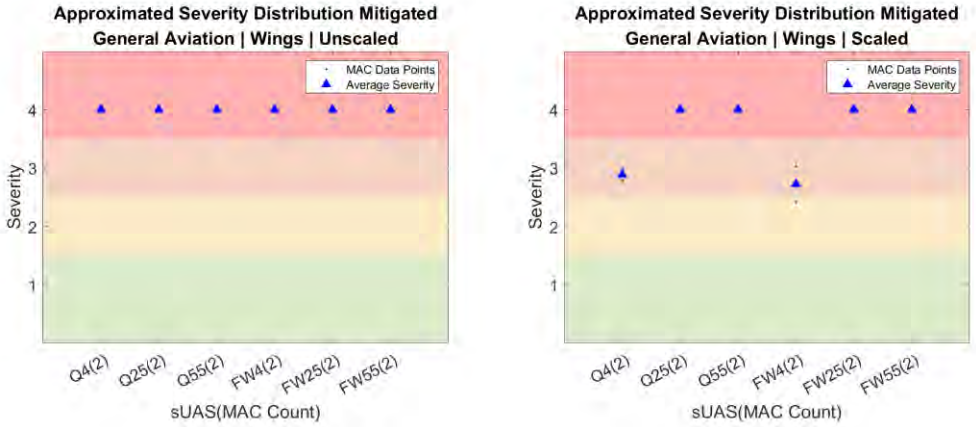

Figure 174. Approximated severity level distribution – Mitigated general aviation & wing.

A.4 Rotorcraft

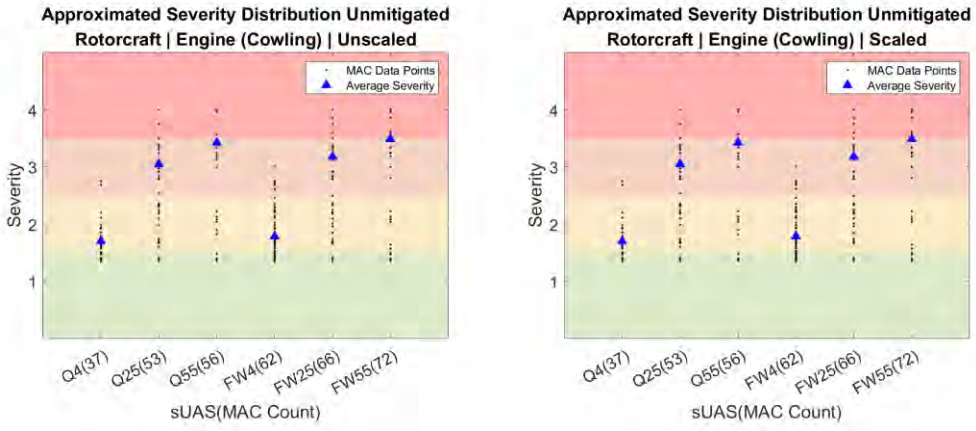

Figure 175. Approximated severity level distribution – Unmitigated rotorcraft & engine (cowling).

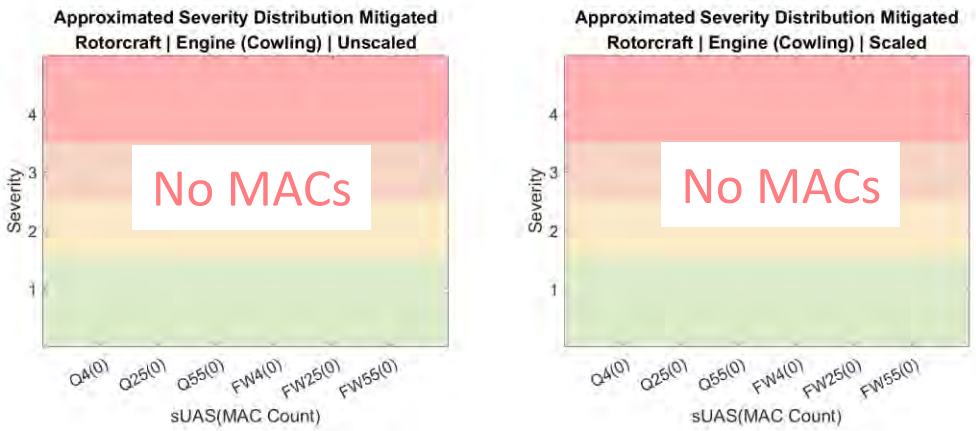

Figure 176. Approximated severity level distribution – Mitigated rotorcraft & engine (cowling).

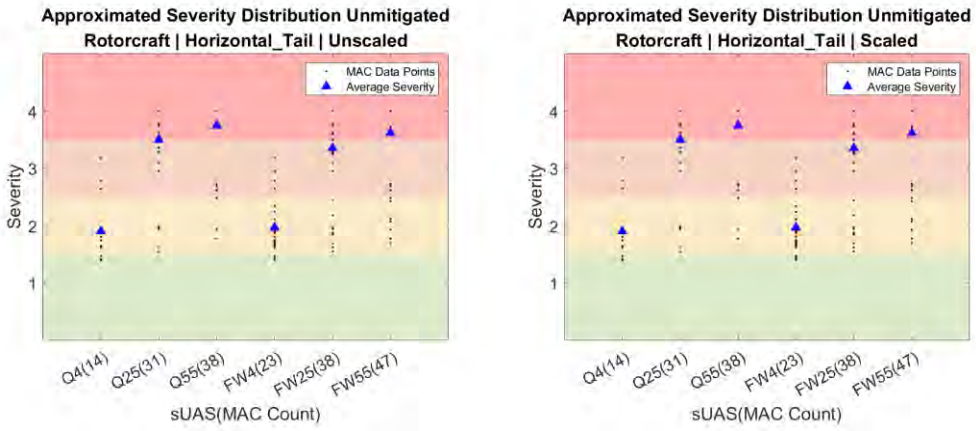

Figure 177. Approximated severity level distribution – Unmitigated rotorcraft & horizontal tail.

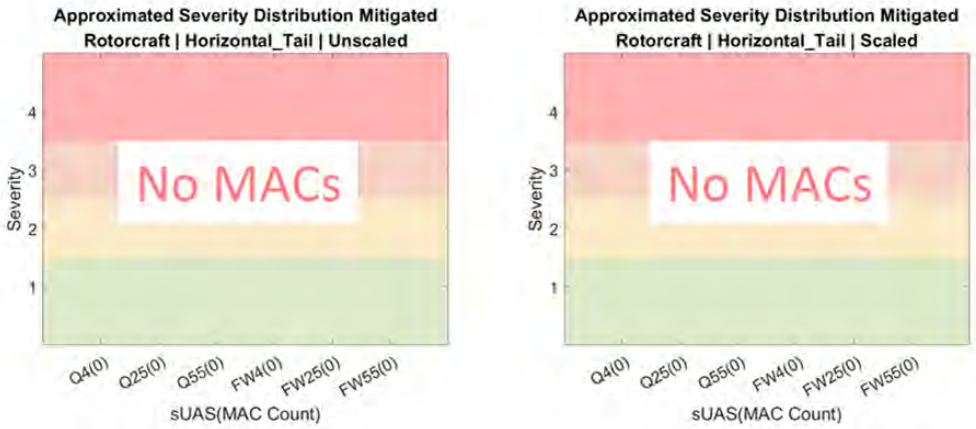

Figure 178. Approximated severity level distribution – Mitigated rotorcraft & horizontal tail.

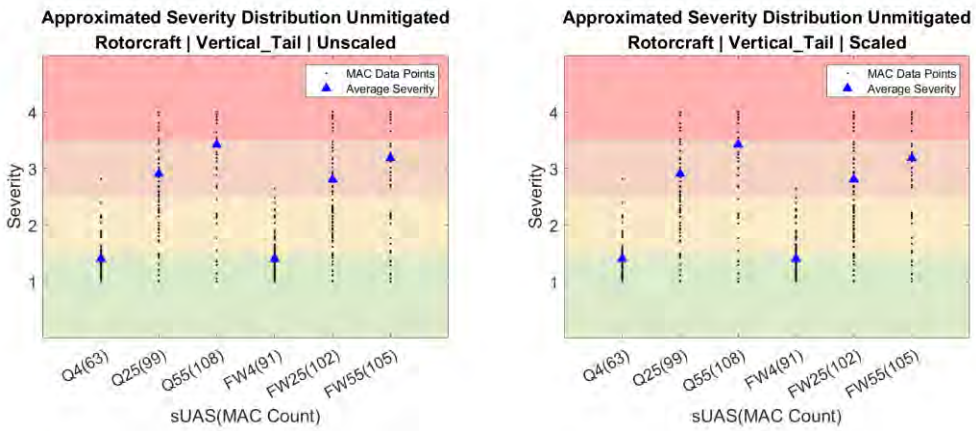

Figure 179. Approximated severity level distribution – Unmitigated rotorcraft & vertical tail.

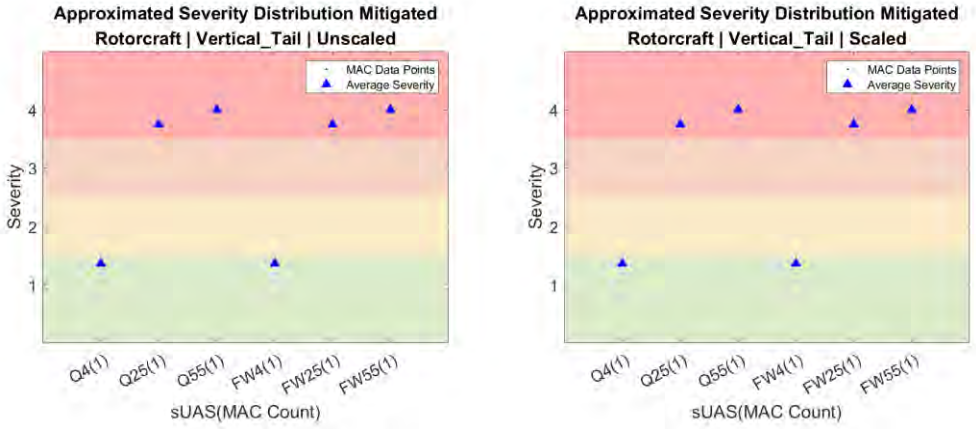

Figure 180. Approximated severity level distribution – Mitigated rotorcraft & vertical tail.

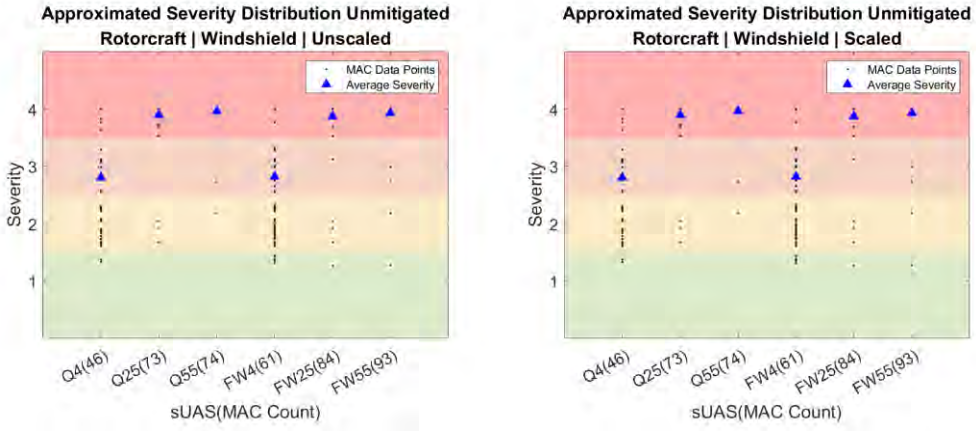

Figure 181. Approximated severity level distribution – Unmitigated rotorcraft & windshield.

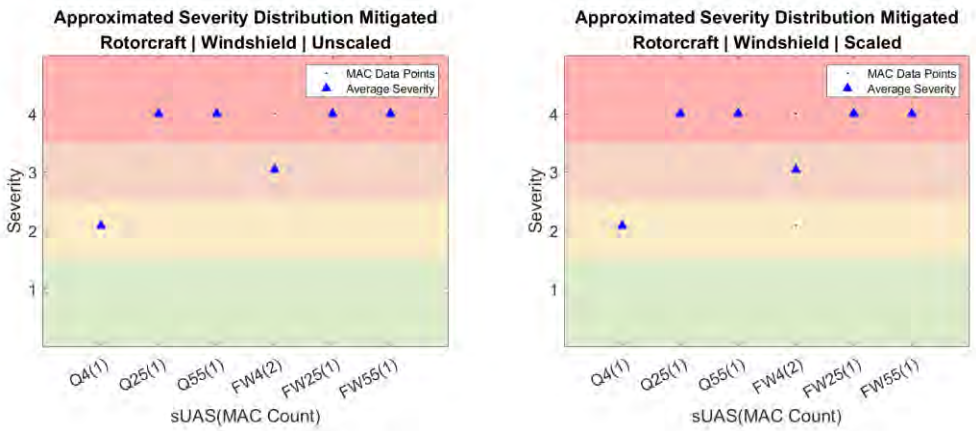

Figure 182. Approximated severity level distribution – Mitigated rotorcraft & windshield.

Appendix B Approximation Function vs. Impact Kinetic Energy for all Manned Aircraft Parts

B.1 Commercial Transport

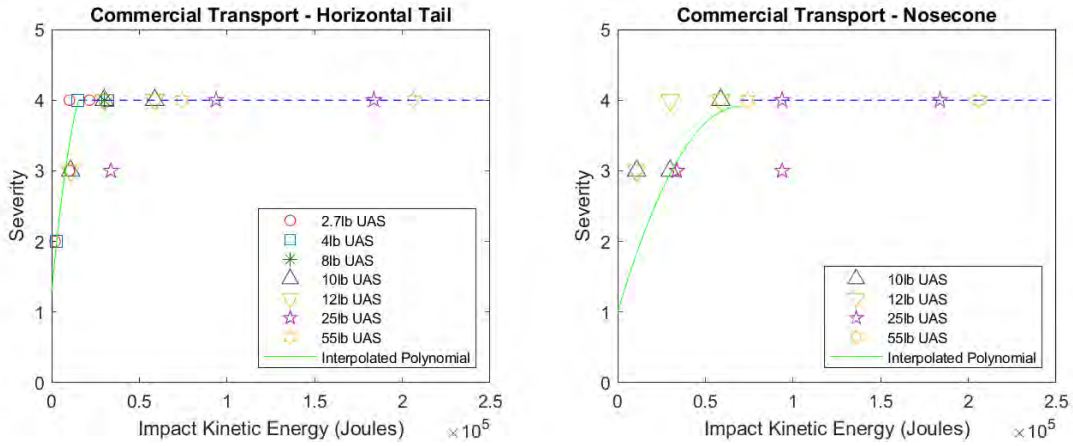

Figure 183. Commercial transport approximation function – Horizontal tail & nose cone.

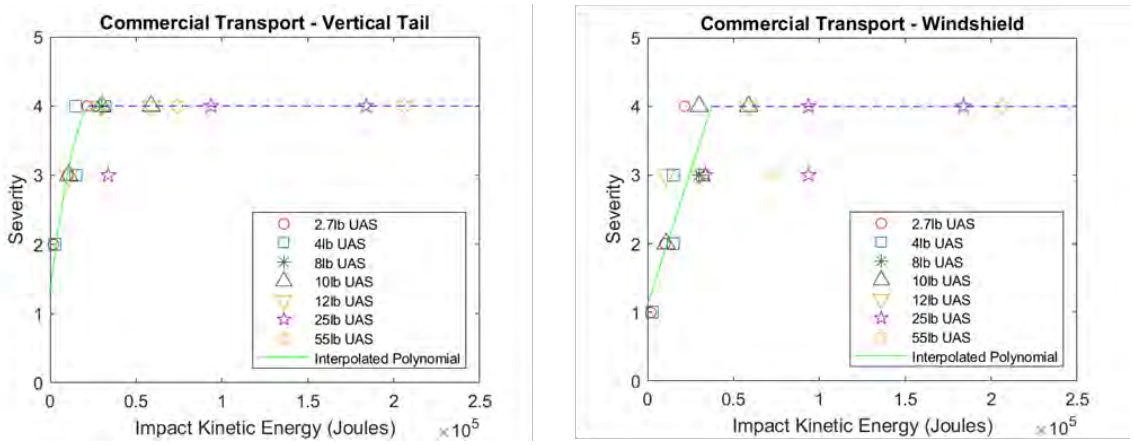

Figure 184. Commercial transport approximation function – Vertical tail & windshield.

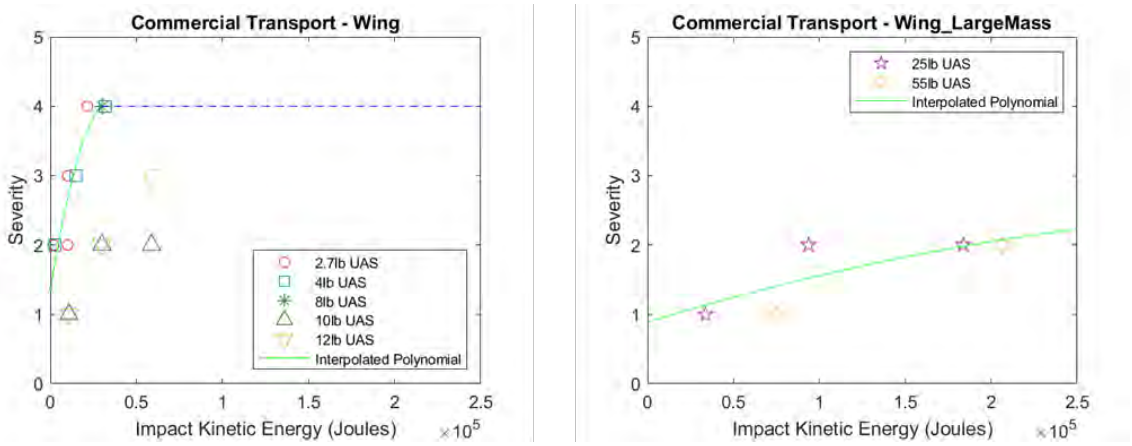

Figure 185. Commercial transport approximation function – Wing for small & large sUAS mass.

B.2 Business Jet

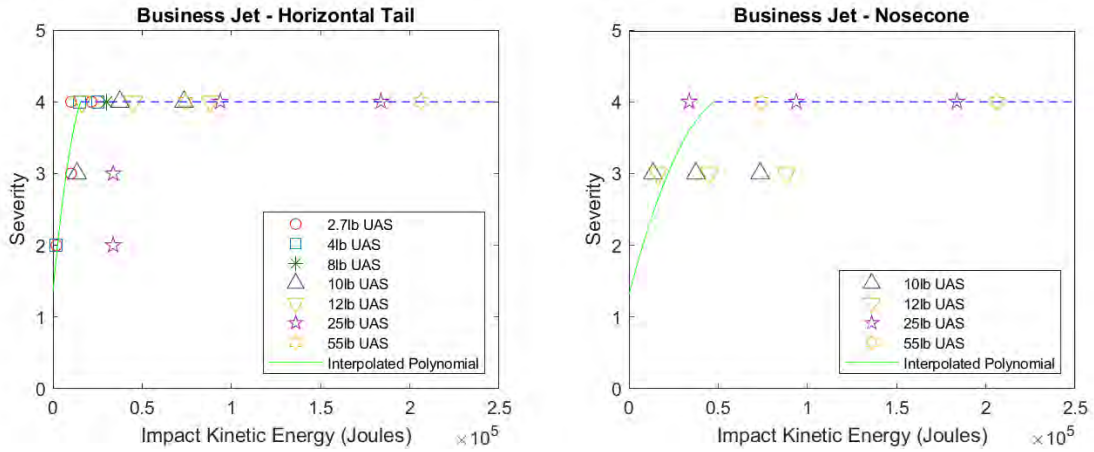

Figure 186. Business jet approximation function – Horizontal tail & nose cone.

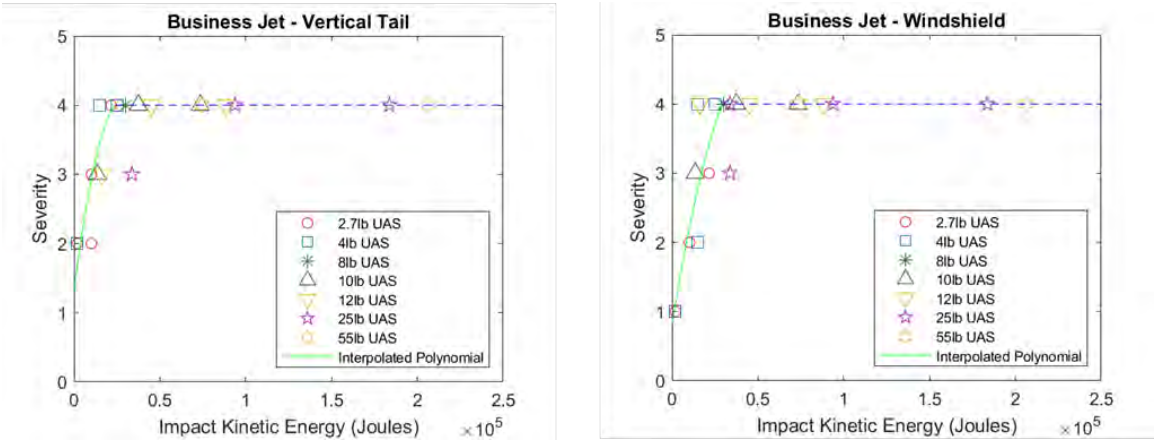

Figure 187. Business jet approximation function – Vertical tail & windshield.

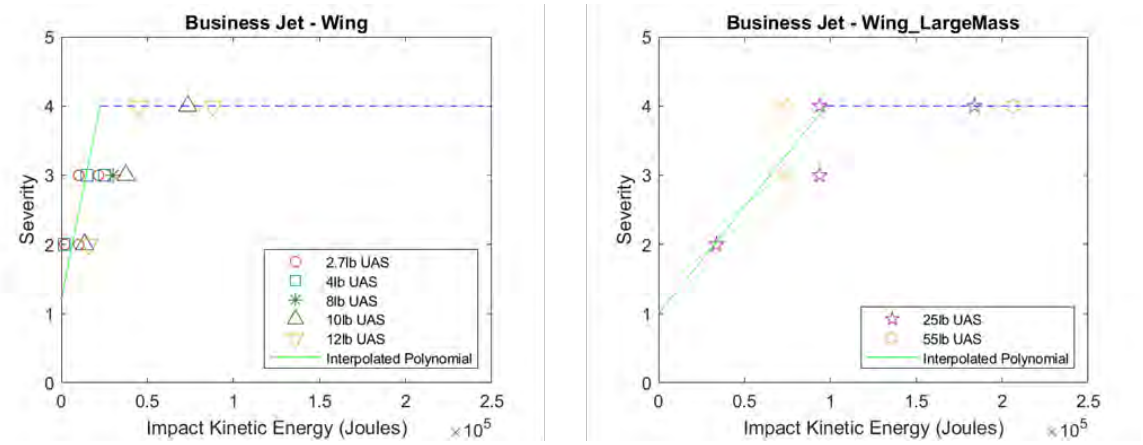

Figure 188. Business jet approximation function – Wing for small & large sUAS mass.

B.3 General Aviation (Single-Engine)

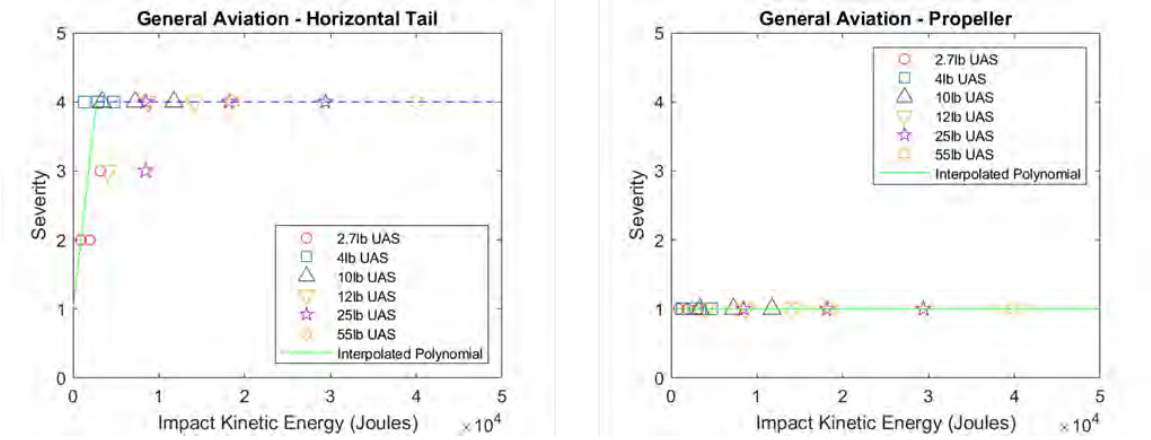

Figure 189. General aviation single-engine approximation function – Horizontal tail & propeller.

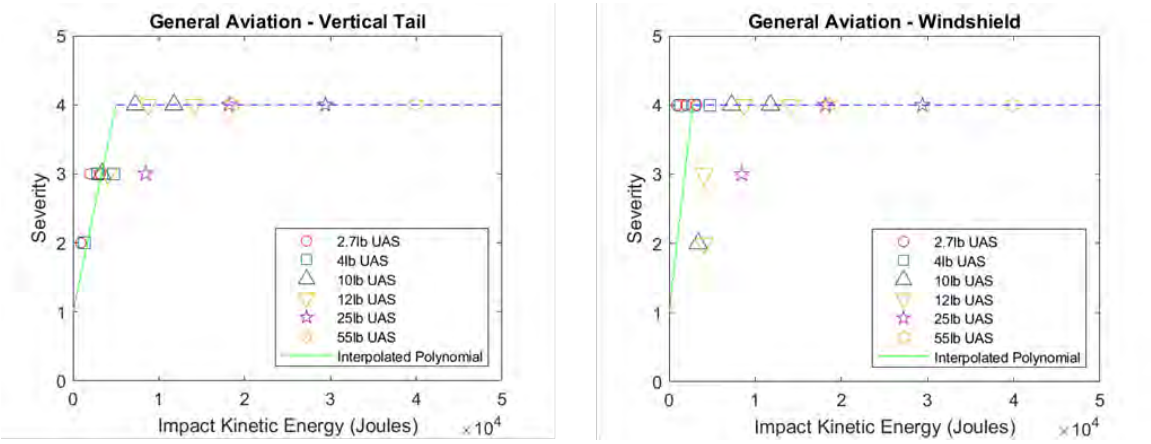

Figure 190. General aviation single-engine approximation function – Vertical tail & windshield.

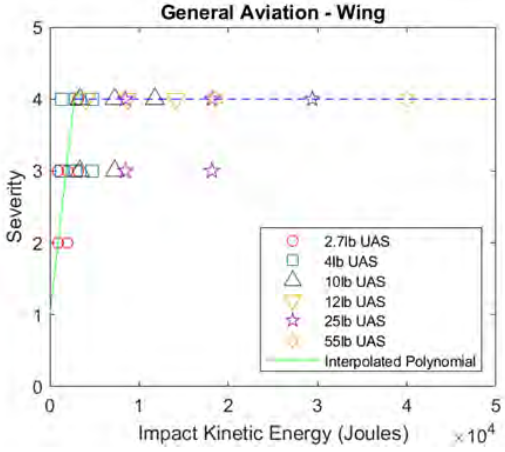

Figure 191. General aviation single-engine approximation function – Wing.

B.4 Rotorcraft

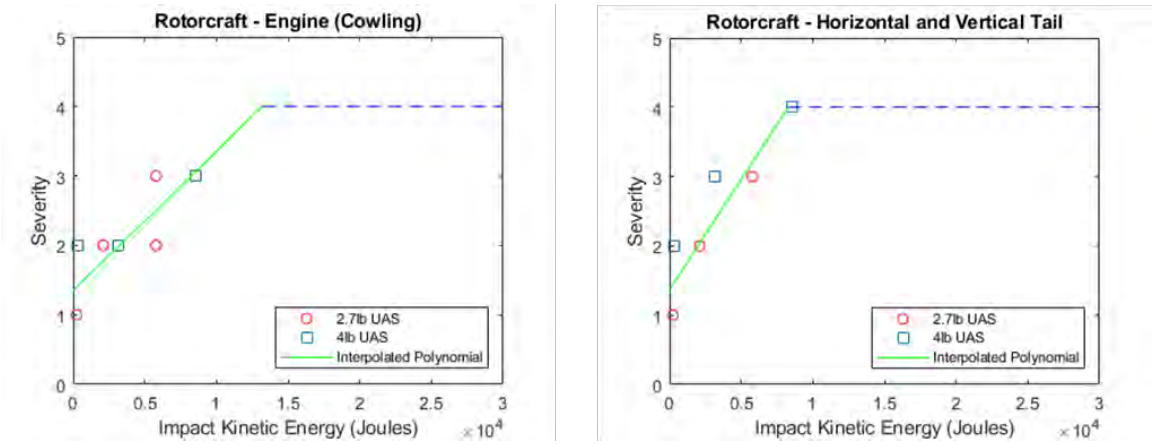

Figure 192. Rotorcraft approximation function –Engine (cowling) & horizontal tail.

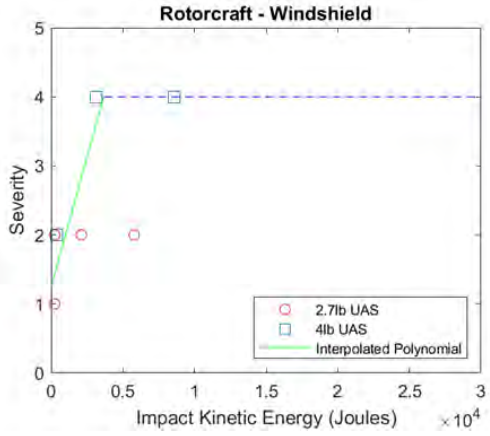

Figure 193. Rotorcraft approximation function – Windshield.

Appendix C FEA Setup and Results

This appendix presents the documentation of all FEA cases analyzed in Table 45 from Section 5.4. Detailed model descriptions and validations are documented in the reports from previous collision severity research (Olivares et al., 2020; 2022; 2021; 2017). No new FE models were developed for the analysis presented herein. The boundary conditions and position for each FEA were extracted from its corresponding encounter simulation. In the FEA, the aggregate velocity vector is applied to the sUAS as its initial condition, while the manned aircraft part is fixed in space. The velocity components are calculated according to Eq. (28) and Eq. (29). The vertical velocity, *Vz*, is negligible in most cases. For non-negligible cases, the vertical speed recorded from the encounter is used directly as *Vz*. The variables from the encounter simulation are shown in *(a)* of each figure and the equivalent FEA boundary conditions are shown in *(b)* of each figure. *(c)* of each figure highlights the damage observed in the manned aircraft.

$$Vx = speed_{Manned\ Aircraft} - speed_{sUAS} * \cos(heading_{Relative\ sUAS-manned}) \quad (28)$$

$$Vy = -speed_{sUAS} * \sin(heading_{Relative\ sUAS-manned}) \quad (29)$$

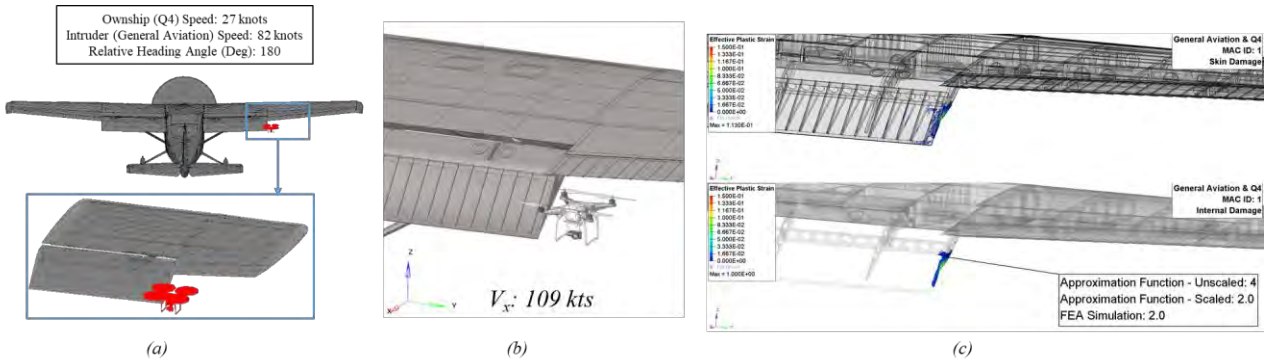

Figure 194. MAC id:1 (a) Encounter Simulation (b) FEA Setup (c) FEA severity assessment.

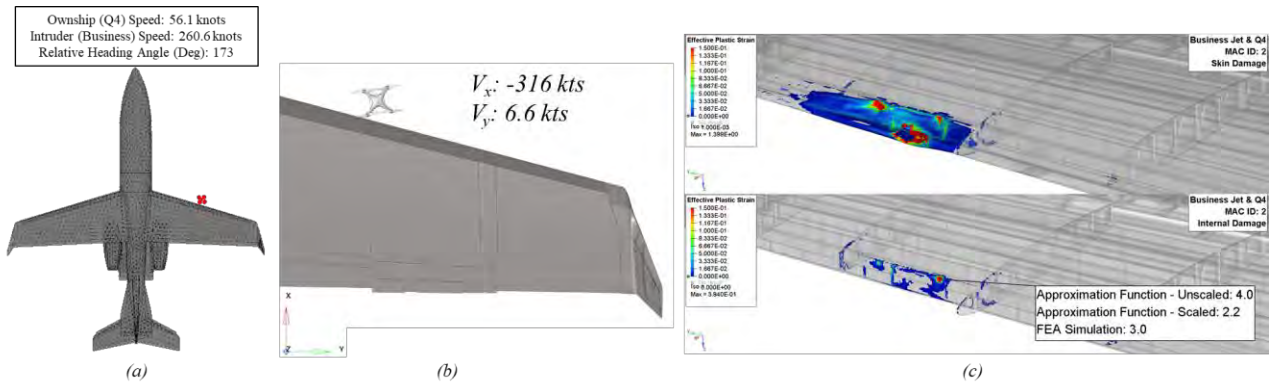

Figure 195. MAC id:2 (a) Encounter Simulation (b) FEA Setup (c) FEA severity assessment.

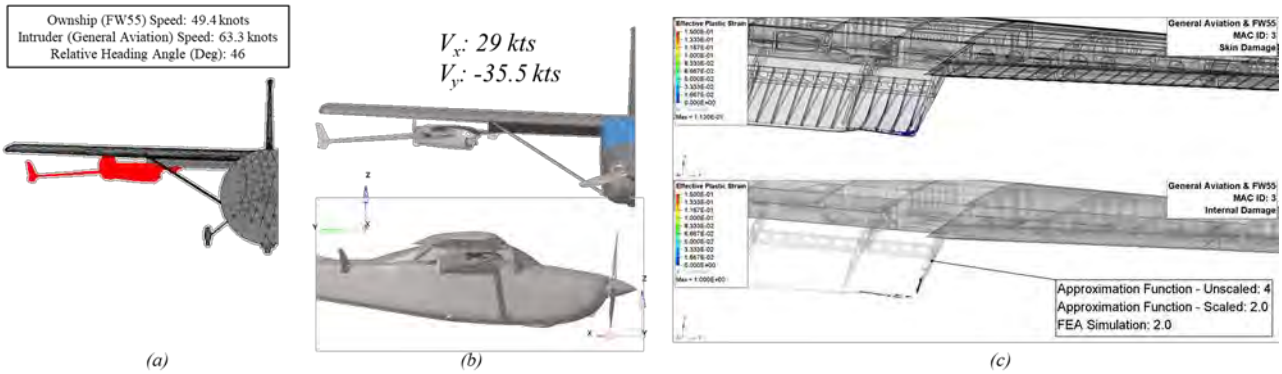

Figure 196. MAC id:3 (a) Encounter Simulation (b) FEA Setup (c) FEA severity assessment.

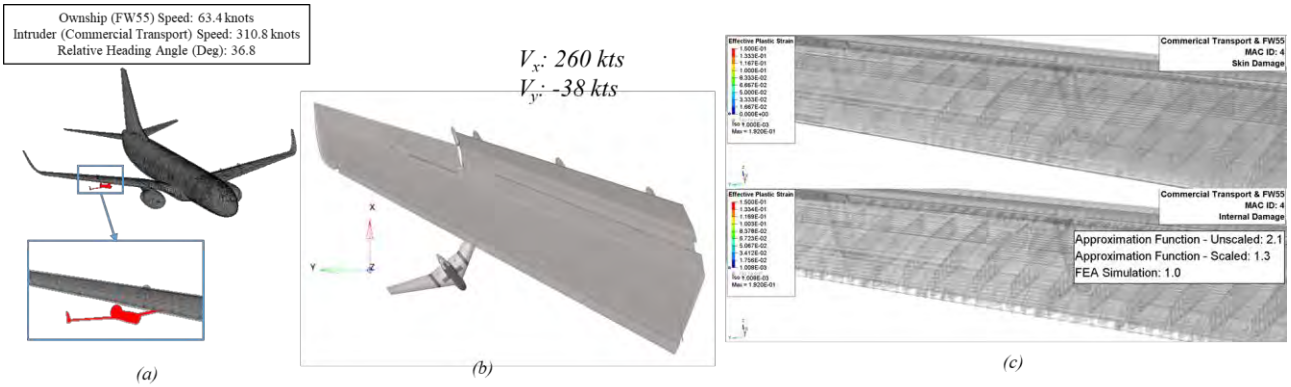

Figure 197. MAC id:4 (a) Encounter Simulation (b) FEA Setup (c) FEA severity assessment.

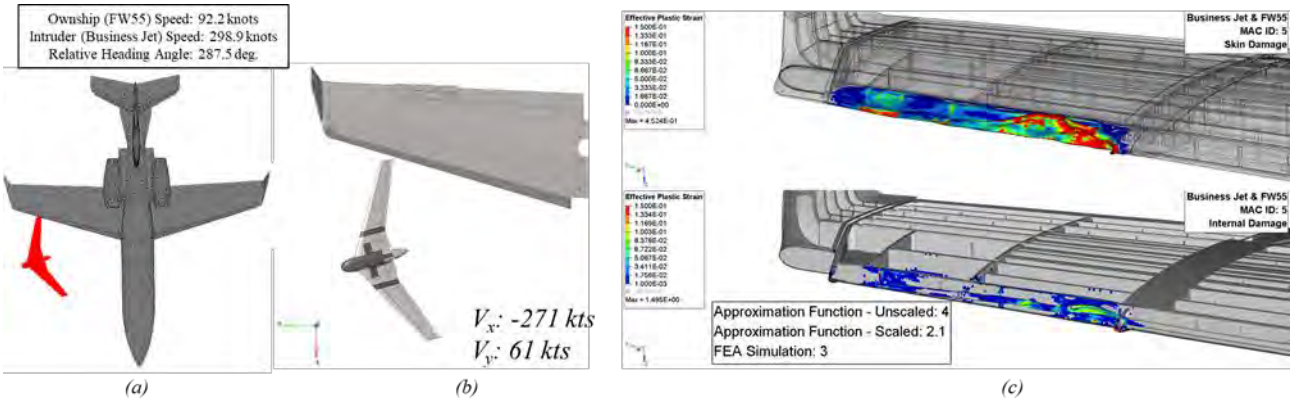

Figure 198. MAC id:5 (a) Encounter Simulation (b) FEA Setup (c) FEA severity assessment.

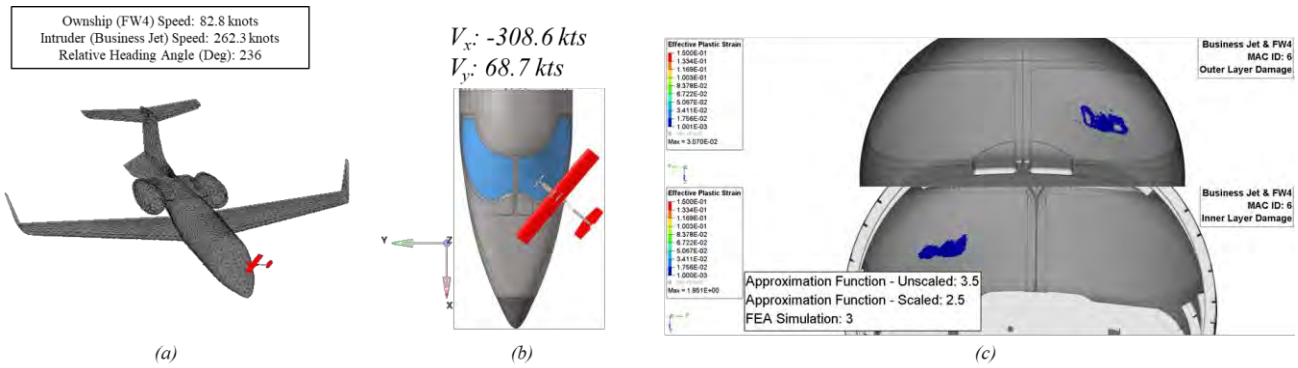

Figure 199. MAC id:6 (a) Encounter Simulation (b) FEA Setup (c) FEA severity assessment.

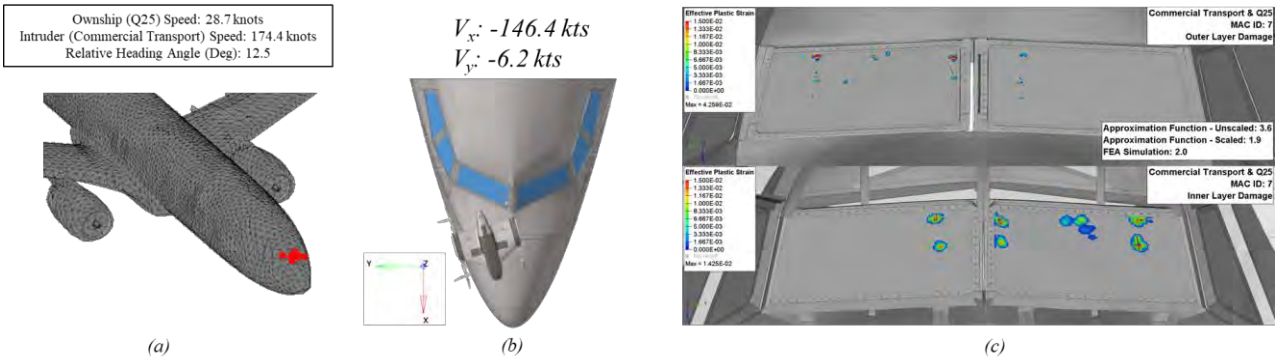

Figure 200. MAC id:7 (a) Encounter Simulation (b) FEA Setup (c) FEA severity assessment.

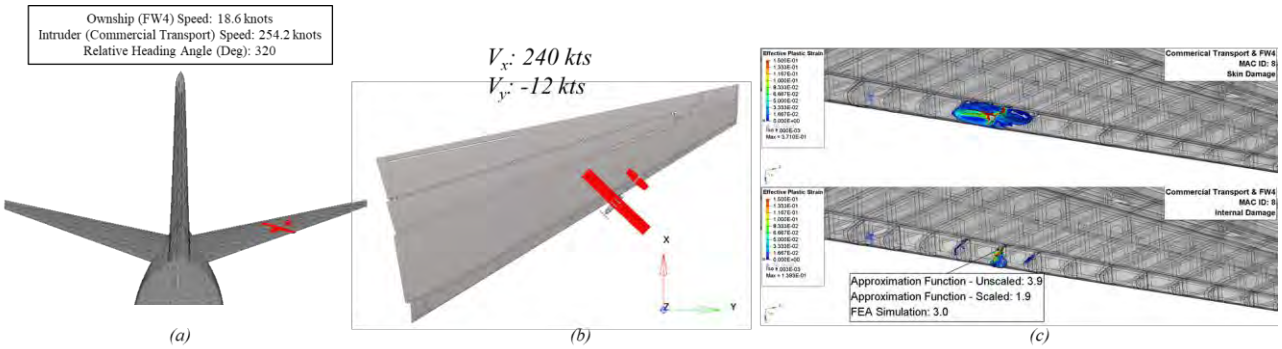

Figure 201. MAC id:8 (a) Encounter Simulation (b) FEA Setup (c) FEA severity assessment.

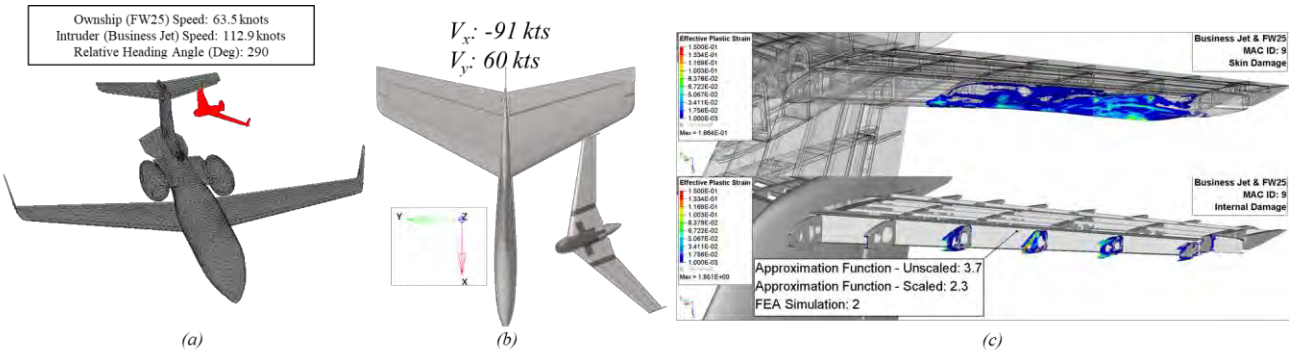

Figure 202. MAC id:9 (a) Encounter Simulation (b) FEA Setup (c) FEA severity assessment.

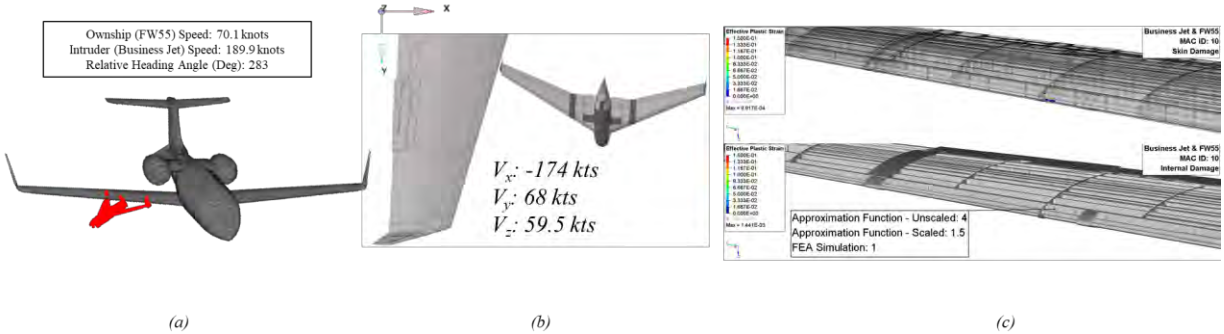

Figure 203. MAC id:10 (a) Encounter Simulation (b) FEA Setup (c) FEA severity assessment.

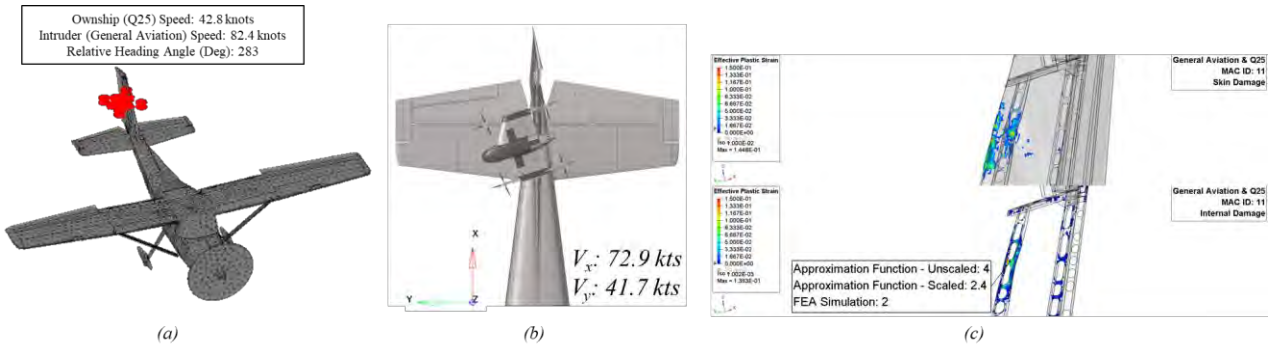

Figure 204. MAC id:11 (a) Encounter Simulation (b) FEA Setup (c) FEA severity assessment.

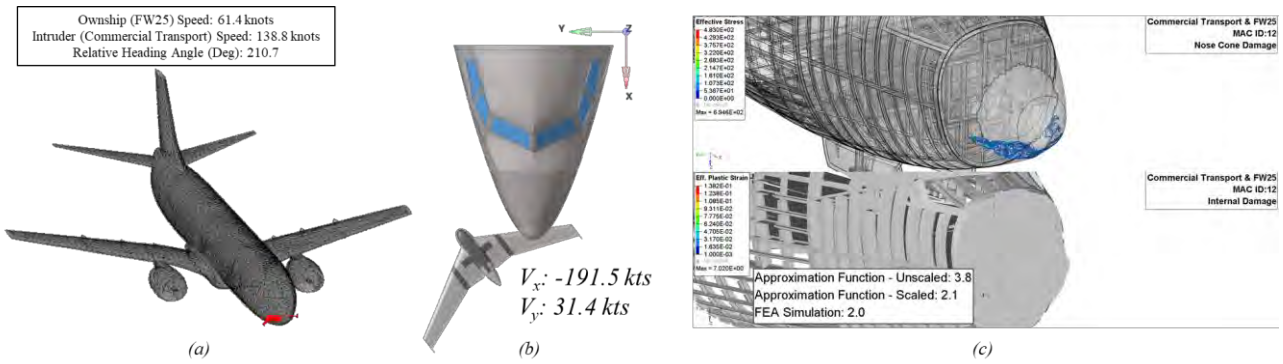

Figure 205. MAC id:12 (a) Encounter Simulation (b) FEA Setup (c) FEA severity assessment.

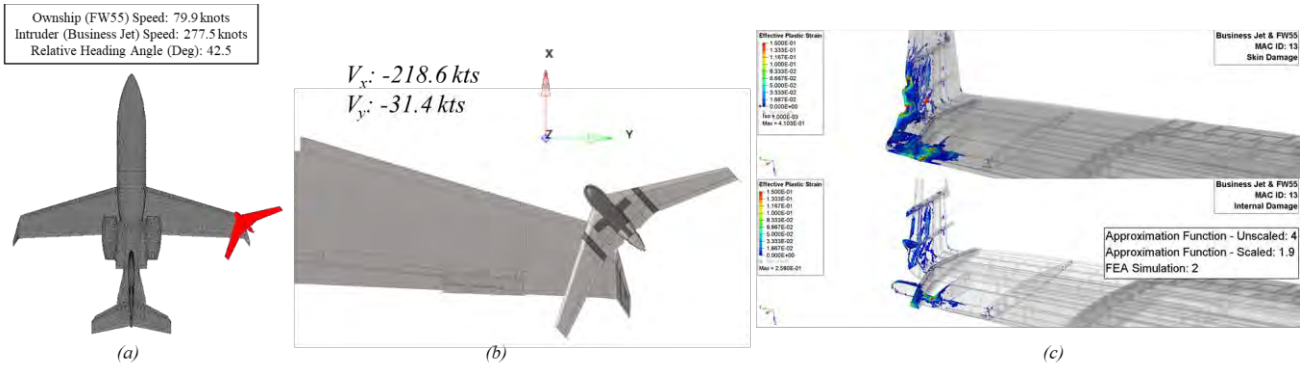

Figure 206. MAC id:13 (a) Encounter Simulation (b) FEA Setup (c) FEA severity assessment.

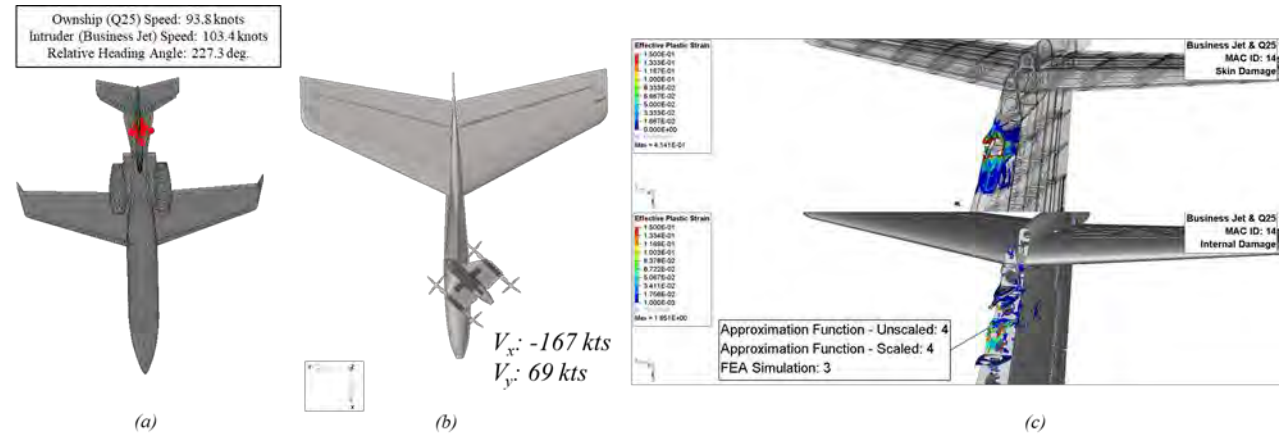

Figure 207. MAC id:14 (a) Encounter Simulation (b) FEA Setup (c) FEA severity assessment.

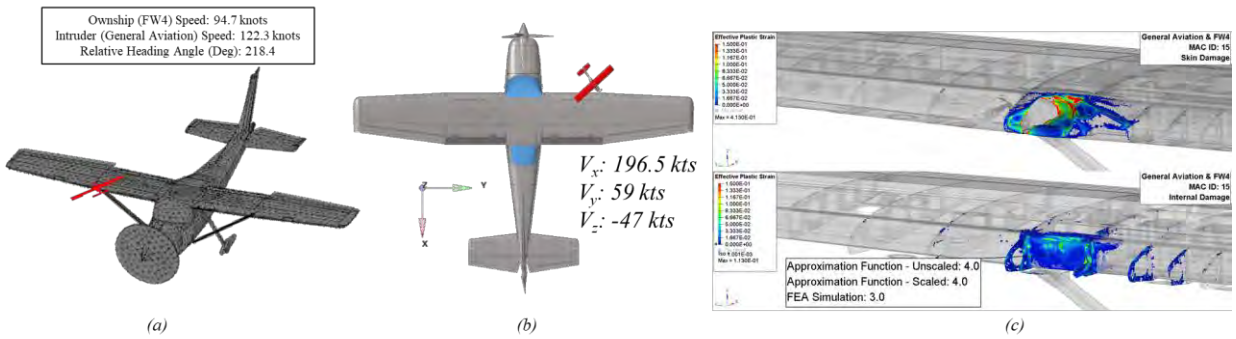

Figure 208. MAC id:15 (a) Encounter Simulation (b) FEA Setup (c) FEA severity assessment.

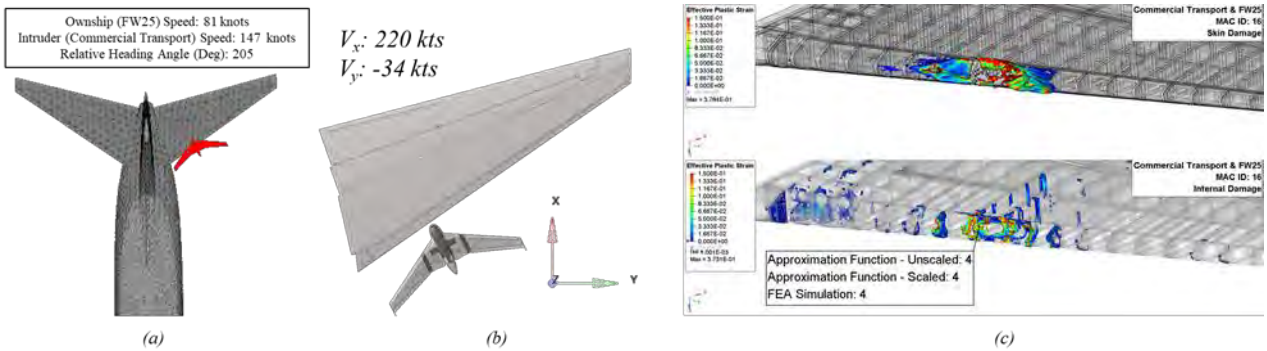

Figure 209. MAC id:16 (a) Encounter Simulation (b) FEA Setup (c) FEA severity assessment.

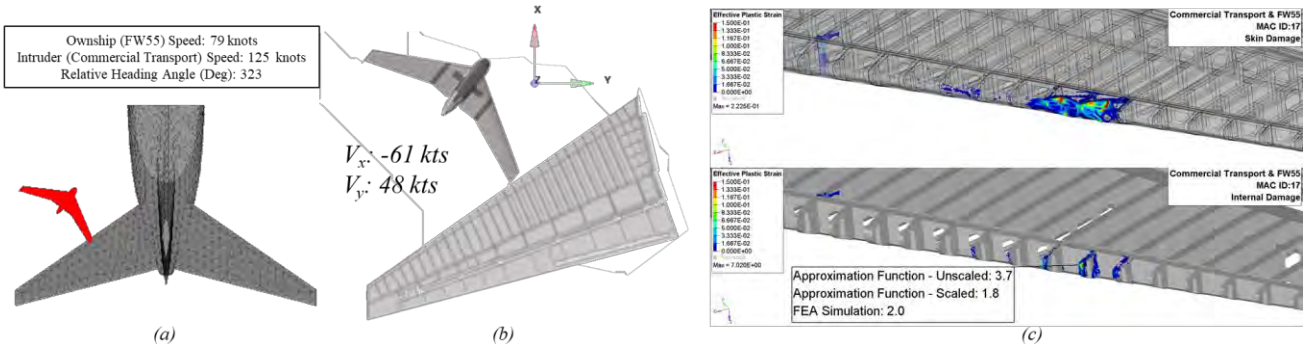

Figure 210. MAC id:17 (a) Encounter Simulation (b) FEA Setup (c) FEA severity assessment.

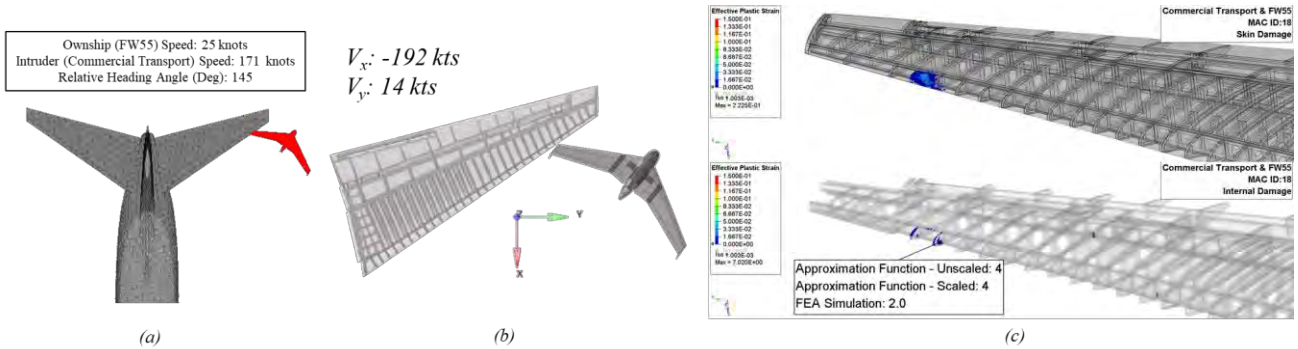

Figure 211. MAC id:18 (a) Encounter Simulation (b) FEA Setup (c) FEA severity assessment.

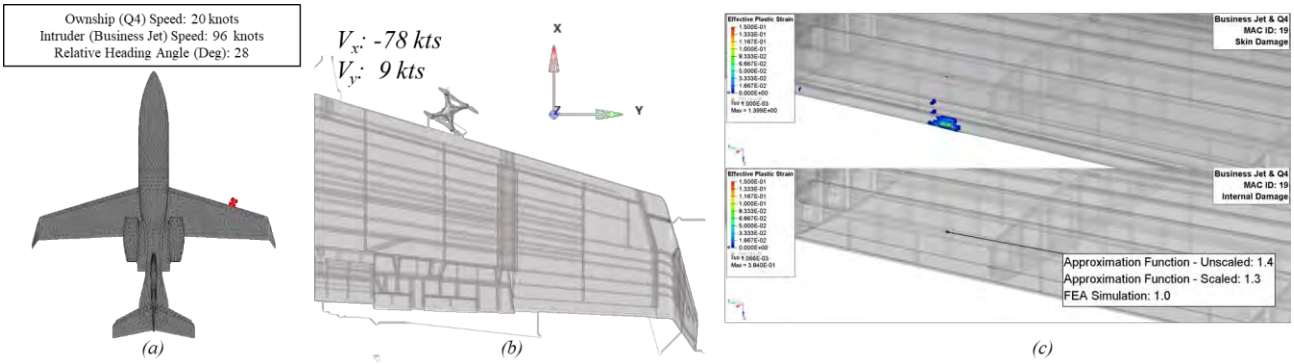

Figure 212. MAC id:19 (a) Encounter Simulation (b) FEA Setup (c) FEA severity assessment.

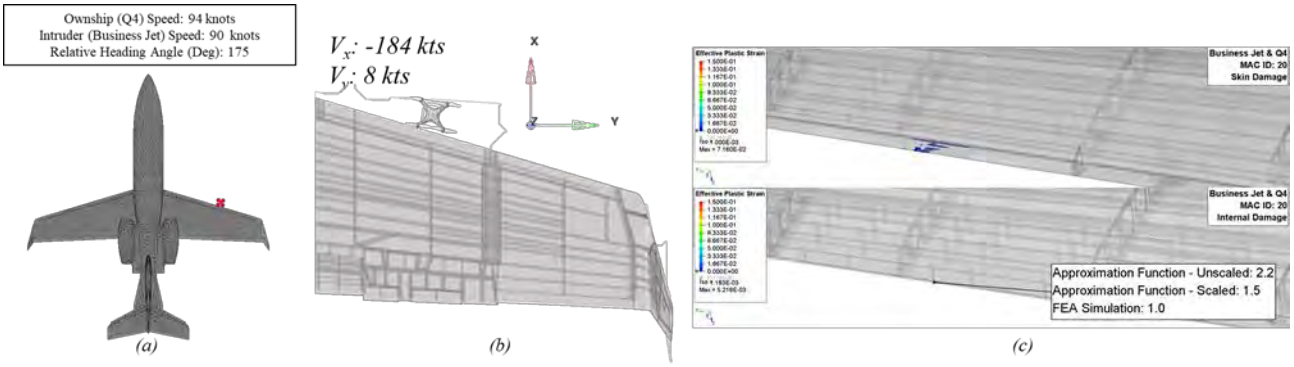

Figure 213. MAC id:20 (a) Encounter Simulation (b) FEA Setup (c) FEA severity assessment.

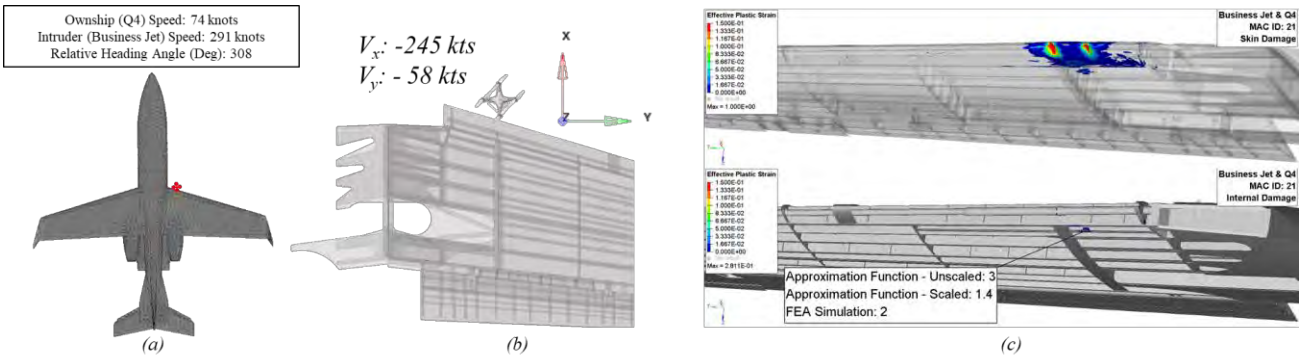

Figure 214. MAC id:21 (a) Encounter Simulation (b) FEA Setup (c) FEA severity assessment.

Appendix D Relative Heading Distribution of all Manned Aircraft & sUAS for unmitigated and mitigated MACs

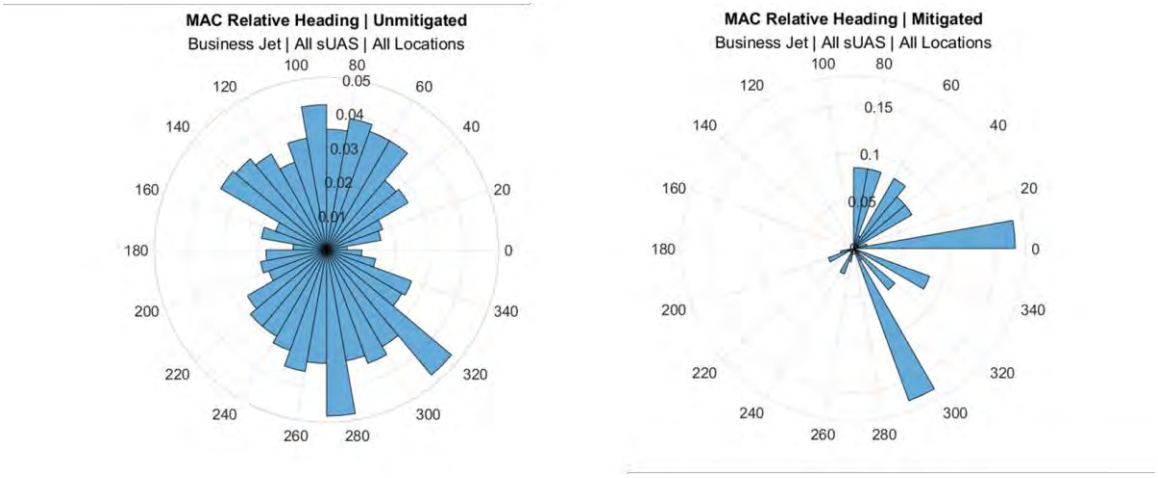

Figure 215. MAC relative heading distribution – Business jet & all sUAS.

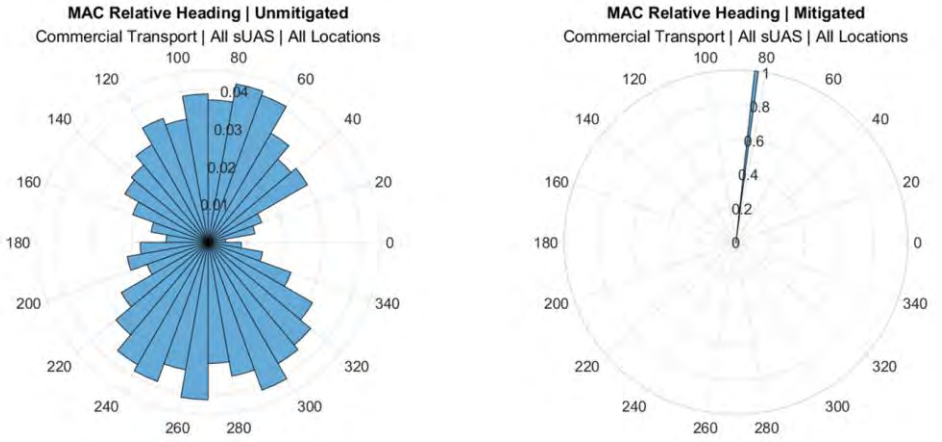

Figure 216. MAC relative heading distribution – Commercial transport & all sUAS.

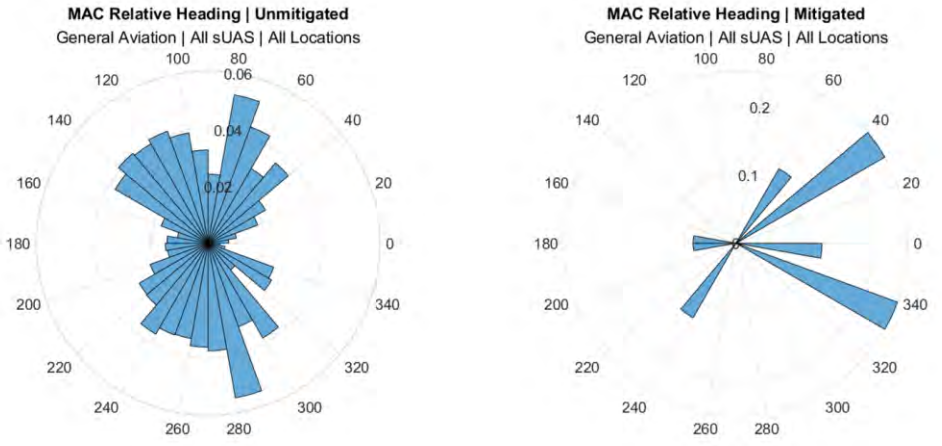

Figure 217. MAC relative heading distribution – General aviation & all sUAS.

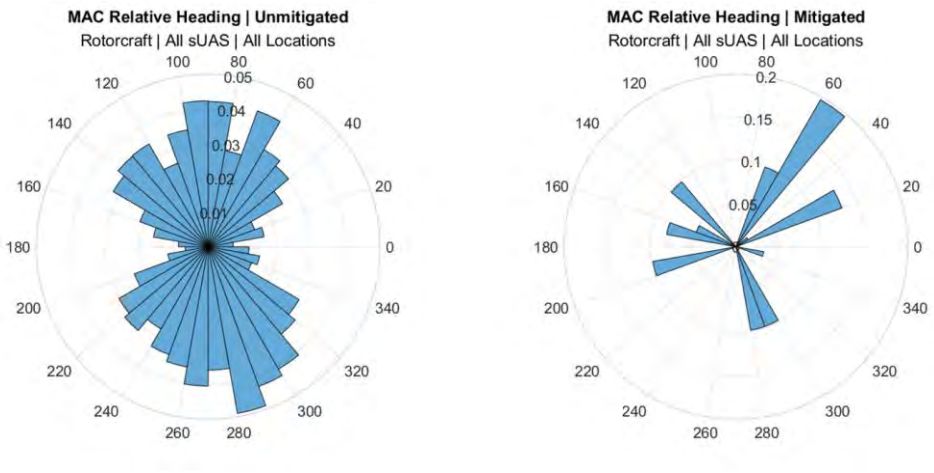

Figure 218. MAC relative heading distribution – Rotorcraft & all sUAS.

Appendix E Relative Heading at MAC

This appendix highlights the top views of each manned aircraft-sUAS pair relative heading at the moment the MAC was detected. The relative heading is represented as an arrow at the center of gravity of the sUAS. Interactive plots for each pair are also documented in an annex report, shown below:

ASSURE_A47_FinalReport_Annex_I.pdf

E.1 Commercial Transport

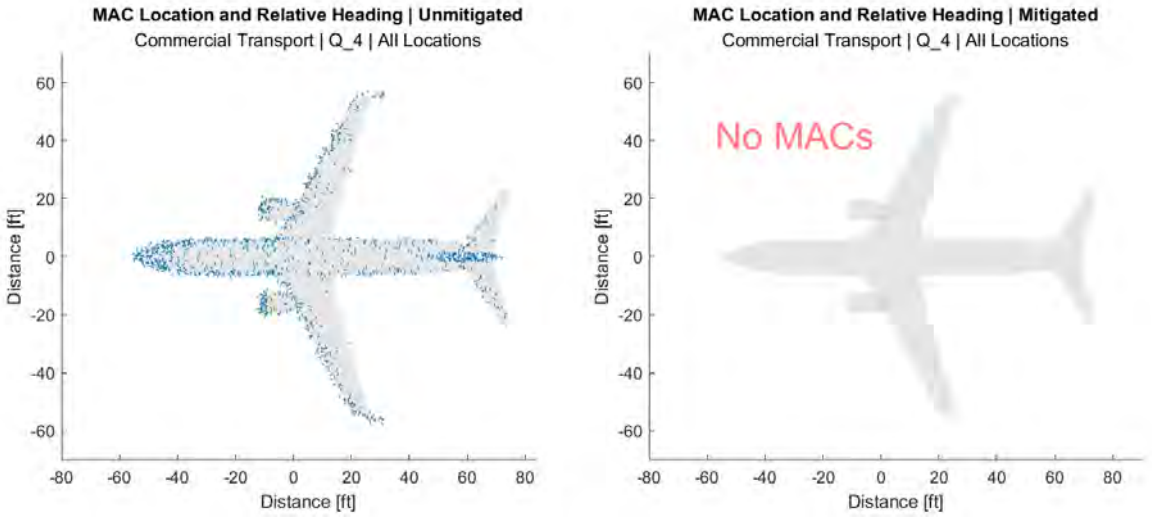

Figure 219. MAC location and relative heading – Unmitigated (left) and mitigated (right) commercial transport-Q4 pair.

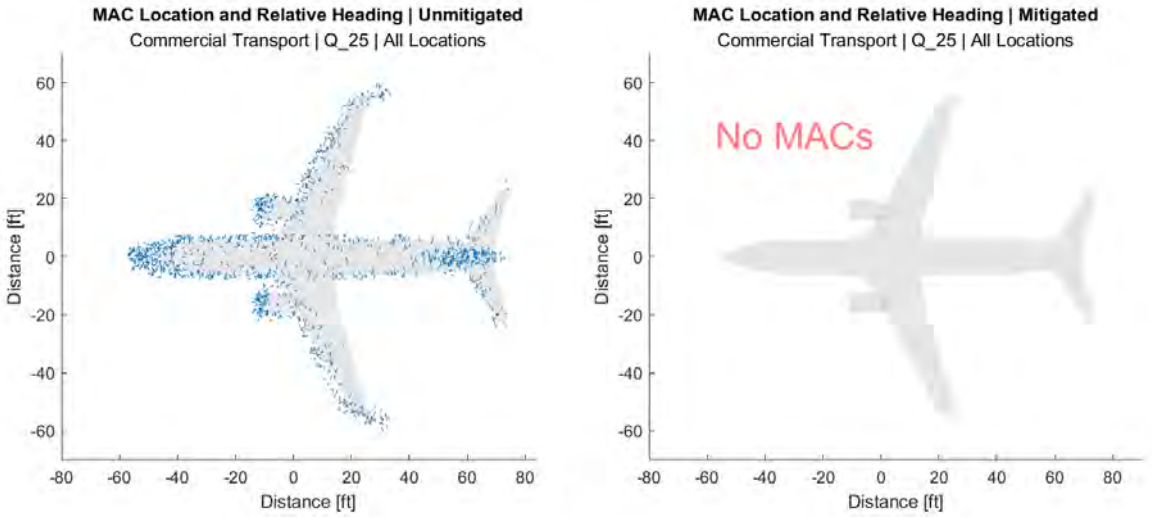

Figure 220. MAC location and relative heading – Unmitigated (left) and mitigated (right) commercial transport-Q25 pair.

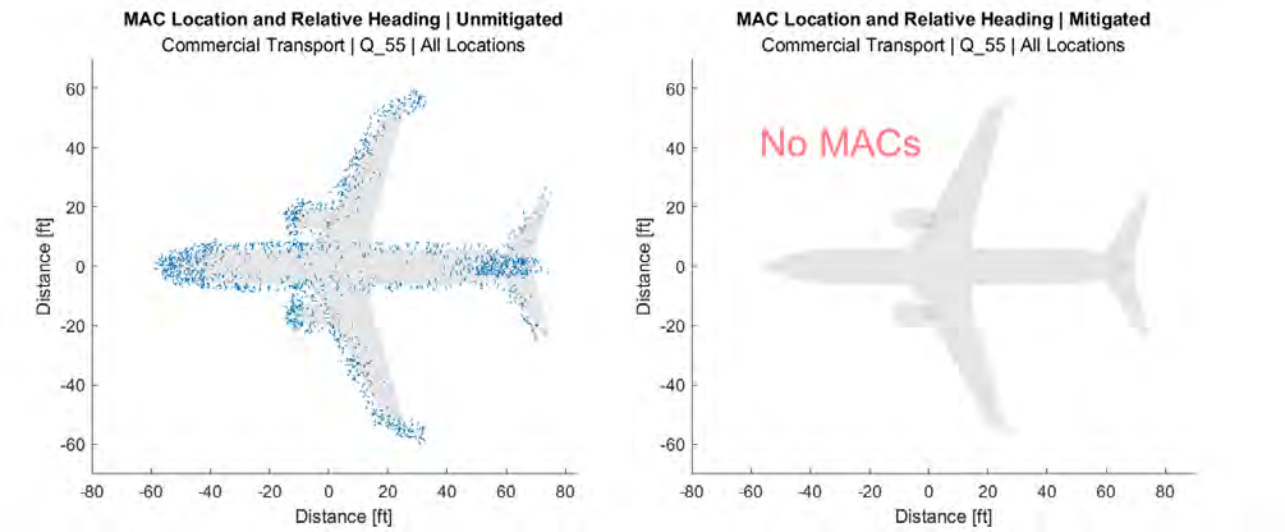

Figure 221. MAC location and relative heading – Unmitigated (left) and mitigated (right) commercial transport-Q55 pair.

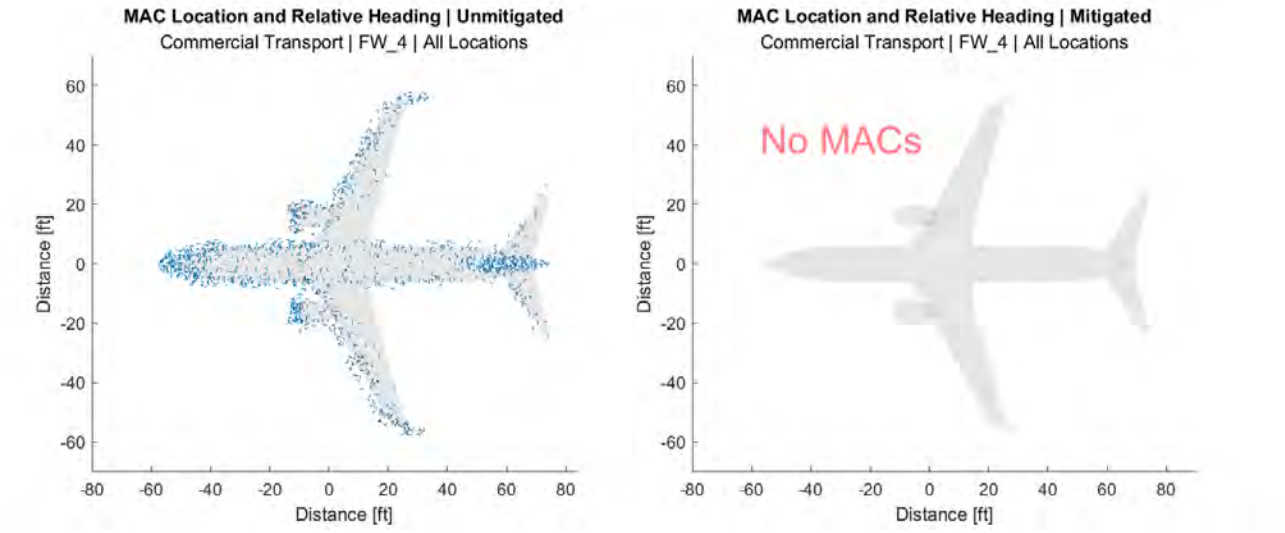

Figure 222. MAC location and relative heading – Unmitigated (left) and mitigated (right) commercial transport-FW4 pair.

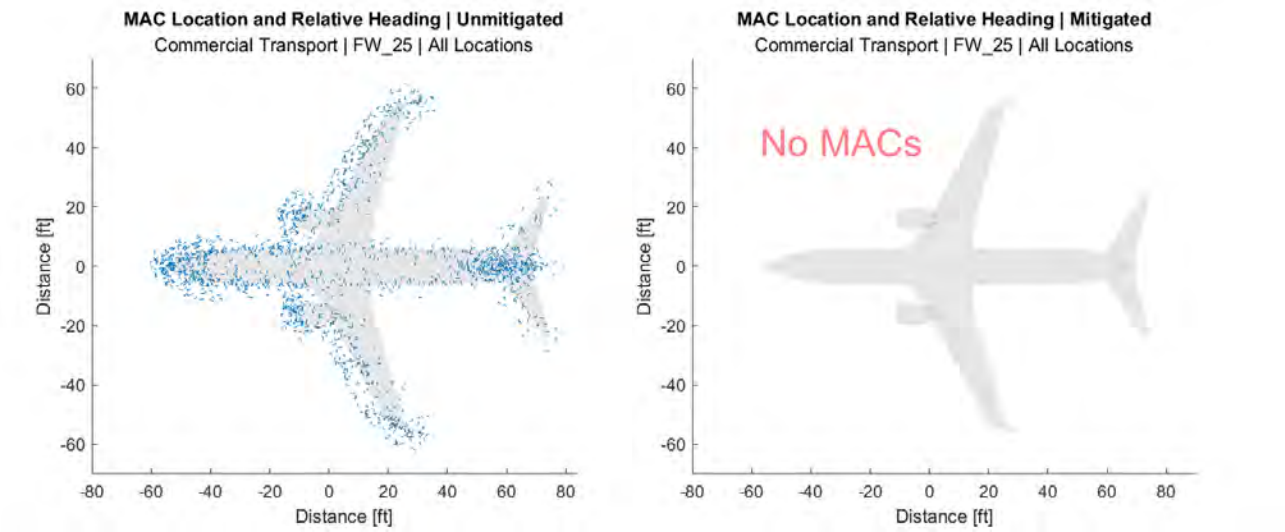

Figure 223. MAC location and relative heading – Unmitigated (left) and mitigated (right) commercial transport-FW25 pair.

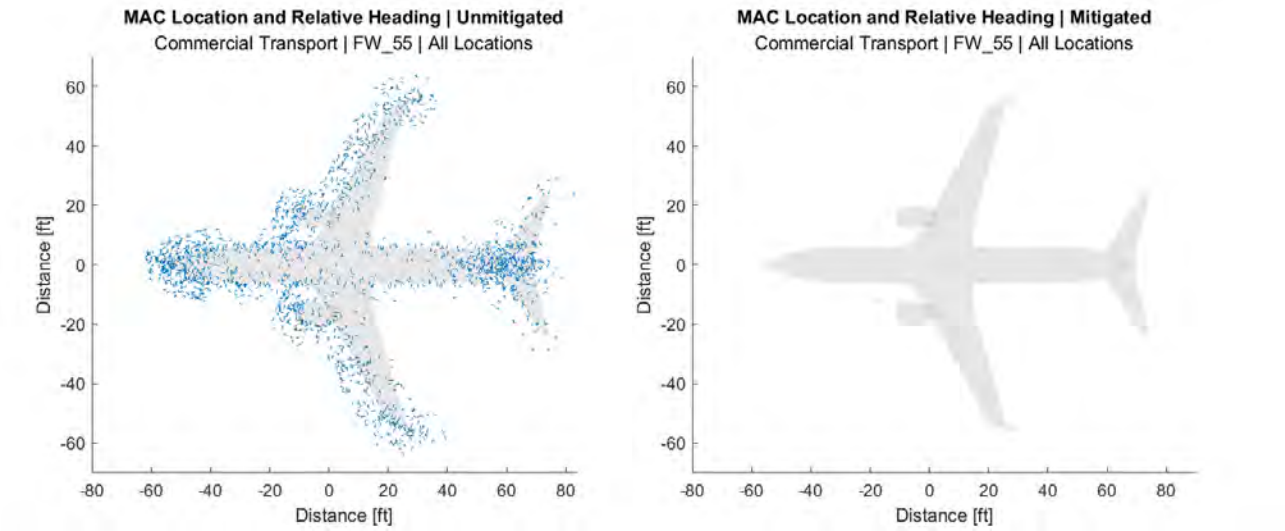

Figure 224. MAC location and relative heading – Unmitigated (left) and mitigated (right) commercial transport-FW55 pair.

E.2 Business Jet

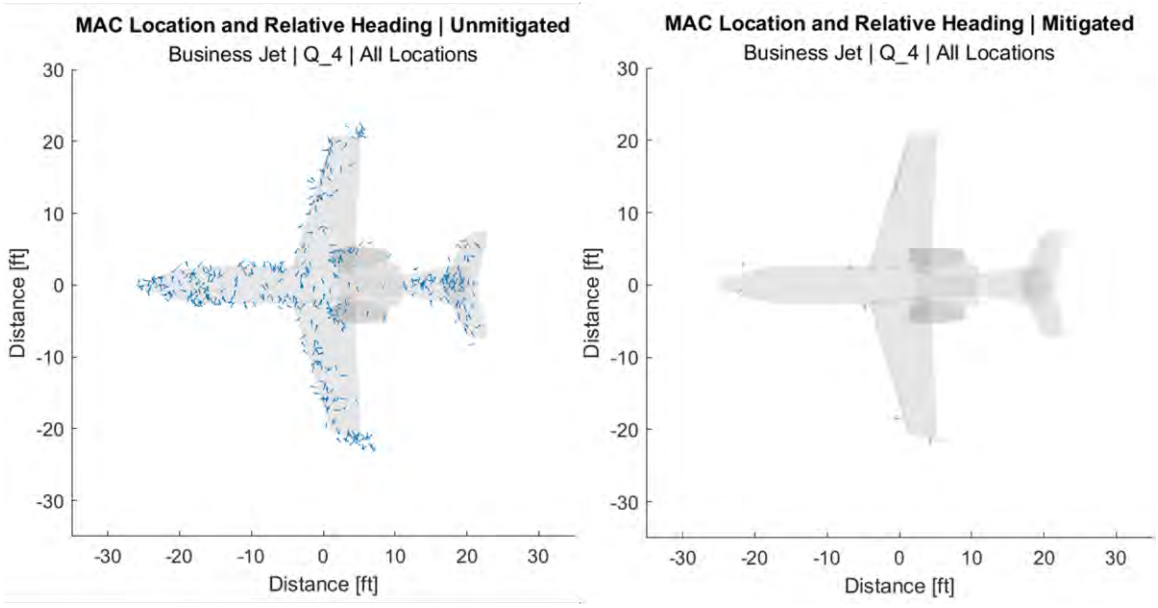

Figure 225. MAC location and relative heading – Unmitigated (left) and mitigated (right) business jet-Q4 pair.

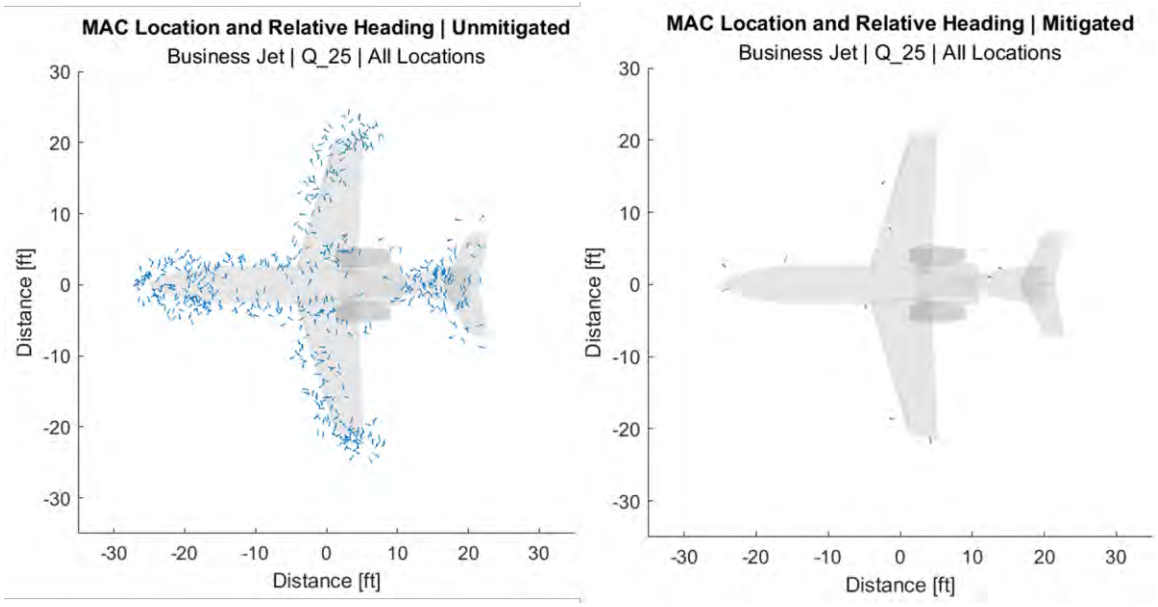

Figure 226. MAC location and relative heading – Unmitigated (left) and mitigated (right) business jet-Q25 pair.

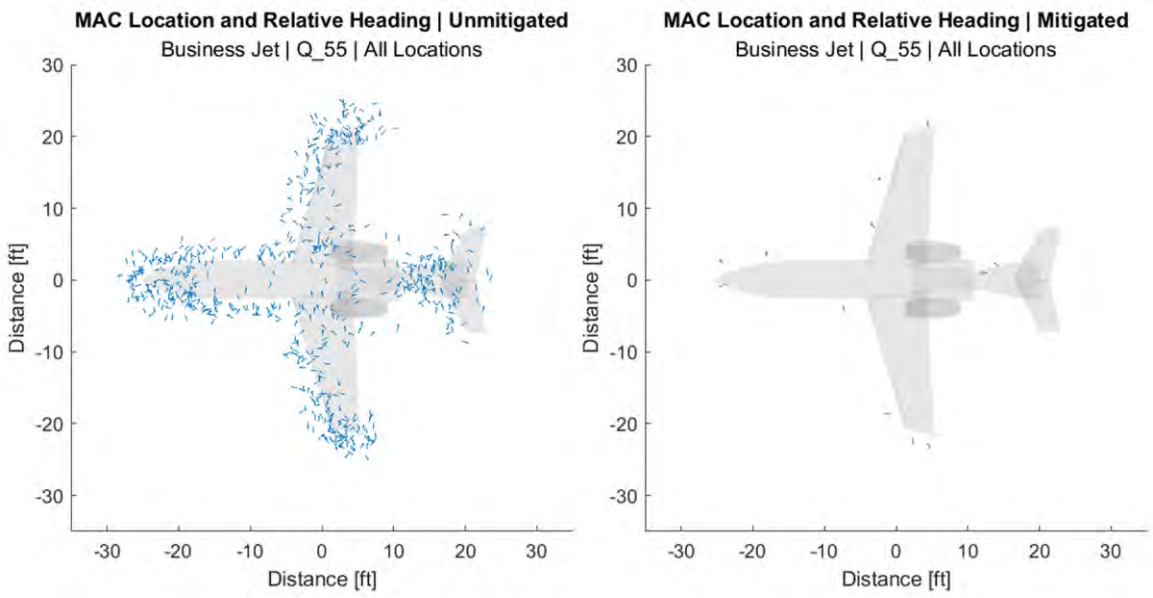

Figure 227. MAC location and relative heading – Unmitigated (left) and mitigated (right) business jet-Q55 pair.

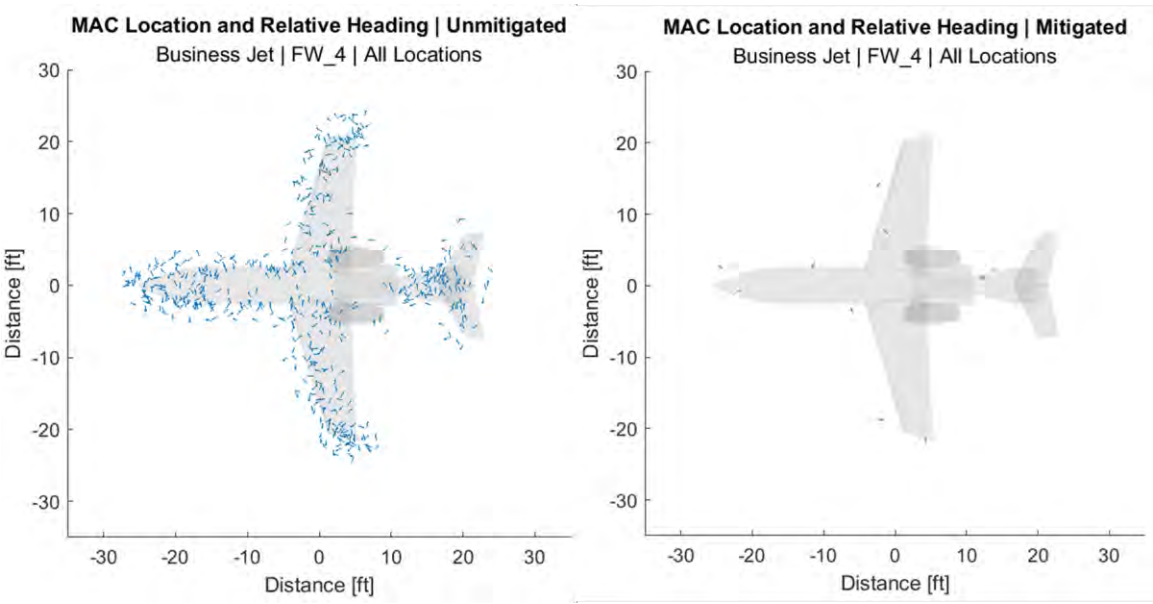

Figure 228. MAC location and relative heading – Unmitigated (left) and mitigated (right) business jet-FW4 pair.

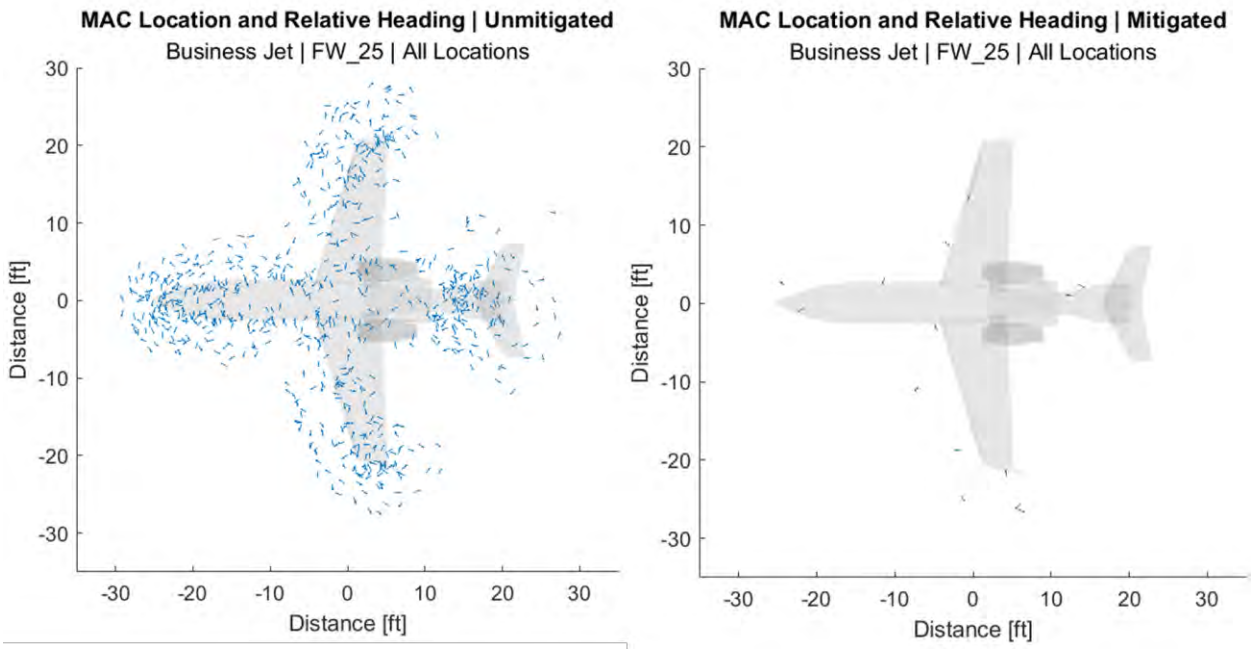

Figure 229. MAC location and relative heading – Unmitigated (left) and mitigated (right) business jet-FW25 pair.

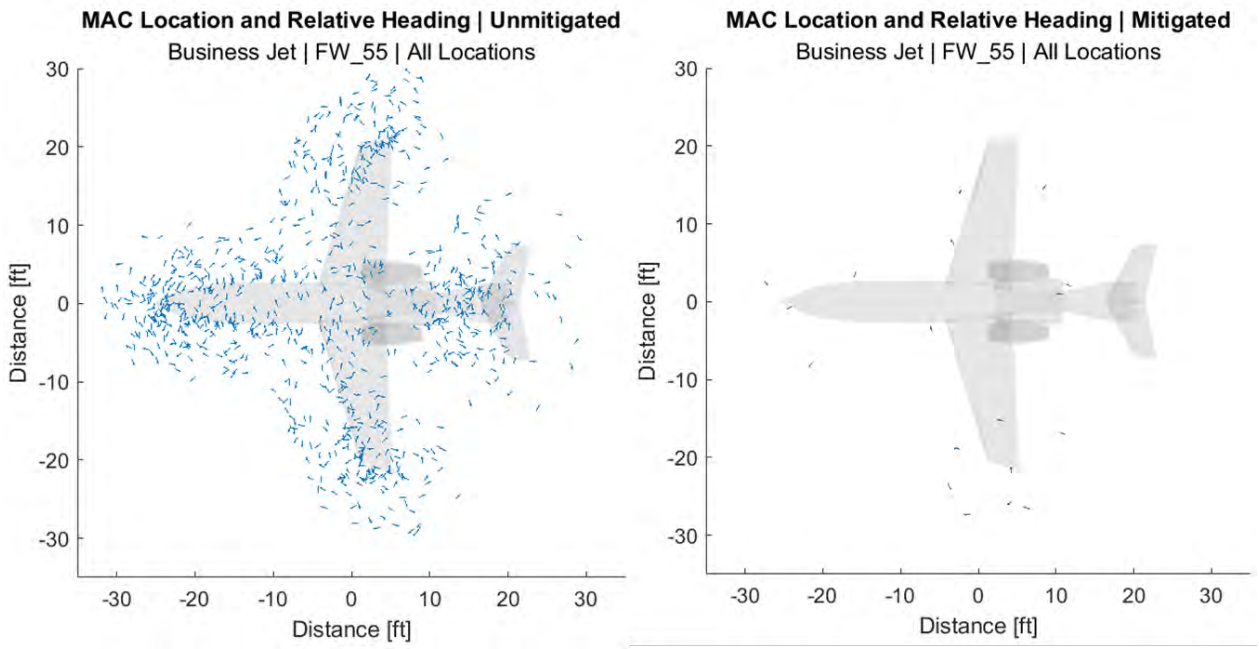

Figure 230. MAC location and relative heading – Unmitigated (left) and mitigated (right) business jet-FW55 pair.

E.3 General Aviation (Single-Engine)

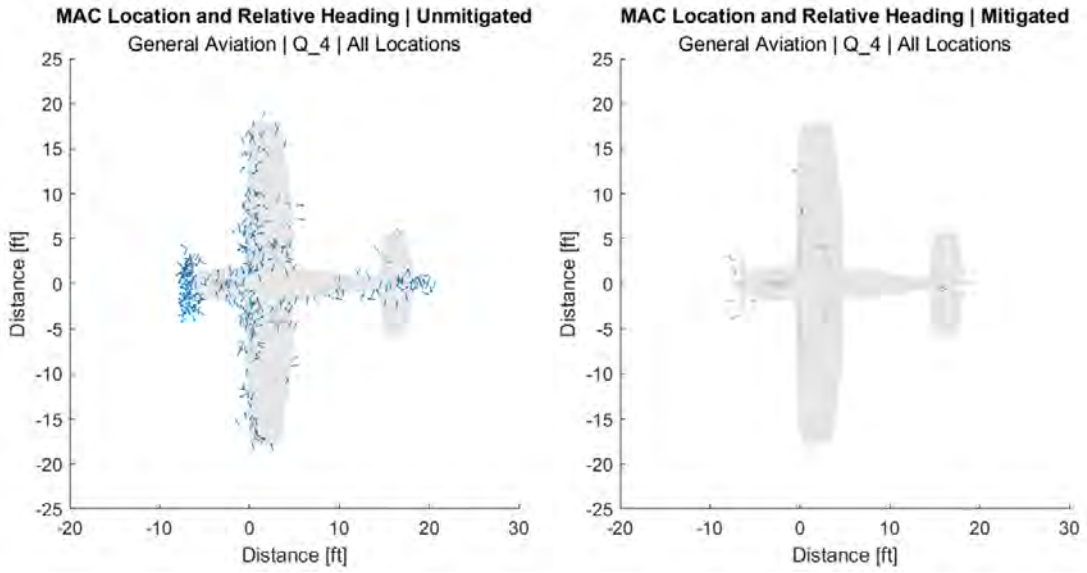

Figure 231. MAC location and relative heading – Unmitigated (left) and mitigated (right) Single-Engine General Aviation-Q4 pair.

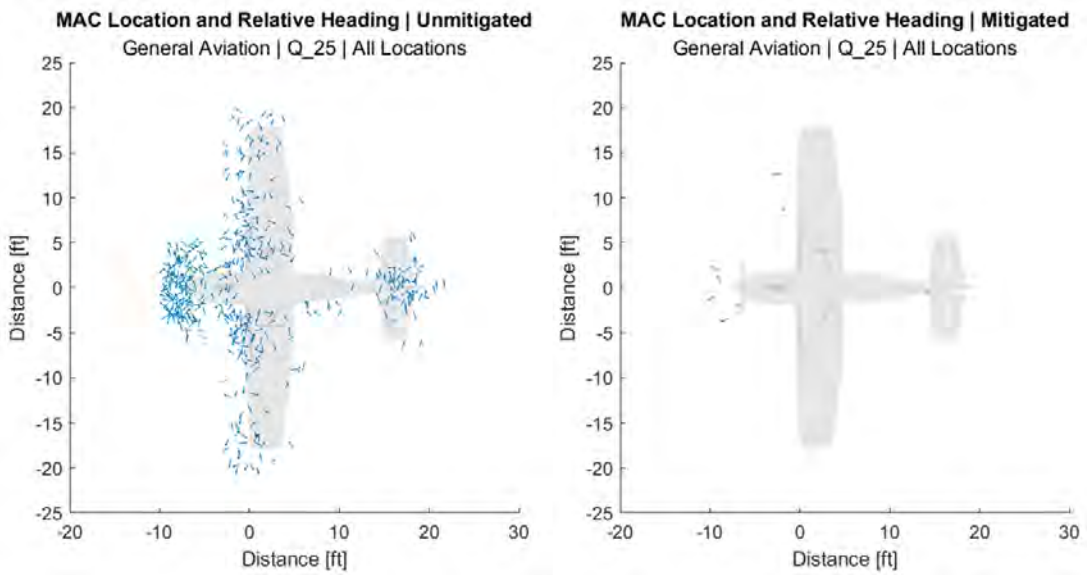

Figure 232. MAC location and relative heading – Unmitigated (left) and mitigated (right) Single-Engine General Aviation-Q25 pair.

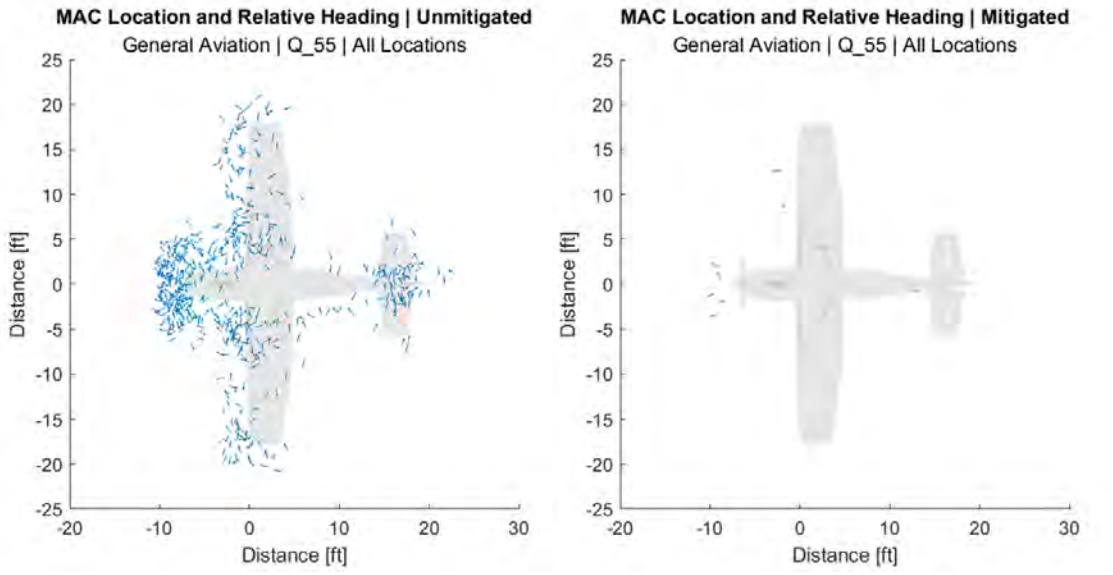

Figure 233. MAC location and relative heading – Unmitigated (left) and mitigated (right) Single-Engine General Aviation-Q55 pair.

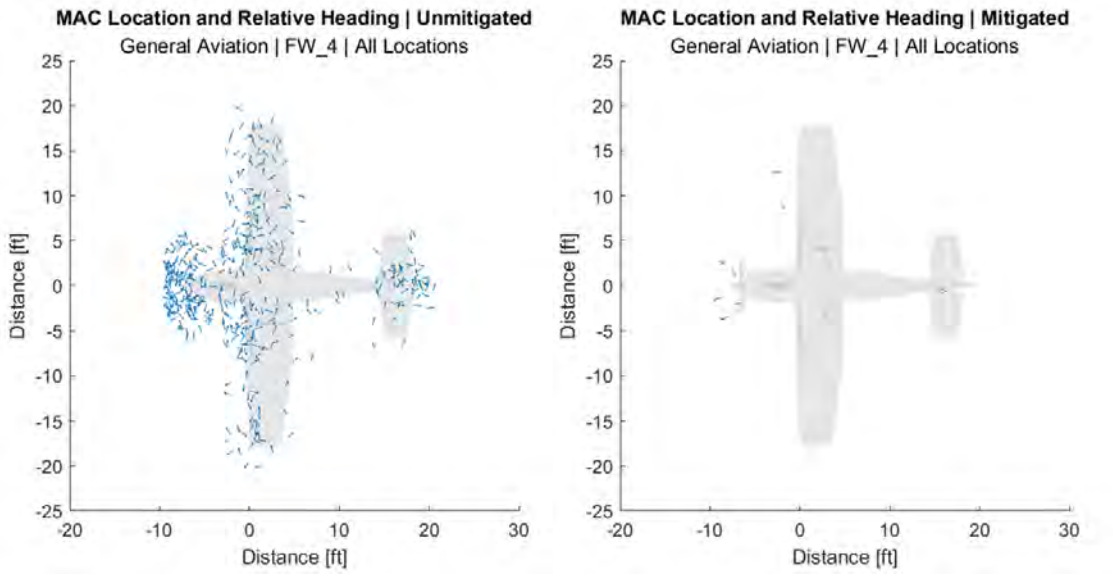

Figure 234. MAC location and relative heading – Unmitigated (left) and mitigated (right) Single-Engine General Aviation-FW4 pair.

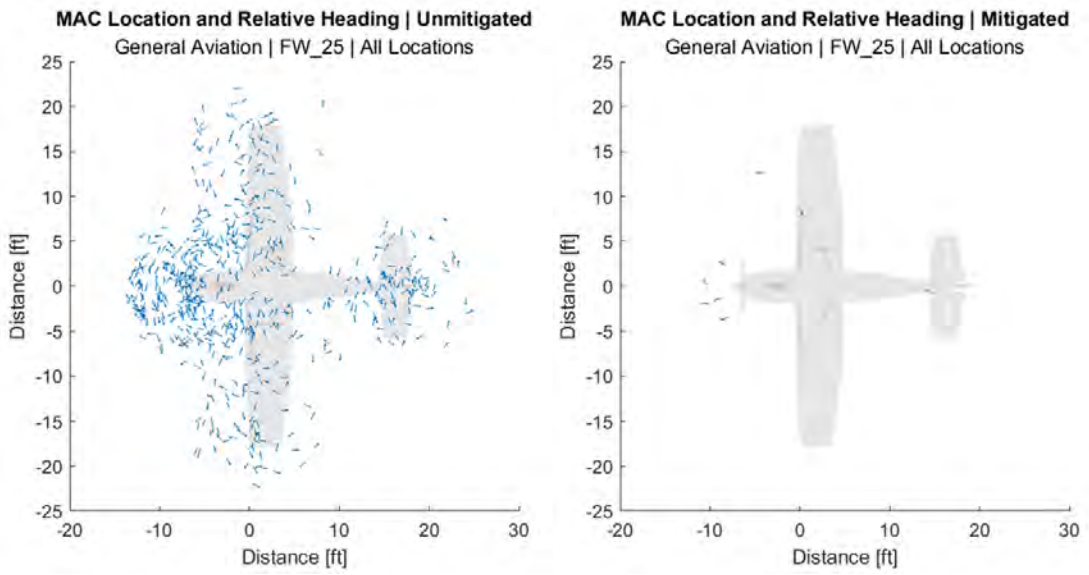

Figure 235. MAC location and relative heading – Unmitigated (left) and mitigated (right) Single-Engine General Aviation-FW25 pair.

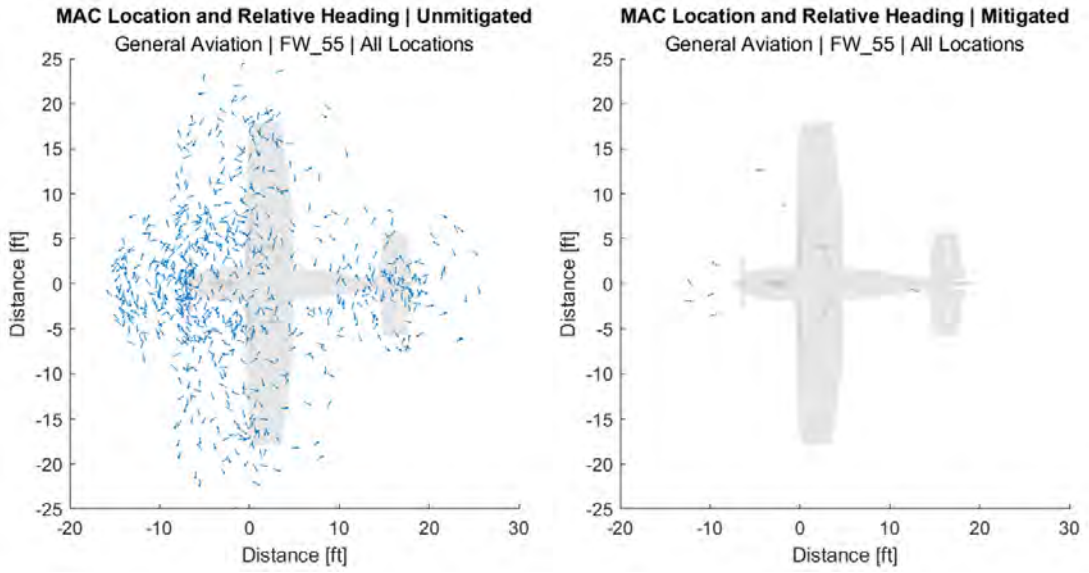

Figure 236. MAC location and relative heading – Unmitigated (left) and mitigated (right) Single-Engine General Aviation-FW55 pair.

E.4 Rotorcraft

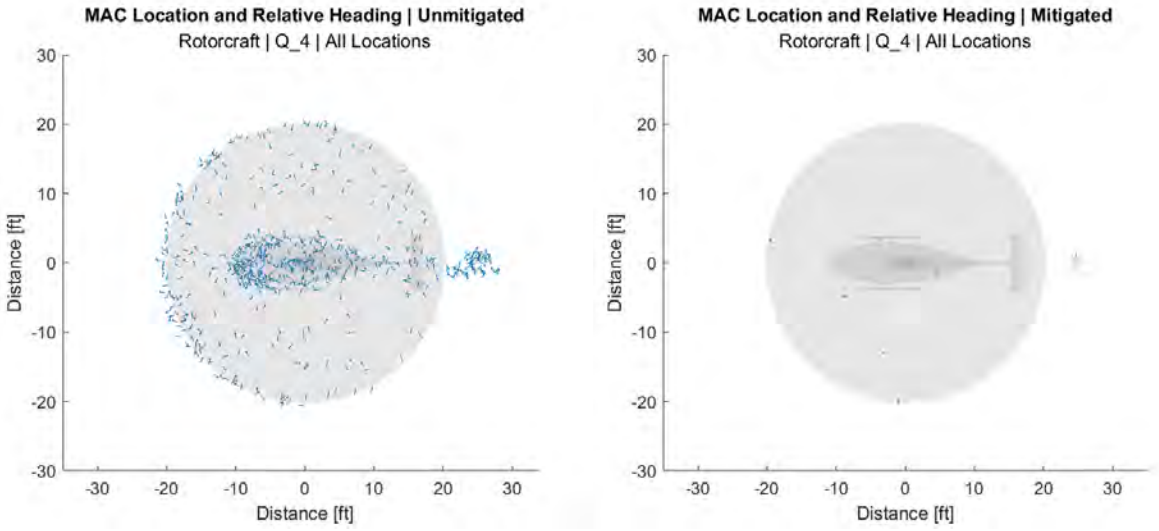

Figure 237. MAC location and relative heading – Unmitigated (left) and mitigated (right) Rotorcraft-Q4 pair.

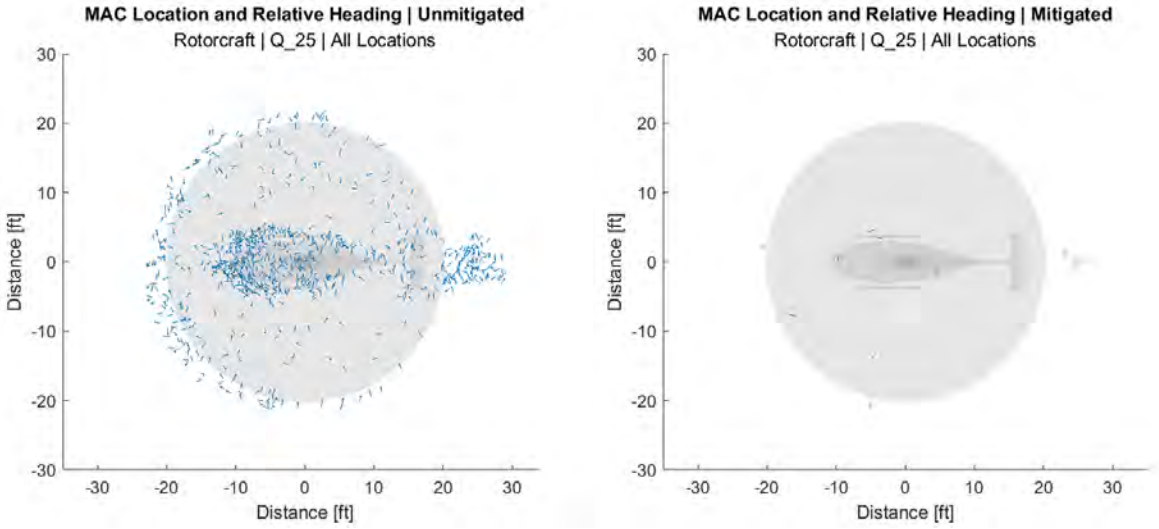

Figure 238. MAC location and relative heading – Unmitigated (left) and mitigated (right) Rotorcraft-Q25 pair.

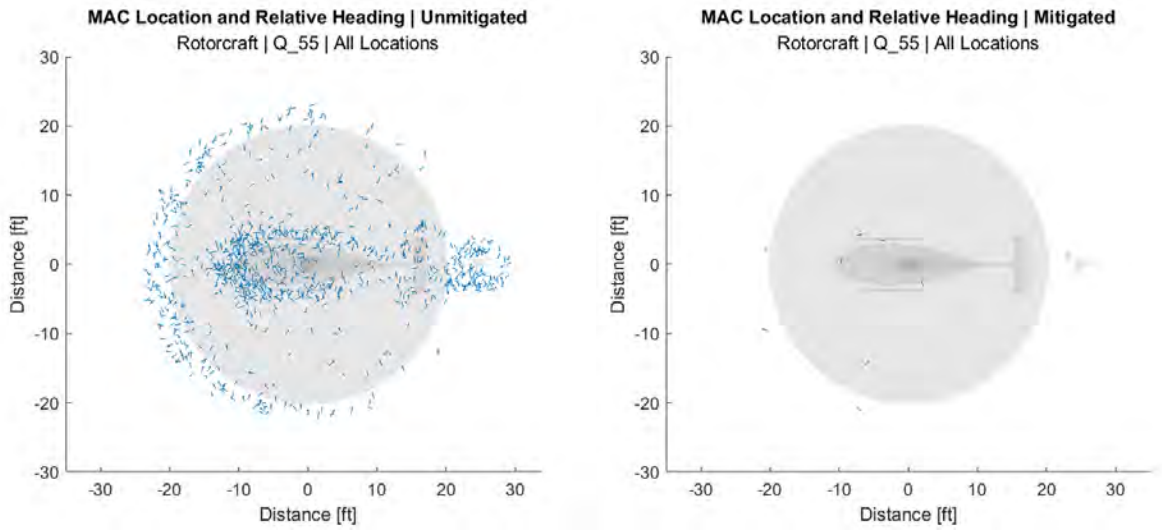

Figure 239. MAC location and relative heading – Unmitigated (left) and mitigated (right) Rotorcraft-Q55 pair.

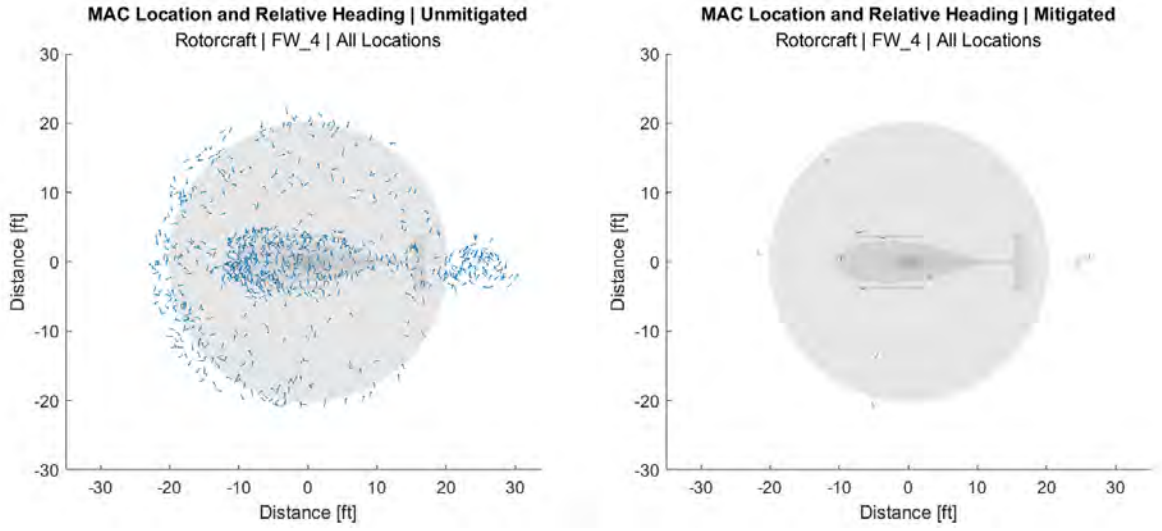

Figure 240. MAC location and relative heading – Unmitigated (left) and mitigated (right) Rotorcraft-FW4 pair.

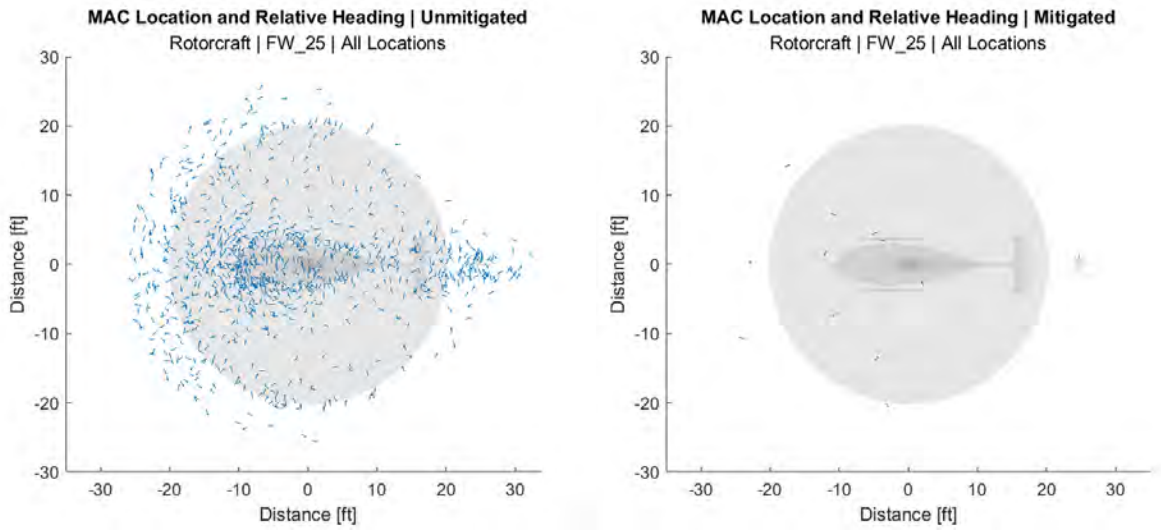

Figure 241. MAC location and relative heading – Unmitigated (left) and mitigated (right) Rotorcraft-FW25 pair.

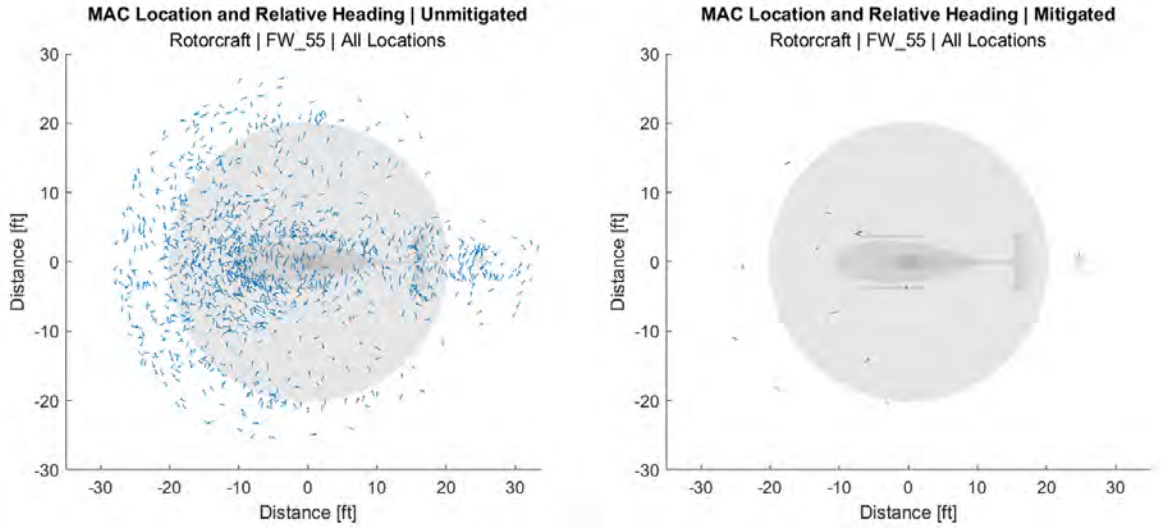

Figure 242. MAC location and relative heading – Unmitigated (left) and mitigated (right) Rotorcraft-FW55 pair.

Appendix F LEVERAGING UAS DETECTION DATA AND ADS-B TO BETTER UNDERSTAND AIRCRAFT-SUAS ENCOUNTERS

This appendix discusses sUAS detections and UAS sighting reports to estimate sUAS encounters with manned aircraft. Most sUAS detected are expected to be operating under Part 107 rules.

F.1 Introduction & Background

Encounters between unmanned aircraft and manned aircraft are still not well understood. In 2014, the Federal Aviation Administration began collecting data of UAS sighting reports, a proxy measurement of UAS encounters with aircraft. According to the FAA (2022), sighting reports are [reports of visual UAS sightings] received from pilots, law enforcement officials, and other stakeholders.

F.1.1 UAS Sighting Reports

As of September 2022, the agency had received more than 15,000 reports since the reporting program's inception (FAA, 2022b)(see Figure 243).

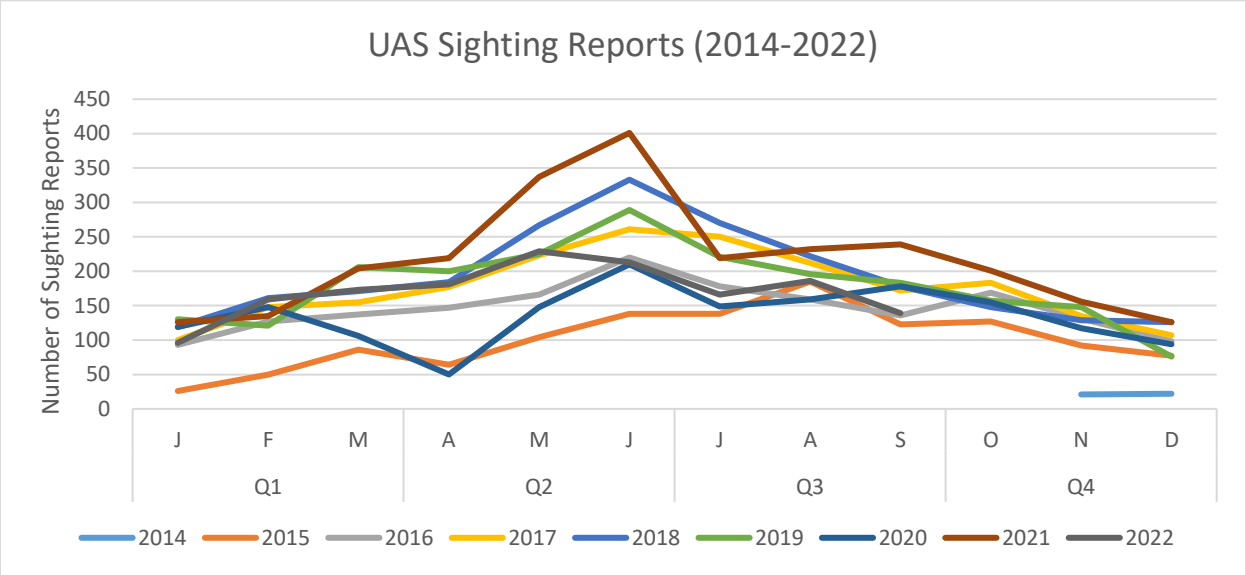

Figure 243. UAS Sighting Reports (November 2014-September 2022).

The UAS sighting report system can be credited with highlighting the problem of potentially-hazardous encounters between UAS and manned aircraft within the National Airspace System. Figure 244 demonstrates an example of such hazards, with pilots repeatedly spotting drones while on approach to Los Angeles International Airport in 2014-2015 (Gettinger & Michel, 2015).

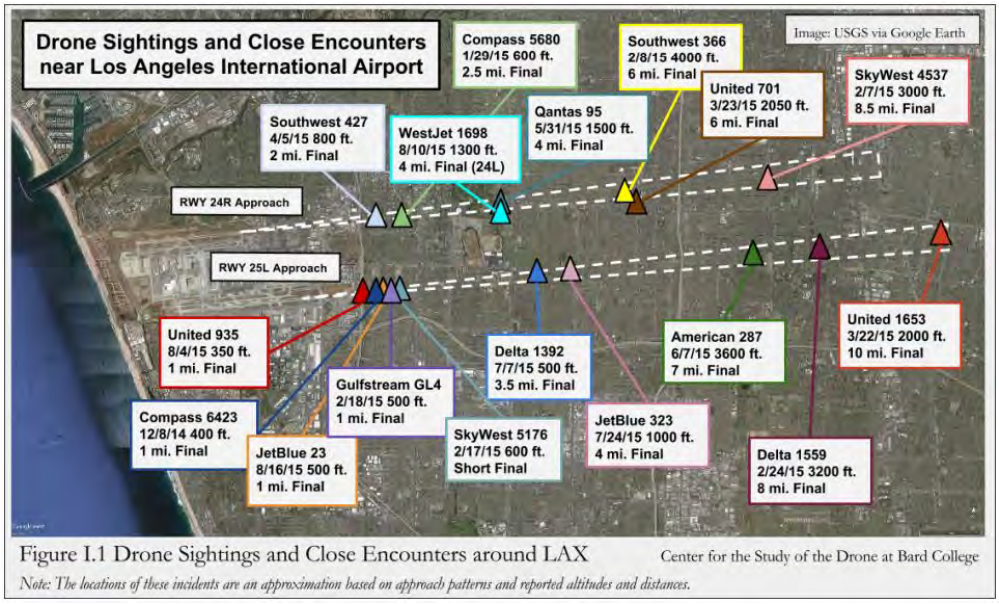

Figure 244. Drone Sightings and Close Encounters around LAX. Reprinted with permission, Center for the Study of the Drone at Bard College (Gettinger & Michel, 2015).

A number of reports have attempted to codify the potential risk of UAS encounters. An overview of these findings is presented in Table 48.

Table 48. UAS Sighting Report Studies.

Criteria	Wang & Hubbard (2021)	Unmanned Aircraft Safety Team (2017)	Academy of Model Aeronautics (2016)	Academy of Model Aeronautics (2015)	Gettinger & Michel (2015)
No. Analyzed Sighting Reports	6,544	3,417	582	764	921
Years Included	2016-2019	2015-2017	2016	2015	2014-2015
Near Miss*	N/A	16.0%	3.5%	3.3%	35.5%
Required A/C Course Change*	3.3%	3.3%	2.4%	1.3%	3.0%
Drone Was Over 400 Feet	91.0%	70.4%	N/A	N/A	90.2%

*Note: Studies utilized varied metrics for determining near miss / evasion criteria.

In one of the most detailed reports of its kind, Wang and Hubbard (2021) performed an assessment of more than 6,544 sightings reports to identify characteristics of UAS sightings. Their reporting highlighted several unique findings, including seasonality trends, time of day, altitudes, relative trajectories, and closest point of approach distances of UAS encounters (Wang & Hubbard, 2021).

While UAS sighting reports aid in the identification of potential hazards, several studies have documented the inadequacies of UAS sighting reports as an accurate measure of UAS encounters. A series of studies analyzing segments of the UAS sightings database performed by the Academy of Model Aeronautics ([AMA], 2016, 2017) revealed that several sighting reports contained descriptions of objects other than drones, including balloons, birds, blimps, and model rockets. Both AMA (2016, 2017) reports contain reports of sightings when a drone was operating below 400 feet—an altitude where UAS flight is generally permissible. The reports further highlight the

subjective nature of sightings—reliance on the observer's perception—as well as the lack of objective criteria for further skewing sightings report data (AMA, 2016, 2017). Perhaps most importantly, sighting reports only capture incidents in which the pilot of the manned aircraft becomes aware of the encounter. A series of visibility experiments by Kephard and Braasch (2010), Maddocks and Griffitt (2015), Loffi et al. (2016), Wallace et al. (2018), Wallace et al. (2019), and Loffi et al. (2021) indicate that pilots are highly unlikely to spot unmanned aircraft while in flight (see Figure 245).

Figure 245.Multi-engine aircraft encounter with a small multirotor UAS. In-flight visibility experiments by Wallace et al. (2019) highlight the difficulty in a crewmember's ability to spot a small UAS during landing.

To address the validity issues and data gaps presented by UAS sighting reports, the research team sought to assess UAS encounters using solely direct observational data. Data methodology was adapted from a prior sUAS-aircraft encounter study conducted at Dallas-Fort Worth International Airport (DFW) by Wallace, Winter et al. (2022).

F.1.2 Pilot Study

A pilot study of sUAS-aircraft encounters was conducted at DFW airport in Dallas, Texas, from August of 2018 through September of 2021 (Wallace, Winter et al., 2022). Researchers collected 36 months of sUAS detection data using an RF sensor suite and combined it with ADS-B/Mode S data collected from the same time period. During the sampling period, DFW recorded 1,840,667 aircraft operations (FAA, n.d.e); and, sUAS detection technology recorded 459,549 sUAS flights from a population of 28,995 sUAS platforms. During the sampling period, 203 sighting reports

were reported to the FAA in the Dallas/Fort Worth areas (FAA, 2022b). The research team identified 24 encounters, defined as an incursion of an sUAS within 500 feet of an aircraft at the same point in time. Results are presented in Figure 246.

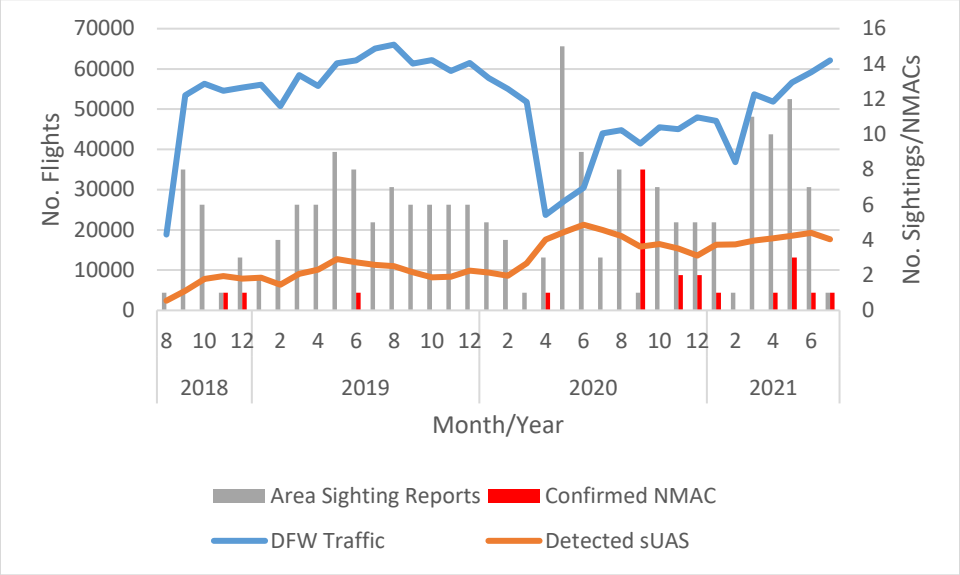

Figure 246. sUAS Encounter and Contextual Data (derived from Wallace, Winter, et al., 2022).

F.2 Methodology

The research team performed an assessment of historical UAS encounters based on telemetry data collected from UAS detection sensors and ADS-B/Mode S datasets from a sample of locations around the US.

F.2.1 Instrumentation

F.2.1.1 UAS Detection Data & Equipment

This project employed an array of Radio-Frequency (RF) sensors at 10 locations around the US. The sensors detected the datalink communications protocols emitted from DJI-manufactured sUAS. The RF sensors enabled continuous, passive monitoring of sUAS status, telemetry, and identification data, sampled at one-second intervals.

F.2.1.2 Air Traffic Data

Open Sky Network (OSN). The research team acquired ADS-B and Mode S data from the Open Sky Network. OSN collects and archives aircraft telemetry data from a network of more than 5,000 ground stations in 190 countries worldwide. "Researchers from different areas primarily use the database to analyze and improve air traffic control technologies and processes" (OSN, 2022, p. 1).

Automatic-Dependent Surveillance-Broadcast (ADS-B). UAS detection data was fused with Automatic Dependent Surveillance-Broadcast data, "an advanced surveillance technology that combines an aircraft's positioning source, aircraft avionics, and ground infrastructure . . . ADS-B (Out) works by broadcasting information about an aircraft's GPS location, altitude, ground speed, and other data to ground stations . . . " (FAA, n.d.a, p. 1).

Mode S. Mode S transponders are allocated a unique identification code. Aircraft equipped with Mode S can be positively identified. Mode S interrogation methods enable improved detection and positional accuracy in dense or closely-spaced traffic conditions (FAA, n.d.c).

F.2.2 Analysis Tools

The research team utilized Unmanned Robotics Systems Analysis (URSA), Inc.'s Airspace Awareness Platform (AAP), to integrate, store, and analyze all datasets. According to URSA (2022), AAP integrates vendor-agnostic data from multiple sources and enables data analysis and visualization of traffic, trends, compliance, and safety risk. The platform utilizes the power of web-based cloud computing to provide custom analysis for large Geographical Information Systems (GIS) datasets.

F.2.3 Data Cleaning & Datum Adjustment

Before conducting the analysis, the AAP system filtered invalid data elements. Since some sensor placements were arrayed, there was an overlap in data coverage. Duplicated data elements were removed. Data points from outside the selected capture regions were also removed. The system filtered the dataset for illegal values, including zero-values, null datasets, and related spurious or incomplete data. All lateral and vertical distance measurements were converted from metric units to imperial feet (ft). UAS altitude data was aligned to represent AGL values. Altitude conversions to Mean Sea Level (MSL) altitude values were applied using Open Elevation, a publicly-accessible source of GIS elevation data (Lourenco, n.d.). All GIS data was aligned to the World Geodetic System 1984 (WGS84) standard. All times were converted from their respective local times to universal coordinated time (UTC/Zulu).

F.2.4 Procedure

The research team defined vertical, lateral, and temporal encounter criteria within the AAP analysis software to identify the CPA between sUAS and manned aircraft platforms. The AAP system segregates and processes each day of data independently, initially evaluating the lateral and vertical distance between sUAS and manned aircraft telemetry data points using a Haversine calculation, then validating that any identified encounters occurred within the established temporal limits. The sampling of sUAS detection data and ADS-B data occurred at different rates; only observed values were used (the research team did not interpolate points for the sensor with the lower sampling rate). To address this limitation, the research team set a temporal sampling range of 2 seconds within the analysis. Sensor data within this temporal range was presumed to correlate in time. The research team defined an encounter as an sUAS coming within a three-dimensional encounter envelope with a lateral distance of 4,000 feet horizontally, and 500 feet vertically, within a temporal space of 2 seconds. To simplify the data comparison, the research team also reported how the number of encounters in each location varied when the encounter envelope distances were further confined. According to the FAA (n.d.d), "A NMAC is an incident associated with the operation of an aircraft in which the possibility of a collision occurs as a result of a proximity of fewer than 500 feet feel to another aircraft . . . (p. 1).

For contextual purposes, additional location-specific data was collected, including the estimated population of sUAS platforms in the area during the sampling period and the number of manned aircraft flights that occurred. The population of sUAS platforms was determined by conducting a census of unique drone electronic serial numbers detected during the sampling period. The population of manned aircraft was determined by counting distinct aircraft IDs, using ADS-B data.

Although more accurate manned aircraft flight operations data was available using the FAA (n.d.e) Operations Network (OPSNET) database, the deployed sUAS detection sensors were often offset from airport locations; thus, this data did not enable direct comparison.

F.2.5 Assumptions & Limitations

The UAS detection technology employed during this research project could only detect sUAS platforms manufactured by DJI. Research by market analyst Asia Perspective (2021) estimates DJI commands nearly 76% market share, based on sales volumes; conversely, Drone Analyst (2021) applies a more conservative estimate of 54% market share for the Chinese drone manufacturer. Although drones manufactured by other companies were not included in this study, the research team believes the results to be reasonably representative due largely to the preponderance of DJI-manufactured platforms being operated in the National Airspace System.

The UAS detection technology utilized during this study relies on the receipt of datalink radio frequency communications exchanged between the remote controller and aerial vehicle. These signals are subject to interference, attenuation, and blockage by obstacles or terrain. The research team assumed that signal attenuation, interference, or other blockages did not adversely impact the study findings since these factors are generally encountered near the ground, where obstacles are more numerous.

Both UAS platforms and aircraft rely on Global Navigation Satellite Systems (GNSS), such as the U.S. Global Positioning System (GPS) or the Russian Global Navigation Satellite System (GLONASS), for positioning and navigation. These signal-based systems are subject to error, interference, and other factors, which can reduce positional accuracy. The research team assumed that reported GNSS positions were accurate.

F.3 Findings

Data collection was carried out from July 1, 2021, through January 31, 2022. UAS detection data was collected from 10 locations around the U.S. using convenience sampling. A total of 237 sUAS-aircraft encounters were identified where the CPA fell within established encounter envelope criteria. Detailed data for each of the sampling locations is contained in Table 49.

Table 49. Table of Aircraft-sUAS Encounters by Location.

Location	Encounters	AC Flights (ADS-B)	UAS Flights	UAS Platforms	Sample Days
BatonRouge, LA	3	93	650	175	66
Boston, MA	111	194131	1540	679	179
Brooklyn, NY	63	595438	1660	785	179
Brownsville, TX	21	11244	3627	942	109
Chillicothe, OH	3	35433	527	152	179
Concorde, NH	12	47254	97	41	179
Ferndale, WA	8	90166	398	196	179
Kankakee, IL	2	129102	710	191	179
Sacramento, CA	8	104432	242	137	179
Yuma, AZ	6	6911	3218	729	179

F.3.1 Encounters by Aircraft Type

Using the reported N-numbers derived from ADS-B data, the research team referenced the FAA (n.d.b) [Aircraft] Registry to identify aircraft type. Aircraft types were broadly categorized as: Fixed-Wing-Prop (FWP); Fixed-Wing Jet (FWJ); Helicopter/Rotorcraft (HEL); and Unknown (UNK). Unknown aircraft were primarily comprised of those registered outside the U.S. Of the 237 encounters, 24.1% (n=57) involved fixed-wing prop aircraft; 51.1% (n=121) involved fixed-wing jets; 16.0% (n=38) involved helicopters/rotorcraft; and, 8.9% of aircraft (n=21) were unknown (see Figure 247). Results were further distributed by area (see Figure 248). The number of encounters between fixed-wing jets and helicopter/rotorcraft was much more prominent in larger, urban sampled areas such as Boston and Brooklyn. Conversely, smaller airports experienced more encounters with fixed-wing prop aircraft.

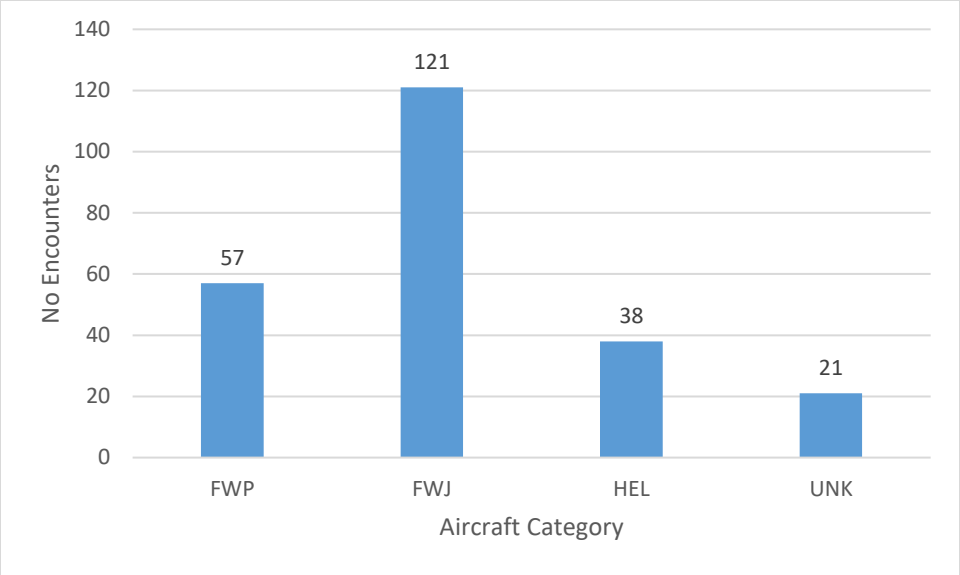

Figure 247. Encounters by Aircraft Category.

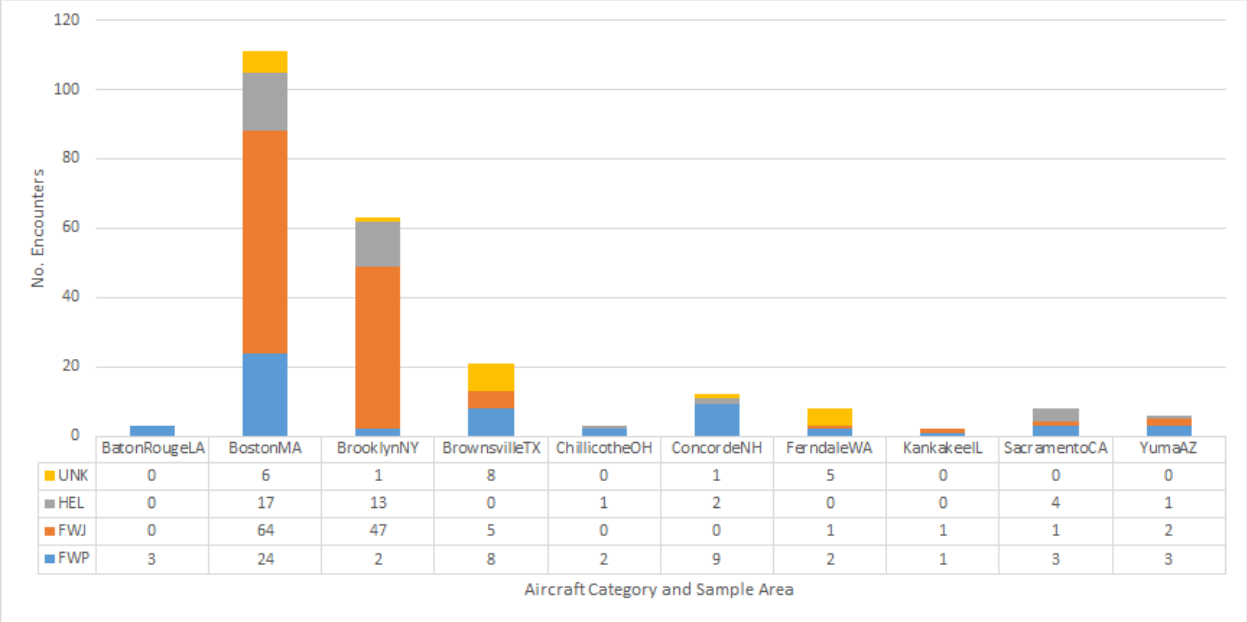

Figure 248. Encounters by Location and Aircraft Category.

F.3.2 Dates & Time of Encounters

An analysis was performed to identify if any date or time trends could be found within the dataset. A histogram of aircraft encounters is presented in Figure 249. It is unclear why some months experienced no encounters, whereas other months experienced high levels of encounters. Twenty-one encounters were identified on December 5, 2021, with 15 encounters in Boston, 5 in Brooklyn, and 1 in Concorde. It is unclear why this date experienced such a disproportionately-high volume of encounters over other sample dates.

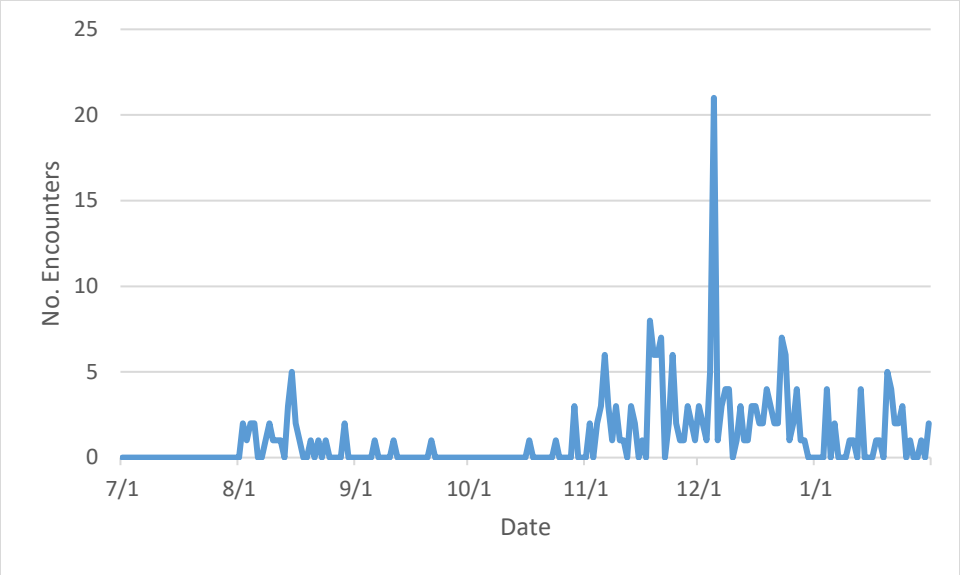

Figure 249. Dates of Aircraft-sUAS Encounters.

An evaluation was also performed on the day of the week in which an encounter was experienced. Results are presented in Figure 250. The data is relatively consistent, except for Thursdays and Sundays, which show elevated encounter counts. The Sunday finding is consistent with other drone detection data that suggests that higher levels of drone activity are performed on Sundays (Wallace, Terwilliger, et al., 2022). The Thursday finding is still under investigation.

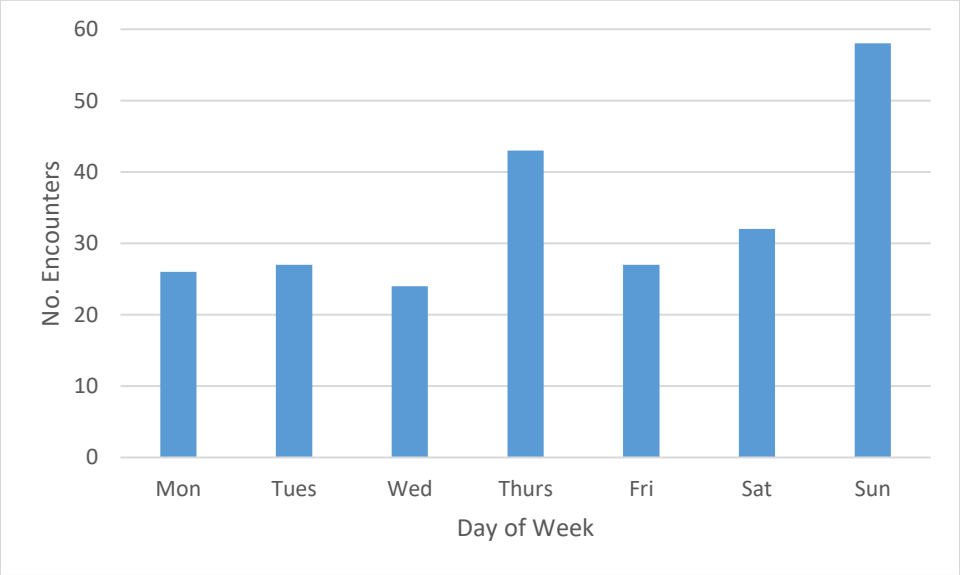

Figure 250. Encounters by Day of Week.

A similar analysis was conducted to identify encounter trends based on the time of day. An evaluation of encounter times is presented in Figure 251 in Universal Coordinated Time (UTC). More than 68.4% (n=162) of encounters occurred between the hours of 1300Z – 1900Z. For

context, these times approximate to 8 am – 2 pm EST or 9 am – 3 pm EDT, generally falling within the morning to early afternoon daylight hours.

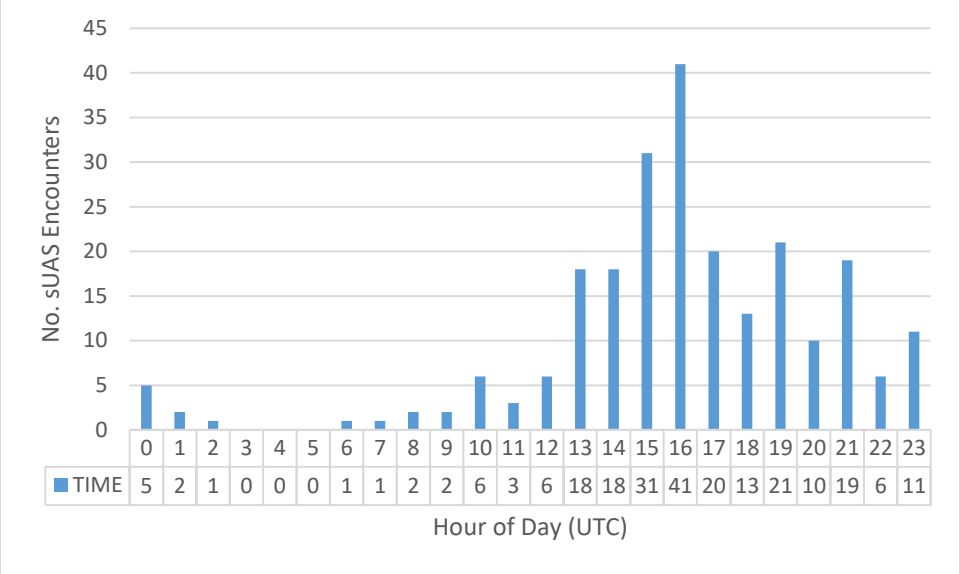

Figure 251. Time Distribution of Aircraft-sUAS Encounters.

F.3.3 Distance from Airfield

The research team identified the most notable airport within each sampling area (see Table 50). Coordinates for each airport were acquired from the FAA (2022a) Digital Chart Supplement Search. Coordinates were converted from degree-decimal minutes format to decimal degree format using Earthpoint (2022), an online coordinate conversion tool. Aircraft and airport coordinates for each encounter CPA were evaluated using a Haversine formula. Results are presented in Figure 252. Distances of encounters from airfields ranged from 4 NM to 18.9 NM, with a mean of 5.4 NM (Median=4.6) and a standard deviation of 3.7. Some of the variability may be due to UAS detection sensor placement and coverage area, which in some cases maybe 10 or more miles from the airport. The research team intends to continue the evaluation of the unique characteristics of encounter locations around these sampled airports to understand influencing factors better.

Table 50. Notable Airports within Each Sampling Area.

Sampling Area	Airport Name	Airport Code
BatonRouge, LA	Baton Rouge Metro Airport	BTR
Boston, MA	Boston Logan International Airport	BOS
Brooklyn, NY	John F. Kennedy International Airport	JFK
Brownsville, TX	Brownsville South Padre Island International Airport	BRO
Chillicothe, OH	Ross County Airport	RZT
Concorde, NH	Concorde Municipal Airport	CON
Ferndale, WA	Bellingham International Airport	BLI
Kankakee, IL	Greater Kankakee Airport	IKK
Sacramento, CA	Sacramento International Airport	SMF
Yuma, AZ	Yuma International Airport	NYL

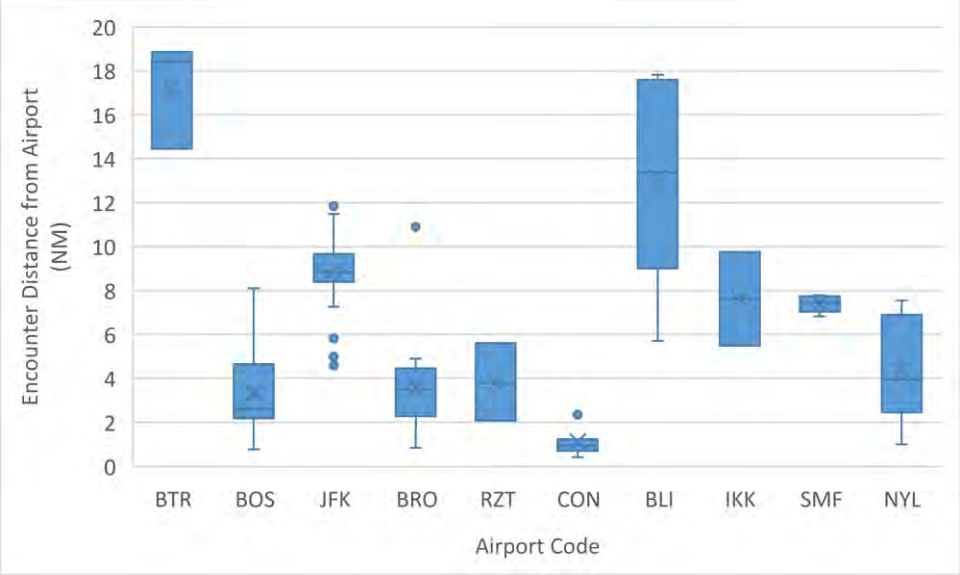

Figure 252. Box and Whisker Plot of Encounter Location Distances from Major Airport in Sampling Areas.

F.3.4 Separation Distances

The distribution of lateral and vertical separation distances for detected encounters between manned aircraft and sUAS is shown in Figure 253. Only one of the encounters resulted in a loss of separation, with the CPA distance measuring 462 feet laterally and 29 feet vertically. Encounter separation distances were further categorized by aircraft type to assess for possible trends (see Figure 254).

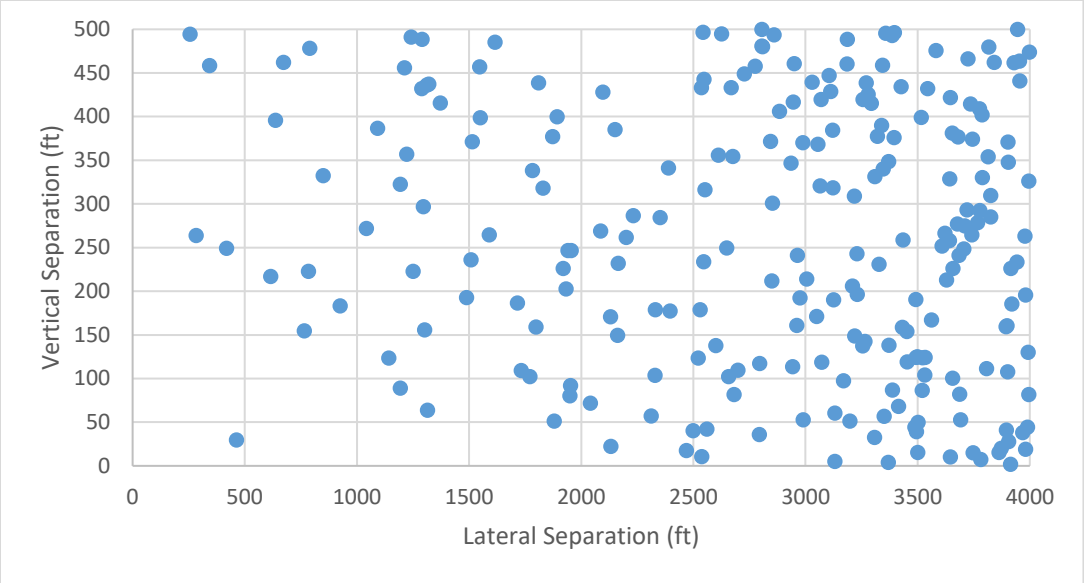

Figure 253. Aircraft-sUAS Encounter Separation Distances at CPA (Absolute Values, n=237, July 2021-January 2022).

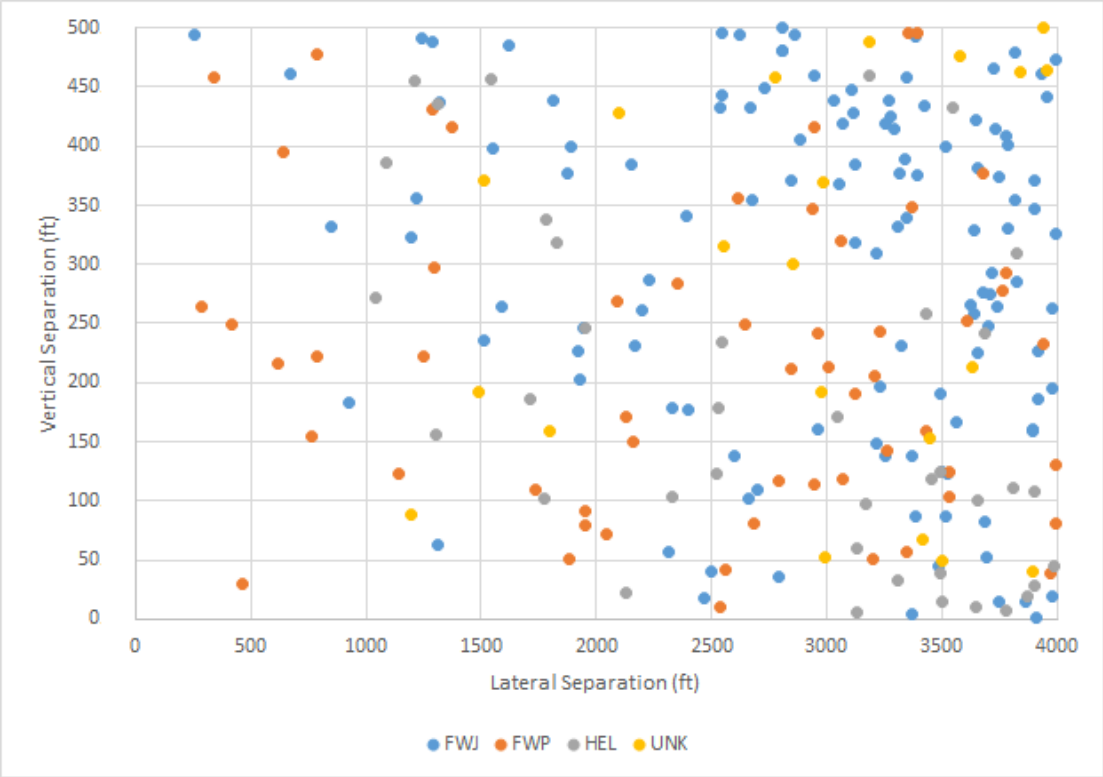

Figure 254. Aircraft-sUAS Separation Distances at CPA by Aircraft Category (Absolute Values, July 2021-January 2022).

The research team evaluated the position of sUAS relative to the aircraft heading at the CPA. More than 71.3% of encounters (*n*=169) with the aircraft positioned above the sUAS (see Figure 255).

More than 51.9% (n=123) of encounters occurred on the portside of the aircraft, nearly equal to the 48.1% (*n*=114) that occurred on the starboard side (see Figure 255).

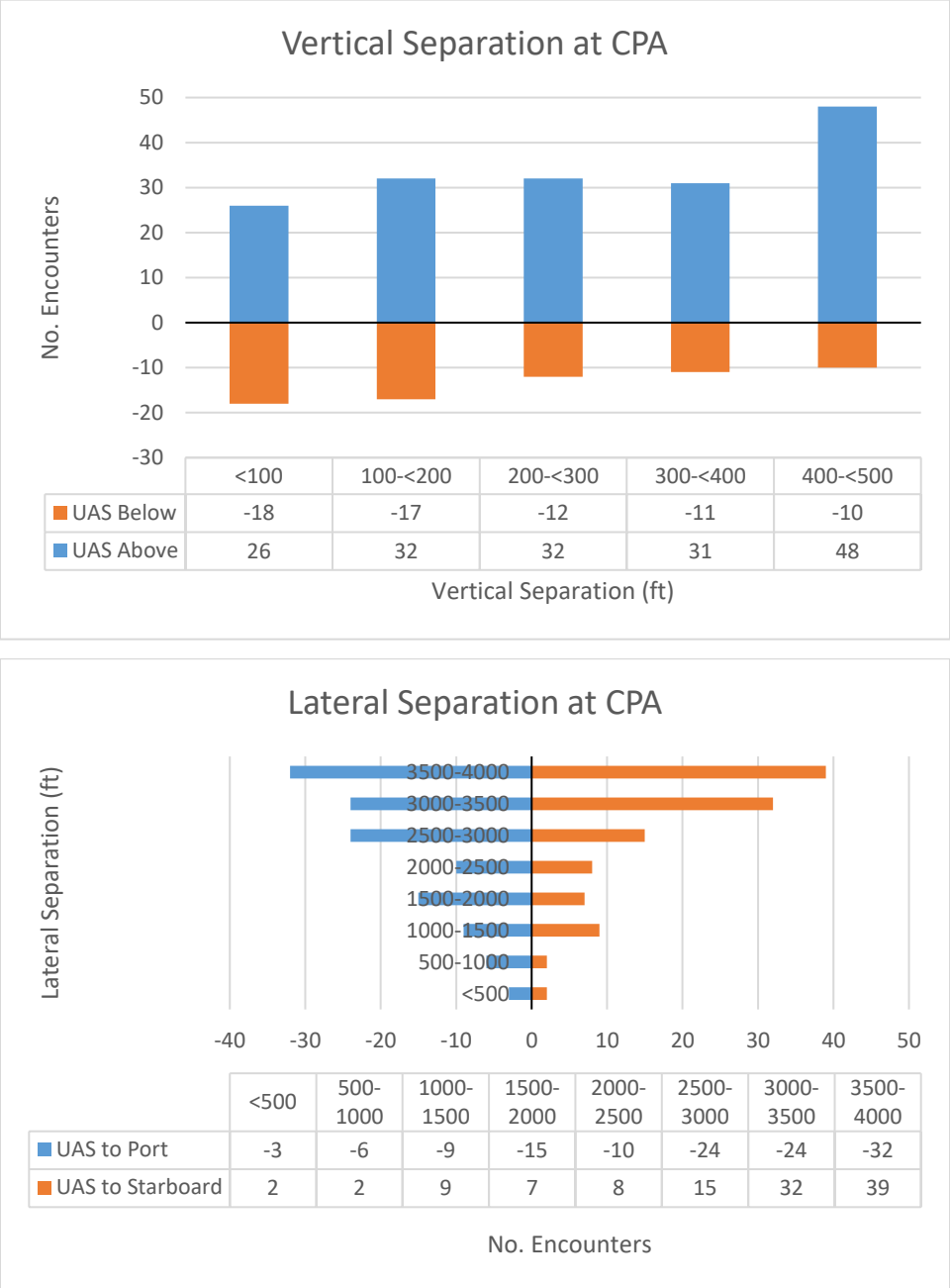

Figure 255. Distribution of Vertical [TOP] and Lateral [BOTTOM] Separation Distances for Encounters at CPA.

A boxplot of vertical and horizontal separation distances for each aircraft category is provided in Figure 256. Vertical separation is highest for fixed-wing jets, lower for fixed-wing prop aircraft, and lower still for helicopter/rotorcraft. A scatterplot of sUAS altitude relative to aircraft altitude at encounter CPA is provided for context in Figure 257. At least 63.2% (n=24) of helicopter/rotorcraft encounters involved sUAS that were above the altitude of the aircraft, a much

higher proportion than for fixed-wing props (33.3%, *n*=19) or fixed-wing jets (14.9%, *n*=19). Lateral separation distances were slightly lower for fixed-wing prop aircraft than for fixed-wing jet or helicopter/rotorcraft.

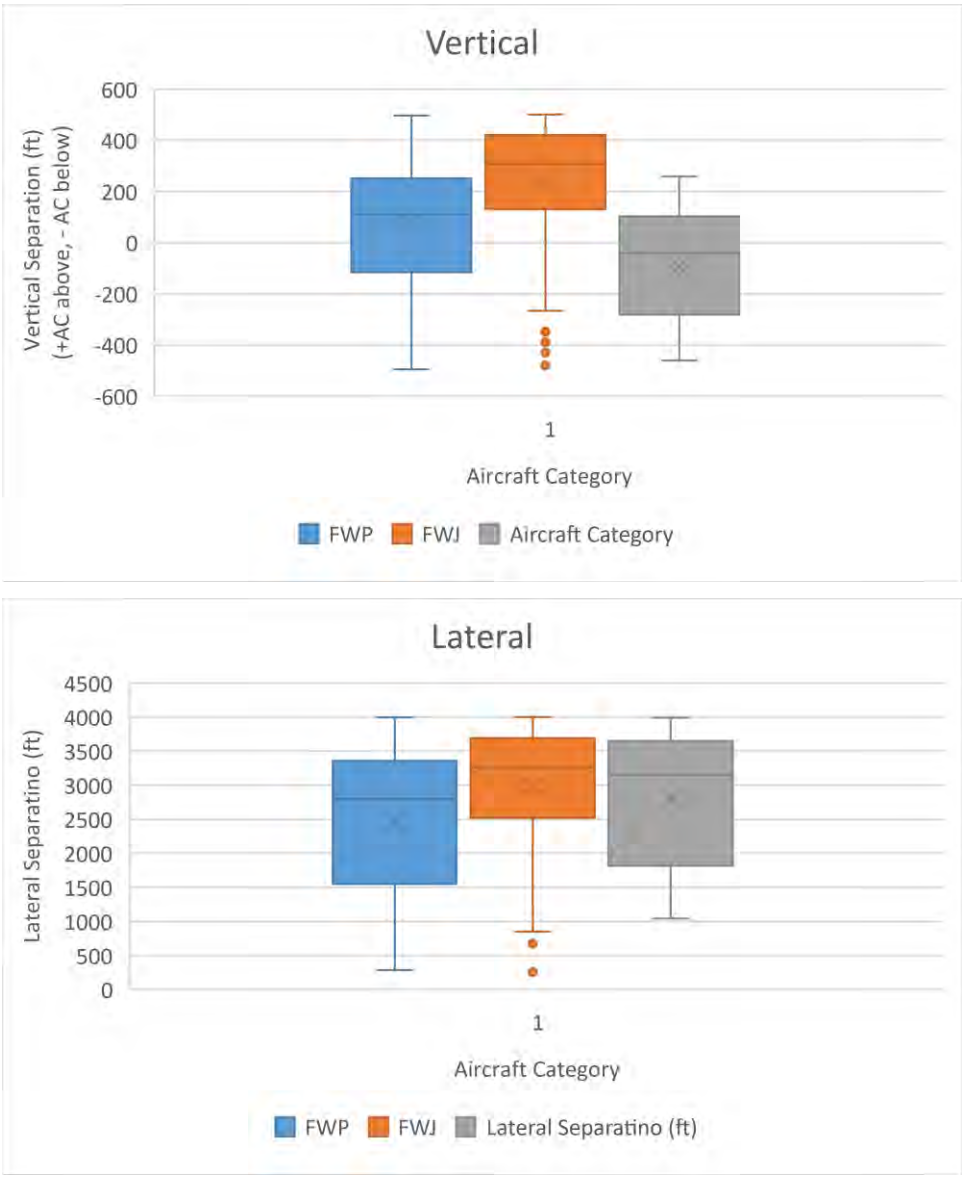

Figure 256.Boxplot of Vertical [TOP] and Horizontal [BOTTOM] Separation Distances for Encounters at CPA by Aircraft Category.

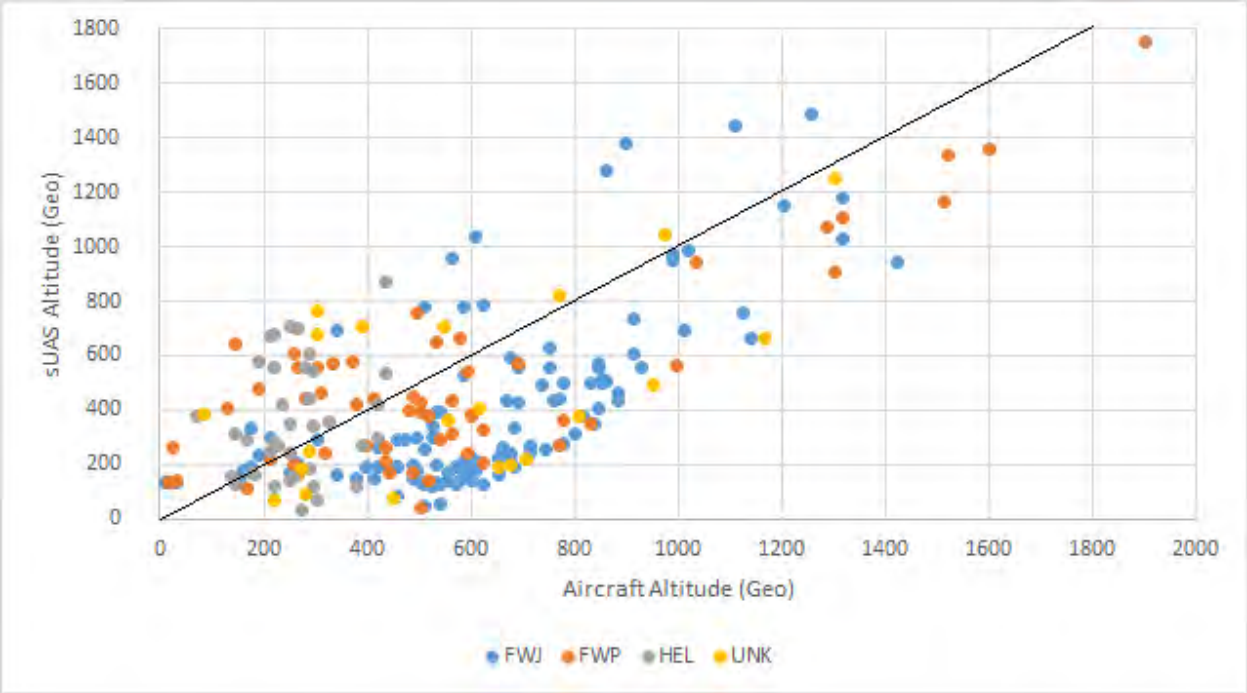

Figure 257.Aircraft Altitude to sUAS Altitude Plot by Aircraft Category. Note: plots above the diagonal line indicate the sUAS was above the altitude of the aircraft, whereas plots below the line indicate the aircraft was above the sUAS.

F.3.5 Encounter Envelopes

The research team established 10 categories of lateral and vertical encounter envelopes of diminishing size to illustrate the number and severity of encounters better. The following encounter envelopes were included:

- Distance Category 1: 4,000 feet horizontal; 500 feet vertical
- Distance Category 2: 2,000 feet horizontal; 400 feet vertical
- Distance Category 3: 1,750 feet horizontal; 350 feet vertical
- Distance Category 4: 1,500 feet horizontal; 300 feet vertical
- Distance Category 5: 1,250 feet horizontal; 250 feet vertical
- Distance Category 6: 1,000 feet horizontal; 200 feet vertical
- Distance Category 7: 750 feet horizontal; 150 feet vertical
- Distance Category 8: 500 feet horizontal; 100 feet vertical
- Distance Category 9: 250 feet horizontal; 50 feet vertical
- Distance Category 10: 0 feet horizontal; 0 feet vertical (suspected collision)

The number of encounters that fell within each encounter envelope category is provided in Figure 258 by location. The number of encounters becomes relatively negligible in number as the encounter envelope is confined below 1,000 feet laterally/200 feet vertically.

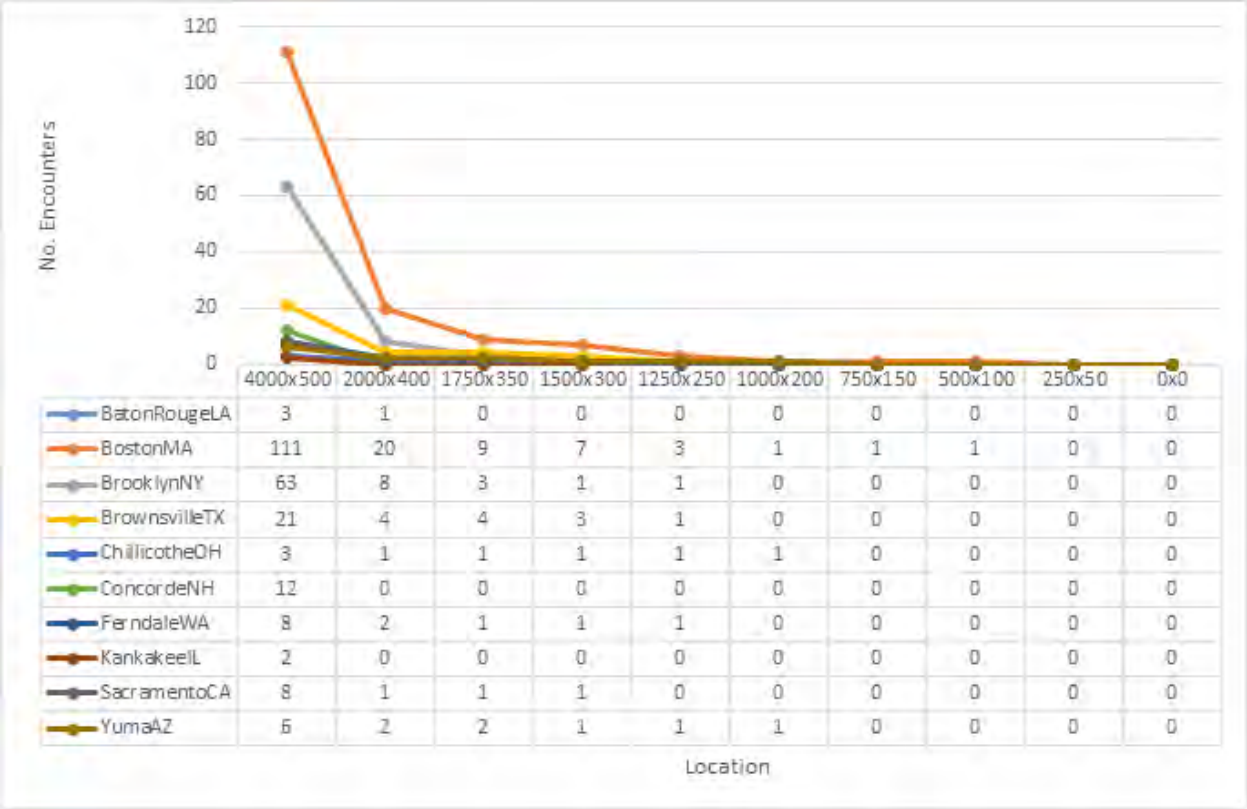

Figure 258. Number of Encounters by Location and Distance Category (July 2021-January 2022).

F.3.6 Likely sUAS Visibility to Flight Crew

The research team calculated the relative bearing and horizontal distance between the aircraft and sUAS at the CPA (see Figure 259). The relative bearing is the angle between the aircraft's forward-facing direction (heading) and the encountered sUAS. This assessment was designed to identify if the encountered sUAS was likely to be within the flight crew's lateral visual cone, as viewed from the flight deck. According to the Civil Aerospace Medical Institute (CAMI, 2017), the normal field of vision for each eye is about 135 degrees vertically and about 160 degrees horizontally . . . (p. 2). However, effective sight used to perceive and focus images is generally limited to the fovea, a one-degree, conical area near the center of the eye (CAMI, 2017). At least 56.1% of encounters occurring on the port side of aircraft (n=123, N=123) and 63.2% of encounters occurring on the starboard side of aircraft (n=72, N=114) would fall outside the normal field of vision for a pilot. However, it is important to note that the normal field of vision to perceive objects outside the aircraft may be further constrained by the fuselage flight deck window assembly.

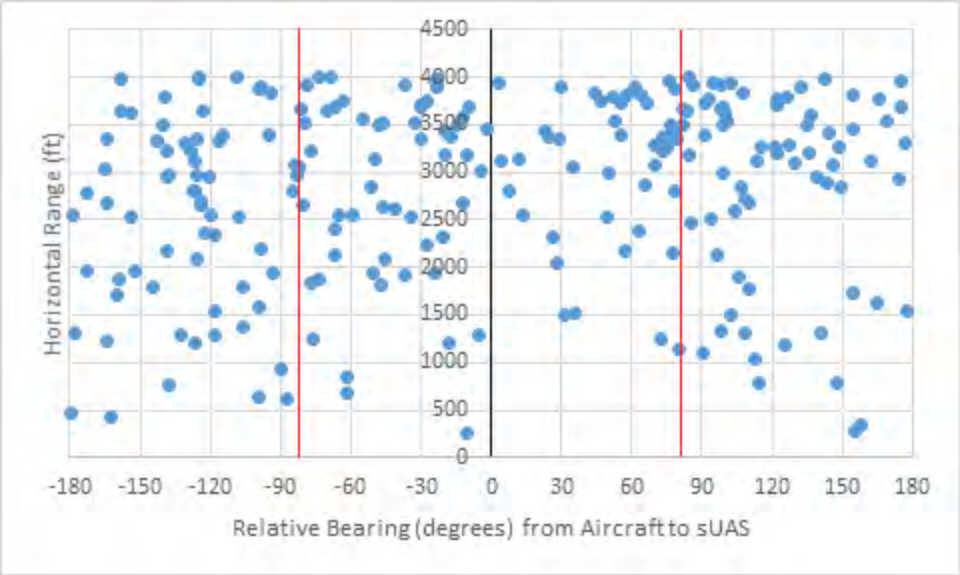

Figure 259. Relative Bearing and Distance from Aircraft to sUAS at CPA. Note: Normal horizontal field of vision limits are displayed as vertical red lines.

The research team analyzed the sUAS platforms involved in each encounter. A calculation was performed to determine the distance at which each platform produced one arc-minute field of view on the eye (see Table 51). One arc-minute is considered the standard visual acuity for an individual with normal, 20/20 vision (Iowa State University, n.d.).

Table 51. sUAS Weight, Size, Endurance, Speed, and Visual Footprint Specifications.

Platform	Weight (g)	Size (mm)	Endurance (min)	Max Speed (mph)	1 Arc-Min (ft)
Mini 2	249	203	31	35.8	2289.6
FPV	795	312	20	100	2842.2
Inspire 1	3060	581	18	49	6552.9
Inspire 2	3440	605	27	58	6823.6
Matrice 100	2400	650	40	49	7331.2
Matrice 200	4690	887	38	50.3	9992.9
Matrice 300	6300	810	55	51.4	9135.7
Matrice 600	9600	1668	40	40.3	18812.9
Mavic 2 Enterprise	905	322	31	44.7	3631.7
Mavic 3	899	448	46	42.5	5052.9
Mavic Air	430	213	21	42.5	2402.4
Mavic Air 2	570	253	34	42.5	2853.5
Mavic Mini	249	202	30	29	2278.3
Mavic Pro	743	335	27	40	3778.4
Phantom 3	1216	350	25	35.8	3947.5
Phantom 4	1380	350	28	35.8	3947.5
Spark	300	170	16	31	1917.4

Note: Weight, size, endurance, and speed are derived from the manufacturer's online product specifications or product manuals.

Applying the 1 arc-minute visualization standard, the research team assessed if the distance of each drone encounter at CPA exceeded the calculated 1 arc-minute threshold (see Figure 260). UAS outside this threshold were considered to be beyond the capability of the flight crew to visually acquire. At least 139 of the 237 encountered drones (58.6%) were found to be outside the maximum visual [1 arc-minute] threshold.

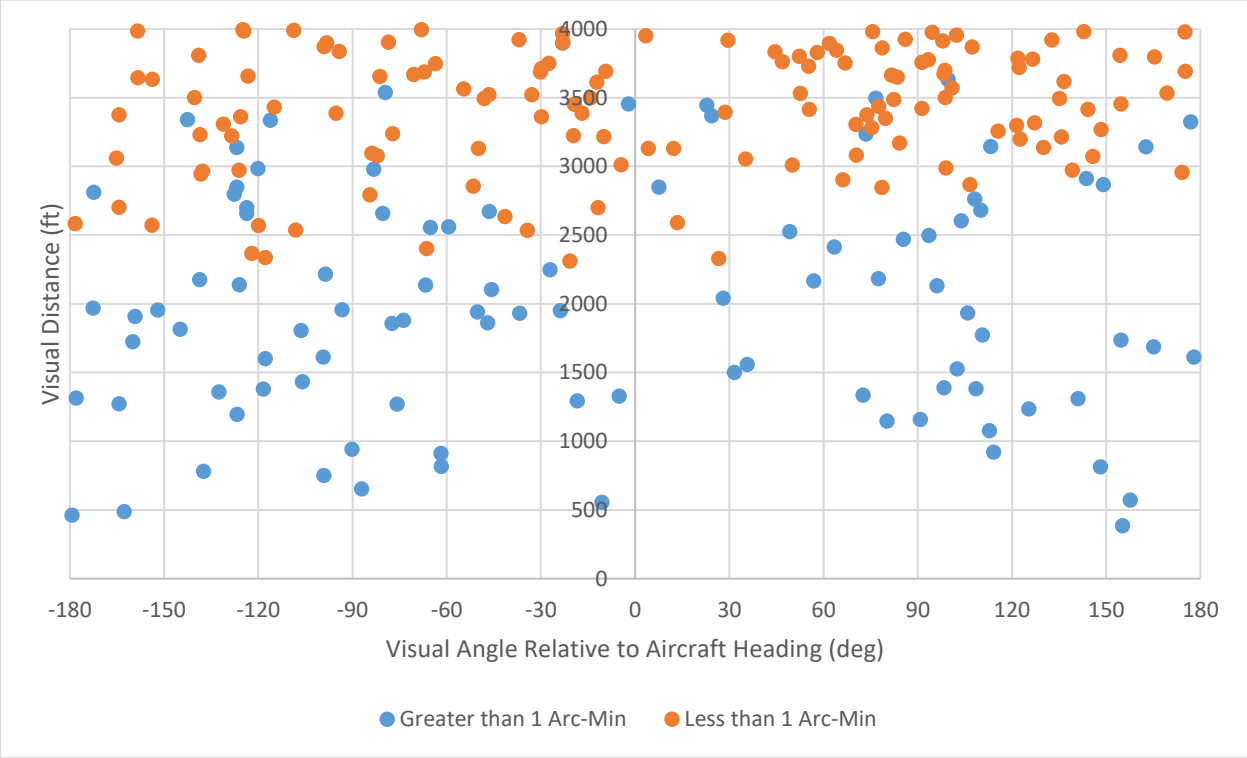

Figure 260. Relative Aircraft Bearing, Range, and Estimated Visibility of sUAS Encounters at CPA.

A similar visual analysis was conducted to assess if sUAS fell within the vertical acuity of flight crew members. The research team used trigonometry to calculate the relative vertical visual angle necessary to spot an sUAS by the flight crew. This data was fused with the [1 arc-minute] visual acuity data (see Figure 261). According to CAMI (2017), the normal vertical vision for a human is 60 degrees upward and 75 degrees downward. Both lateral and vertical thresholds have been added to Figure 261 for context.

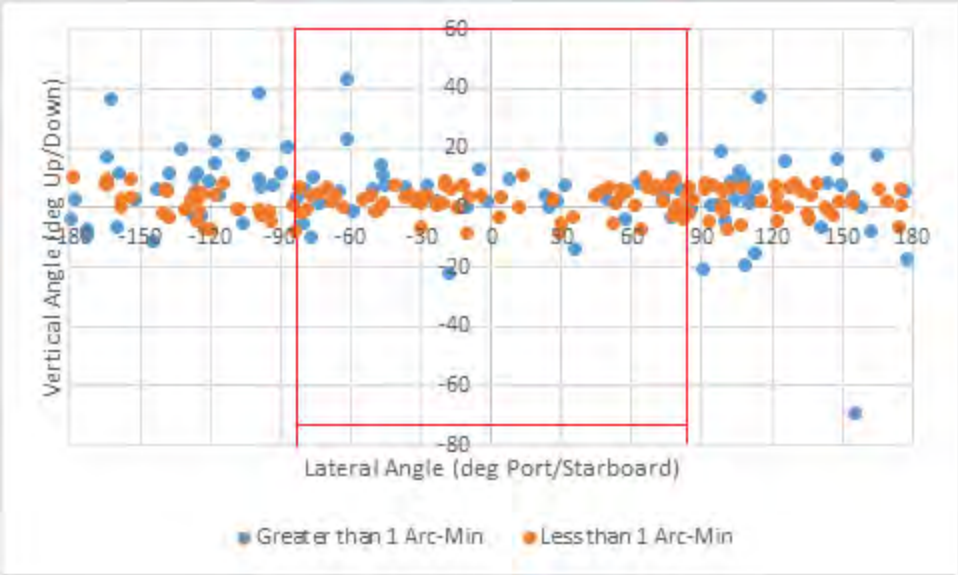

Figure 261. Relative Aircraft Bearing, Vertical Angle, and Estimated Visibility of sUAS Encounters at CPA. Note: Normal lateral and vertical visual acuity field of vision limits are displayed in red.

When considering *all factors*—horizontal field of vision, vertical field of vision, and [1 arc-minute] standard visual acuity—the total number of sUAS *likely* to be visually detectable by a flight crew member falls to 34 (14.3%) of the total 237 encounters. Unless flight crews practice vigilant visual scanning, the actual number of sUAS that are *visually detected* is likely to be much lower.

F.3.7 Weight of Encountered sUAS

An assessment was performed to identify the model and estimated weight of the drones involved in aircraft encounters. UAS detection data identified the model of the sUAS, and the weight was correlated to published online technical specifications. Nine weight categories were established to characterize encountered drone models best (see Table 52). More than 94% of encountered sUAS (n=223) were less than 2 lbs in weight: the sUAS model was unable to be identified in 3.8% of the encounters (n=9). The distribution of encountered drone models is presented in Figure 262.

Table 52. sUAS Weight Categories.

Category	Weight	Grams
0	Unknown	N/A
1	<0.55 lbs	249
2	<1.0 lb	453
3	<1.5 lbs	680
4	<2.0 lbs	907
5	<4.0 lbs	1814
6	<8.0 lbs	3628
7	<10.0	4536
8	<15.0 lbs	6804
9	<25.0 lbs	11340

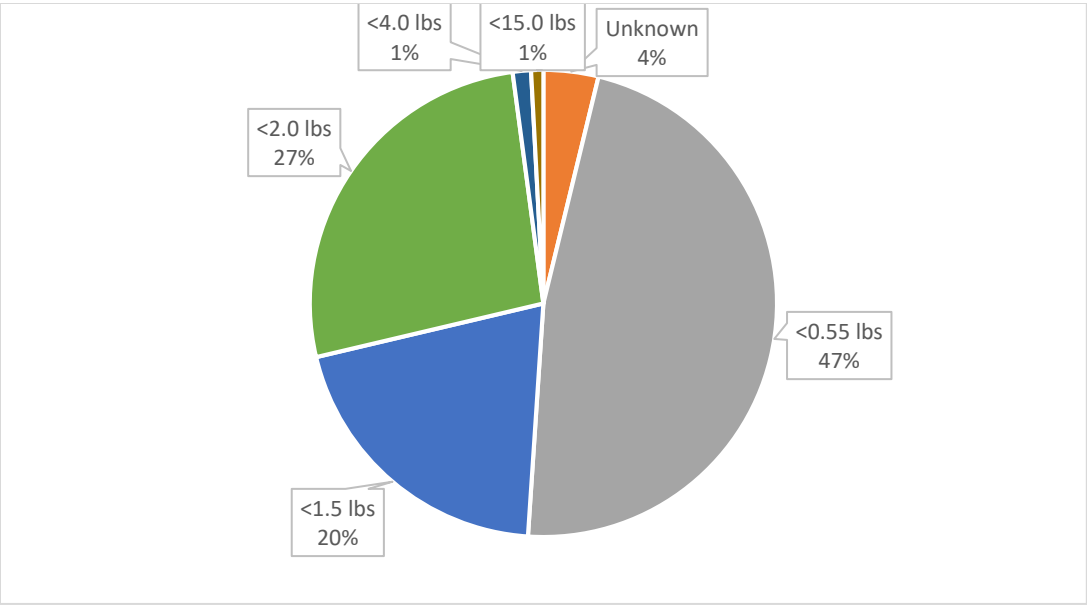

Figure 262. Encountered Drones by Weight Category.

The research team plotted encountered sUAS by absolute vertical and horizontal encounter distance from the CPA, categorizing each sUAS within its respective weight category. The resulting scatterplot did not appear to reveal any identifiable pattern to sUAS weight (see Figure 263).

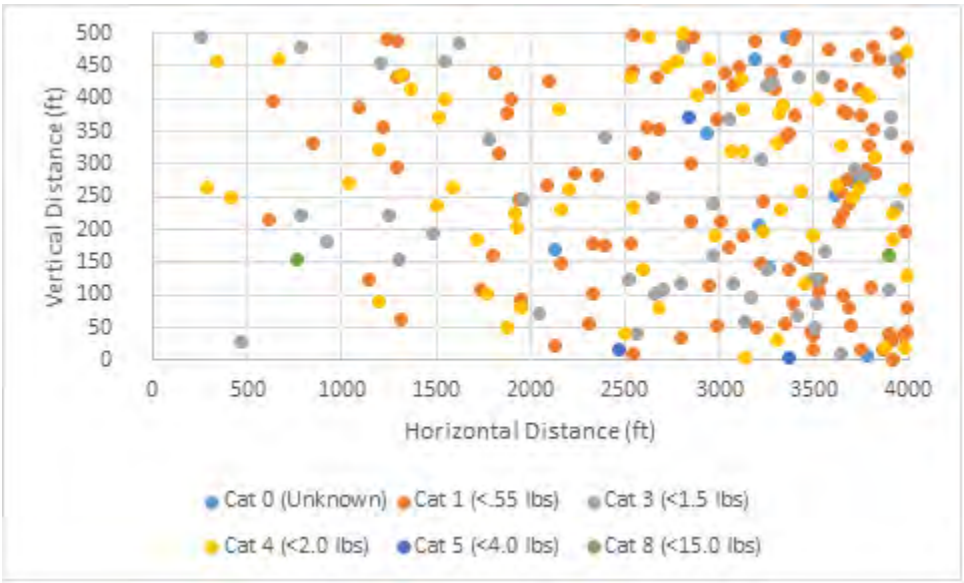

Figure 263. Aircraft-sUAS Encounter Separation Distances at CPA by sUAS Weight Category (Absolute Values, n=237, July 2021-January 2022).

F.3.8 Aircraft Altitudes at Closest Point of Approach

An analysis was conducted to understand better the altitude layers where most encounters occur (see Figure 264 and Figure 265). It is immediately apparent that helicopters/rotorcraft are disproportionately encountering sUAS between 200-300 feet. Similarly, encounters with fixed-

wing propeller aircraft and fixed-wing jet aircraft are encountering sUAS at higher altitudes, generally in the 400-700 foot band.

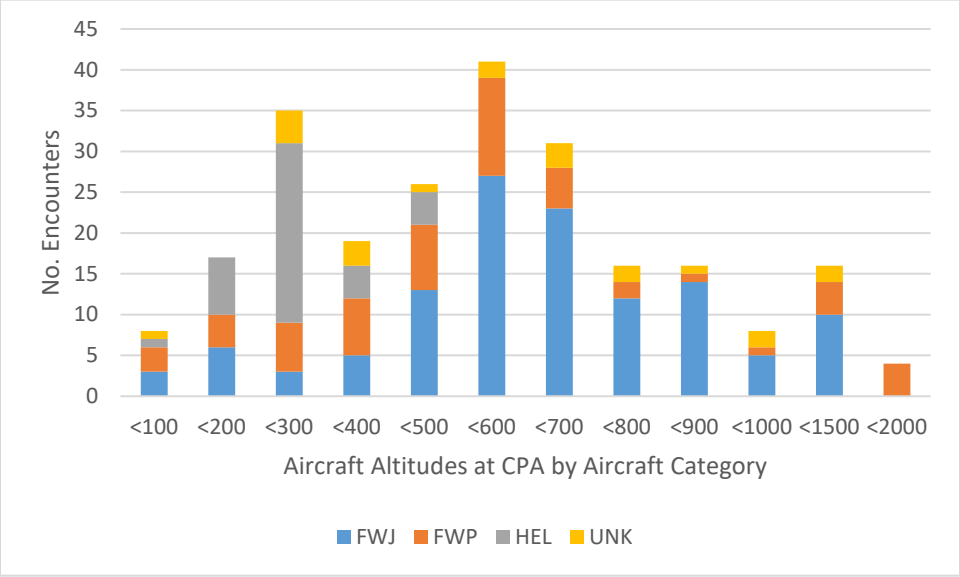

Figure 264. Distribution of Aircraft Altitudes during sUAS Encounters by Aircraft Type.

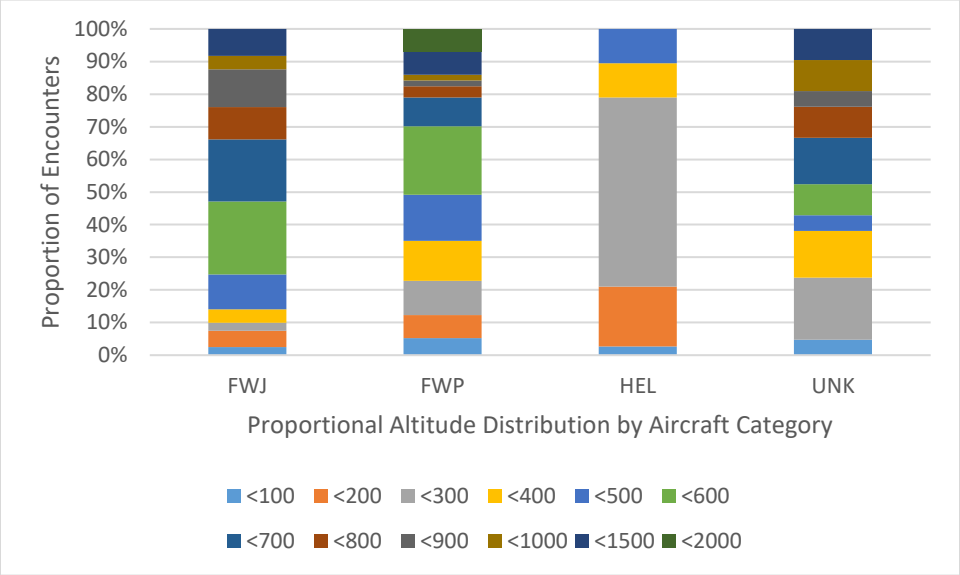

Figure 265. Proportional Distribution of Aircraft Altitudes during sUAS Encounters by Aircraft Type.

F.3.9 sUAS Altitude at Closest Point of Approach

DJI sUAS generally report altitude in meters *above the homepoint or launch location* rather than AGL. Since AGL values vary with terrain elevation, the research team identified the elevation at the CPA location to calculate the AGL altitude of each sUAS (see Figure 266). More than 26.1% of sUAS (n=62) were flown at altitudes exceeding 400 feet AGL, a regulatory limit for sUAS flight. At least 21.5% of the sUAS were flown over 500 feet AGL, impinging on the minimum flight altitudes for most aircraft, as identified in 14 C.F.R. §91.119(c)[other than congested areas]. Perhaps more concerning was that at least 5.1% of sUAS (n=12) had flown over 1,000 feet AGL,

entering into minimum safe altitudes [for aircraft operating over congested areas], as specified in 14 C.F.R. §91.119(b).

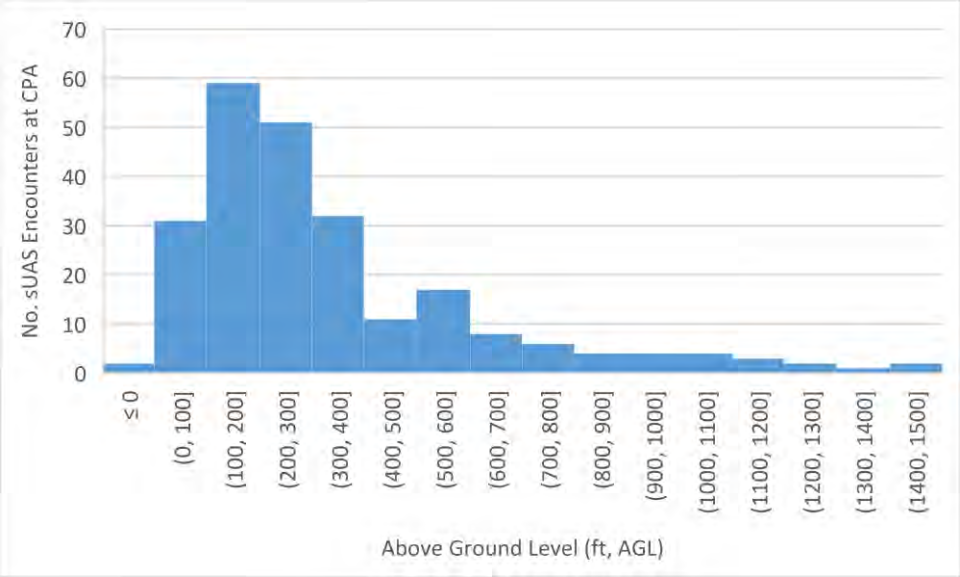

Figure 266. Distribution of sUAS Altitude for Aircraft-sUAS Encounters at CPA Corrected to AGL.

F.3.10 Encounter Rates

Using existing encounter data, the research team attempted to calculate encounter rates to estimate potential encounter risk within the National Airspace System (see Figure 267). The calculated estimates are preliminary in nature and may be revised as additional encounter data becomes available. The research team selected Boston, Massachusetts, as the best sample area from which to derive encounter estimates since this location provided the largest sample, had the most diverse collection of aircraft types involved in encounters, and most encounters occurred within 5 NM of a major airfield. Encounter rates for the remaining sampling areas are provided for comparison and context. The research team believes this sampling accurately reflects sUAS encounter/collision risk at major airports across the U.S. Encounter rates were derived by dividing the number of detected encounters by the number of detected sUAS flights, yielding an encounter rate of .072 per sUAS flight during the sampling period. It is important to note that an encounter was defined as an aircraft and sUAS coming within a 4,000-foot lateral / 500-foot vertical distance of an aircraft. The encounter rate for Boston drops to .009 for encounters that result in a loss of adequate separation [less than 500 feet horizontally / 100 feet vertically].

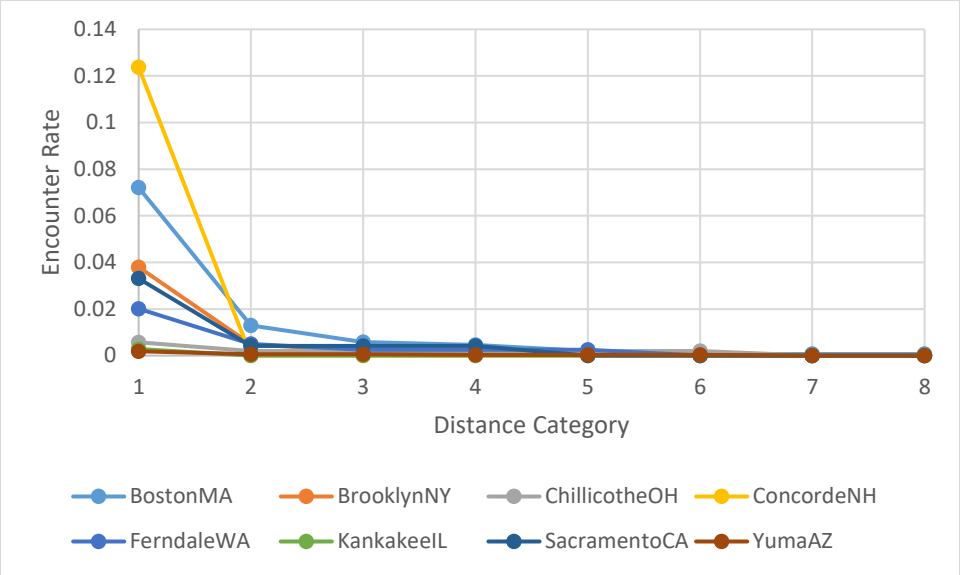

Figure 267. Encounter rates based on number of UAS flights by location.

F.4 Conclusions

Leveraging sUAS detection technology coupled with ADS-B aircraft tracking data and various analytics methods enabled the research team to better understand the problem of aircraft encounters with sUAS. Understanding the unique characteristics of encounters can inform regulatory policymaking to address contributing factors, as well as enable improved measures for assessing National Airspace System safety risks.

F.5 References

Academy of Model Aeronautics [AMA]. (2015). A Closer Look at the FAA's Drone Data. http://www.movoaviation.com/images/AMAAnalysis-Closer-Look-at-FAA-Drone-Data_091415.pdf

Academy of Model Aeronautics [AMA]. (2016). An Analysis of the FAA's March 2016 UAS Sightings. https://amablog.modelaircraft.org/amagov/wp-content/uploads/sites/2/2016/06/AMA-Analysis-FINAL-6-1-16.pdf

Academy of Model Aeronautics [AMA]. (2017). As Drone Sales Soar, Vast Majority of Reports Remain Simple Sightings. https://www.modelaircraft.org/sites/default/files/UASSightingsAnalysisbyAMA5-10-17.pdf

Civil Aerospace Medical Institute [CAMI]. (2017). Pilot Vision Safety Brochure. *Federal Aviation Administration.* https://www.faa.gov/pilots/safety/pilotsafetybrochures/media/pilot_vision.pdf

Drone Analyst. (2021). 2021 Drone Market Sector Report. https://droneanalyst.com/research/2021-drone-market-sector-report

Drone Industry Insights. (2021). The Best Drone Manufacturers in 2021. https://droneii.com/the-best-drone-manufacturers-in-2021?utm_source=email&utm_medium=newsletter&utm_campaign=manufacturers-rank-2021-release&utm_content=read-blog&utm_term=continue-reading-button&mc_cid=433d906d09&mc_eid=3ae0e4ffde

Earthpoint. (2022). Convert coordinates: Calculate a position in a variety of formats. https://www.earthpoint.us/convert.aspx

Federal Aviation Administration [FAA]. (n.d.a). Automatic Dependent Surveillance-Broadcast (ADS-B). https://www.faa.gov/about/office_org/headquarters_offices/avs/offices/afx/afs/afs400/afs410/adsb#:~:text=Automatic%20Dependent%20Surveillance%E2%80%93Broadcast%20(ADS,interface%20between%20aircraft%20and%20ATC.

Federal Aviation Administration [FAA]. (n.d.b). FAA Registry: N-Number Inquiry. https://registry.faa.gov/aircraftinquiry/Search/NNumberInquiry

Federal Aviation Administration [FAA]. (n.d.c). The Mode S Team. https://www.faa.gov/about/office_org/headquarters_offices/ato/service_units/techops/safety_ops_support/nas_engineering/modes_digitizers_sbsm/modes

Federal Aviation Administration [FAA]. (n.d.d). NMACS System Information: FAA Near Midair Collision System (NMACS). https://www.asias.faa.gov/apex/f?p=100:35:::NO::P35_REGION_VAR:1

Federal Aviation Administration [FAA]. (n.d.e). The Operations Network (OPSNET). https://aspm.faa.gov/opsnet/sys/Main.asp

Federal Aviation Administration [FAA]. (2022a). Chart Supplement: Basic Search. https://www.faa.gov/air_traffic/flight_info/aeronav/Digital_Products/dafd/search/

Federal Aviation Administration [FAA]. (2022b). UAS Sightings Report. https://www.faa.gov/uas/resources/public_records/uas_sightings_report

Gettinger, D. & Michel, A.H. (2015). Drone Sightings and Close Encounters: An Analysis. *Center for the Study of the Drone at Bard College.* https://dronecenter.bard.edu/files/2015/12/12-11-Drone-Sightings-and-Close-Encounters.pdf

Iowa State University. (n.d.). Visual acuity of the human eye. *Center for Nondestructive Evaluation.* https://www.nde-ed.org/NDETechniques/PenetrantTest/Introduction/visualacuity.xhtml

Kephart, R.J. & Braasch, M.S. (2010). Comparison of See-and-Avoid Performance in Manned and Remotely Piloted Aircraft. IEEE Aerospace and Electronic Systems Magazine, 25(5), 36-42. DOI: 10.1109/MAES.2010.5486540

Loffi, J.M., Wallace, R.J., Jacob, J.D., & Dunlap, J.C. (2016). Seeing the Threat: Pilot Visual Detection of Small Unmanned Aircraft Systems in Visual Meteorological Conditions. International Journal of Aviation, Aeronautics, and Aerospace, 3(3). https://commons.erau.edu/ijaaa/vol3/iss3/13

Loffi, J.M., Wallace, R.J., Vance, S.M., Jacob, J., Dunlap, J.C., Mitchell, T.A., & Johnson, D.C. (2021). Pilot Visual Detection of Small Unmanned Aircraft on Final Approach During Nighttime Conditions. International Journal of Aviation, Aeronautics, and Aerospace, 8(1). https://commons.erau.edu/ijaaa/vol8/iss1/11

Lourenço, J.R. (n.d.). Open Elevation [database]. https://www.open-elevation.com/

Maddocks, J. & Griffitt, G. (2015). Qualitative Evaluation of Unmanned Aircraft Visibility During Agricultural Flight Operations. Avion. https://coagav.org/resources/Documents/TBYL%20Visibility%20Flight%20Test%20Report_FINAL.pdf

Minimum Safe Altitudes. 14 C.F.R. §91.119 (2010). https://www.ecfr.gov/current/title-14/chapter-I/subchapter-F/part-91/subpart-B/subject-group-ECFRe4c59b5f5506932/section-91.119

Open Sky Network [OSN]. (2022). Open Air Traffic Data for Research. https://opensky-network.org/

Unmanned Aircraft Safety Team [UAST]. Drone Sightings Analysis and Recommendations. https://www.unmannedaircraftsafetyteam.org/wp-content/uploads/2018/01/UAST-Sightings-Executive-Summary-2017.pdf

Unmanned Robotics Systems Analysis. (2022). The URSA Platform: Powerful Analytical Tools to Ensure Safety in Our Skies. https://ursainc.com/

Wallace, R.J., Loffi, J.M., Vance, S.M., Jacob, J., Dunlap, J.C., & Michell, T.A. (2018). Pilot Visual Detection of Small Unmanned Aircraft Systems (sUAS) Equipped with Strobe Lighting. Journal of Aviation Technology and Engineering, 7(2). DOI: 10.7771/2159-6670.1177

Wallace, R.J., Vance, S.M., Loffi, J.M., Jacob, J., & Dunlap, J.C. (2019). Cleared to Land: Pilot Visual Detection of Small Unmanned Aircraft During Final Approach. International Journal of Aviation, Aeronautics, and Aerospace, 6(5). DOI: 10.15394/ijaaa.2019.1421

Wallace, R.J., Winter, S.R., Rice, S., Kovar, D.C., & Lee, S. (2022). *Three Case Studies on Small UAS Midair Collisions with Aircraft: An Evidence-based Approach for Using Objective UAS Detection Technology* [Manuscript Submitted for Publication]. Aeronautical Science Department, Embry-Riddle Aeronautical University.

Wallace, R.J., Terwilliger, B.A., Winter, S.R., Rice, S., Kiernan, K.M., Burgess, S.S., Anderson, C.L., De Abreu, A., Arboleda, G., & Gomez, L. (2022). Small Unmanned Aircraft Systems Traffic Analysis: Initial Annual Report (FAA Grant No. A11L.UAS.91). *Alliance for System Safety of UAS Through Research Excellence (ASSURE).* https://assureuas.com/wp-content/uploads/2021/06/First-Annual-Report-Final-v1.1-11-14-2022-WEBSITE.pdf

Wang, C. & Hubbard, S.M. (2021). Characteristics of Unmanned Aircraft Systems (UAS) Sightings and Airport Safety. *Journal of Aviation Technology and Engineering, 10*(2), pp. 16-33. http://dx.doi.org/10.7771/2159-6670.1238

Appendix G Support Material

The MACs recorded in all the encounter sets in Sections 3.3 and 4.4 are documented in two excel databases. The database includes information for each MAC, such as position, orientation, speed, and an image of the MAC.

G.1 Unmitigated MAC Database

MAC_Database_Nom.xlsx

G.2 Mitigated MAC Database

MAC_Database_Mit.xlsx